SECRET [redacted]

[redacted] COPY

FEASIBILITY STUDY FINAL REPORT

GEODETIC ORBITAL PHOTOGRAPHIC SATELLITE SYSTEM

VOLUME 3 DATA PROCESSING, PART 1

JUNE 1966

SECRET [redacted]

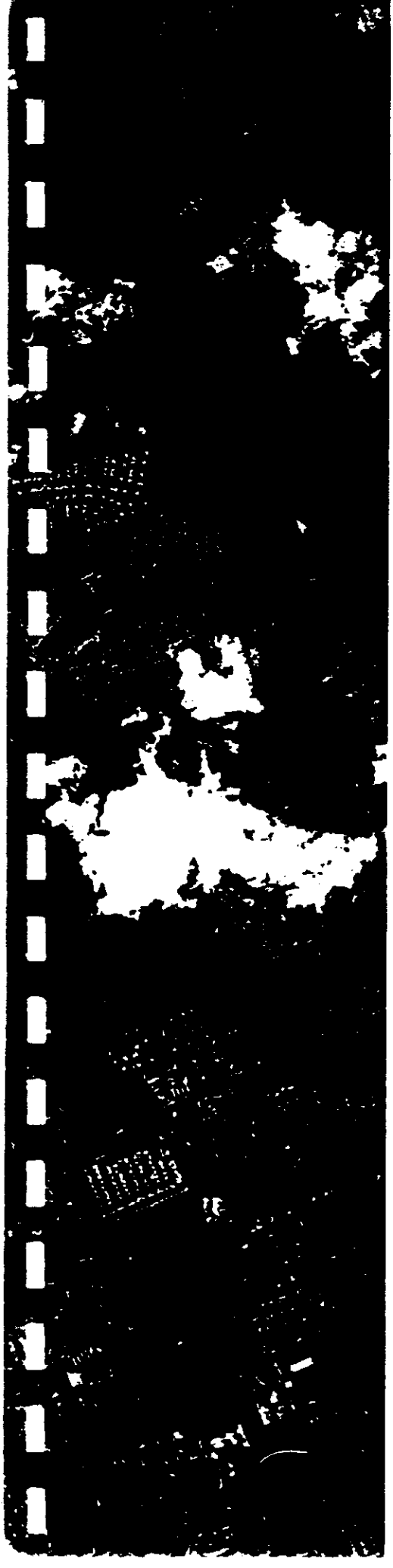

SECRET [redacted]

Copy No. [redacted]

FEASIBILITY STUDY FINAL REPORT

GEODETIC ORBITAL PHOTOGRAPHIC SATELLITE SYSTEM

VOLUME 3 DATA PROCESSING, PART 1

JUNE 1966

Itek

ITEK CORPORATION LEXINGTON 73

SECRET [redacted]

[redacted] VOL 3

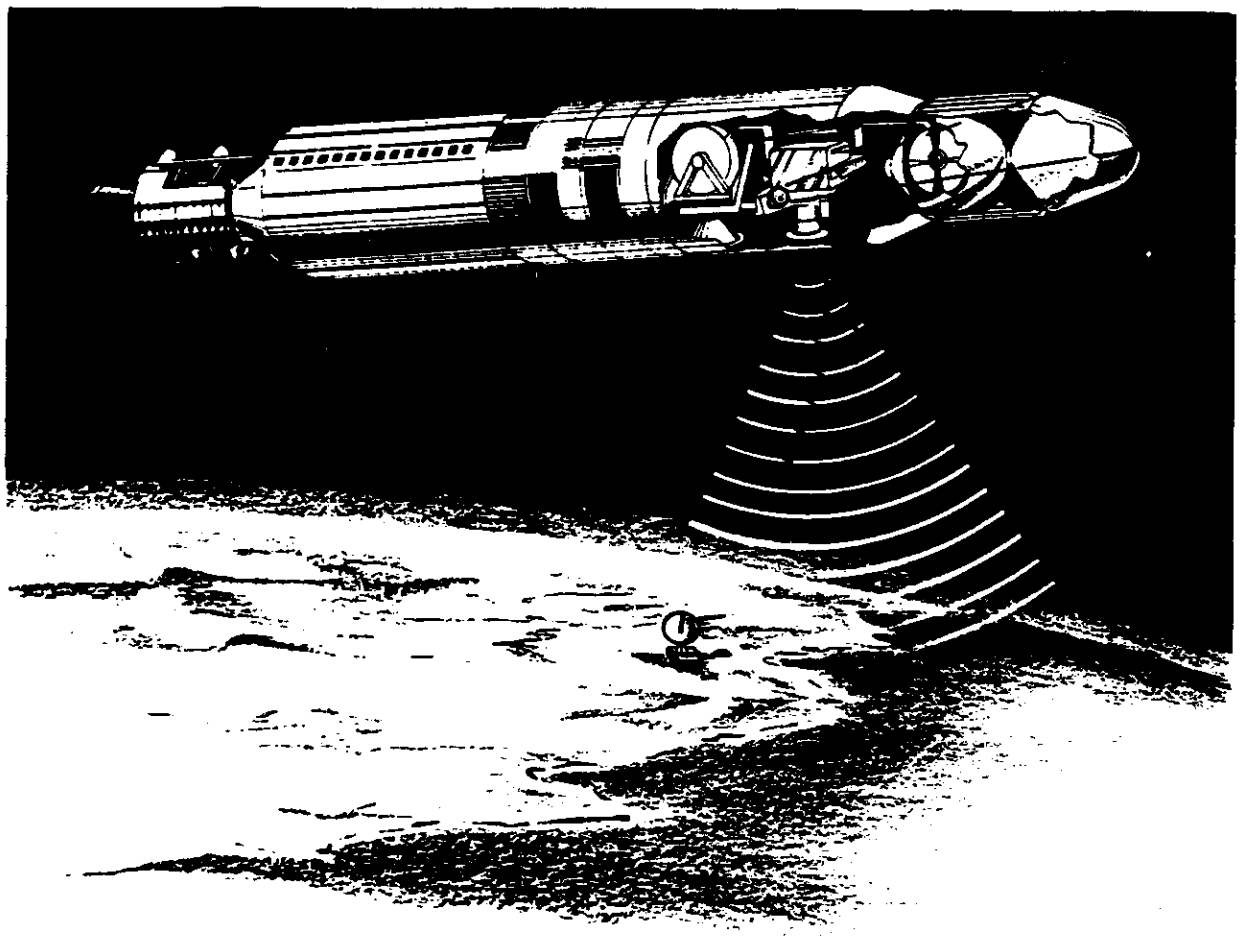

Geodetic Orbital Photographic Satellite System

CONTENTS

Page

TABLES

Page

FIGURES

PREFACE

The objective of the Geodetic Orbital Photographic Satellite System (GOPSS) is to accurately determine the location of landmarks widely distributed over the earth's surface and provide better information concerning the geophysical parameters which affect this system and other systems operating at similar altitudes. The means chosen to accomplish this objective is to orbit a series of data acquisition systems supported by ground-based instrumentation. The data gathered by this system is incorporated into a sophisticated data reduction scheme which determines the geodynamic parameters and landmark locations.

Detailed studies were conducted to determine the feasibility of the GOPSS. The study period was designated as Phase I, and the results of these studies have been compiled into five volumes for reader convenience.

This volume considers the photogrammetric data subject to constraints imposed by orbital and auxiliary data, the mapping capabilities of the system, and ground handling of mission photography.

The division of the remaining volumes and their content are now briefly described for information and reference purposes.

Volume 1, Program Compendium and Conclusions, was prepared to provide briefly the details essential to a comprehensive understanding of the effort conducted during Phase I of the GOPSS feasibility study. System concept and objectives are described plus conclusions which concern the attainment or modification of the initial objectives, along with recommendations for a system configuration and a solution of the attendant data handling problems.

Volume 2, Data Collection Systems, describes the effort for implementation of the data acquisition requirements for the GOPSS program. This volume presents the preliminary design which defines and describes the various sensors, considers their functional interdependencies, and shows their evolvement into an integrated GOPSS.

Volume 4, Data Processing, Part 2, discusses orbital considerations affecting the feasibility of the GOPSS. Physical models and computational procedures are reviewed and error studies involving typical sensors and model inaccuracies are described. Based on these studies, recommendations are made for tracking networks, auxiliary on-board sensors, and detailed orbit plans. In addition, the data reduction procedure, whereby the acquired data are simultaneously located to yield geodynamic parameters and landmark locations is considered.

Volume 5, Phase II-V Program Plan, describes the planning activity as it has been programmed through Phases II to V for the engineering, fabrication, and operational support for the delivery of five systems. Continuing studies which are required are also defined in this volume.

SUMMARY

The basic objective of the photogrammetric study was to evaluate the accuracy of positioning landmarks, well distributed over the earth's surface, with respect to a World Geodetic System. In order to accomplish that objective, prerequisite studies were conducted which showed:

1. Measured photographic data can be corrected for systematic errors, such that the residual errors in the corrected measurements due to calibration, film distortion, etc., are maintained to a maximum value of ±4 microns at the 1-sigma level. This fact is predicated on the use of a prescribed 12-inch focal length lens, and the lens design and its performance characteristics that were generated during the program.

2. That the optimum reseau spacing, assisting the suppression of these errors to the ±4-micron level is 1 centimeter.

3. That the accuracy can be evaluated with which the camera exposure stations may be photogrammetrically determined with respect to the centroid of five landmarks imaged on three adjacent frames.

A theoretical photogrammetric analysis in which the mathematical model for the numerical evaluation of the photographic subsystem is developed. The accuracy with which landmarks can be determined from the reduced photographic data is considered in two segments.

1. The first of these evaluates the accuracy with which landmarks can be determined with respect to the orbit over unknown areas. It is concluded that landmark errors in the order of ±39 feet cross-track, ±42 feet in-track can be obtained and that the inclusion of a radar altimeter in GOPSS will reduce elevation errors to the order of ±42 feet when operating at an altitude of 160 nautical miles.

2. The second segment deals with the accuracy of extending geodetic control from known areas by the method of aerial triangulation. It is concluded that the maximum length of such triangulations that ensure the elevation errors are less than ±40 feet is 640 nautical miles for a vehicle altitude of 160 nautical miles.

The ground handling of the recovered mission photography is discussed, and concludes that the handling of these records presents no serious difficulty with existing equipment.

The final consideration is that of utilizing the GOPSS photography as a mapping medium. It is concluded that for medium scale maps, in the order of 1:200,000, that the criteria for Class A maps can be met. In order that large scale maps, of 1:100,000 scale or better, can be produced consistent with the mapping criteria, supplemental data must be provided to reduce the elevation errors and to increase the relative accuracies.

Section A

PHOTOGRAMMETRIC ANALYSIS

3.1 INTRODUCTION

The mission of the Geodetic Orbital Photographic Satellite System (GOPSS) involves the location of landmarks over the earth's surface to high accuracies from data collected by an orbiting vehicle and the simultaneous accurate evaluation of the geodynamic parameters which influence the motion of the orbiting vehicle. The principal data gathering system for landmark location is photogrammetric, and consists of a set of cameras, one to photograph the earth's surface and two stellar cameras to define orientations. Orbit position is defined by typical tracking networks, re-enforced by selective photogrammetric data. Accurate time in orbit is recorded and auxiliary onboard sensors may be employed.

The GOPSS program might be treated as two independent calculating schemes. The first is the utilization of tracking data as the prime input to determine the orbit; the second is the use of this orbit to position the camera stations from which the location of ground points is obtained. In this positioning task, the camera is considered as the prime sensor, so that the production of a landmark catalog is approached as if it were a photogrammetric problem alone.

This leads to an approach which treats each of the data types according to independent data reduction schemes and can become involved, since functional relationships exist between the various types of data despite the fact that they are independently acquired. For example, ground tracking data provide the most accurate information for the determination of orbital parameters, yet these parameters can be weakly determined from the photogrammetric solution. The independent reduction of ground tracking data and photographic records is theoretically unsound, since these two sets should be consistent with each other through on common factors, namely, the orbital parameters.

Investigating the feasibility of the GOPSS concept using an integrated treatment as described in Volume 4, Section 4.12 requires the complete data reduction scheme that will be necessary to finally reduce the data from the GOPSS. Only partially integrated analyses can be performed in this study. If, by proceeding in this manner, it is concluded that meeting the specification is feasible, then the final data reduction involving complete integration would more strongly re-enforce this conclusion.

In the past, multidata systems have been considered as being composed of a prime sensor that fulfills the basic system objective, and various auxiliary sensors that support and complement the prime sensor. The role assigned to the so-called auxiliary systems has been to provide supplemental information and facilitate the data reduction problem. Nowadays, auxiliary data systems frequently provide better quality and a greater quantity of data than that furnished by the prime sensor. This has led to a revision in the concepts of auxiliary data utilization, such that all related data are used to perform an integrated and simultaneous adjustment to obtain consistent results in achieving the system objectives.

This section of the report is directed toward evaluating the photogrammetric accuracies that can be attained as well as furnishing realistic estimates of the expected input errors to the orbital computations. It is recognized that providing these error estimates implies that the reduction of photogrammetric and orbit tracking data are independently performed. This conflicts with the preceding comments, but is necessitated by the structural organization of this phase of the study. The recommended data reduction scheme, however, will not consist of independent computational schemes, since the combined data acquisition capability of the system provides for a great amount of over-determination of the desired information, even for small orbital segments, so that a constrained adjustment will be mandatory to achieve optimum results.

As previously stated, the GOPSS program can be treated as utilizing tracking data to determine the orbit, and using this orbit to position the camera stations from which the location of ground points are obtained. However, since the camera stations lie on the orbit, inconsistencies will result unless the photogrammetric data are used with the other data in determining the orbital parameters. In this regard, and provided that a sufficiency of ground control points exists, the photographic records furnish a means of determining discrete orbital positions. These positions must conform to those that can be interpolated from an alternate orbit determination. and thus a condition is imposed on the data adjustment. The whole purpose of this adjustment is to eliminate the discrepancies that would otherwise exist, so that no matter whether one determines camera positions photogrammetrically or by using orbital positions, the same location results. The same holds true for landmark determination—after adjustment, the coordinates of such points should be the same, whether resulting from a long photogrammetric strip triangulation or compiled from two exposures whose locations have been orbitally determined.

In this portion of the analysis, the camera positioning and landmark location requirements will be treated as a photogrammetric problem, subject to functional restraints and constrained to various auxiliary and orbit tracking data. This assigns the photogrammetric subsystem the primary role. However, this is only a specific aspect of the overall data reduction scheme, and, provided that the correct functional relationships are enforced, it is irrelevant. In other words, the same data could be equally viewed as an orbit determination in which the photogrammetric data are a minor set of tracking information.

The use of auxiliary data as an integral part of the photogrammetric reduction is one of the strengths of the GOPSS. Individual photogrammetric models possess a reasonable geometric strength. The conjunction of successive models, however, to form a triangulated strip, is subject to an unfavorable error propagation. It is this fact which precludes the attainment of the objectives through photogrammetric techniques alone. These techniques do not have the strength to extend positional control into uncontrolled areas even with such a highly sophisticated camera as this, but must depend on a stable and well-defined orbit determined by other sensors. Additional data, acquired by other sensors, when incorporated into the triangulation with the correct functional constraints suppress the error accumulation to a surprisingly small minimum.

The other considerations in this study consists of a sequence of single and multimodel triangulations. Although it might appear as if this were the whole concern of this study, this is far from the truth. Essentially, the triangulations are performed to determine whether certain system objectives can be achieved, and to demonstrate that the proper use of auxiliary data enables these objectives to be surpassed. Since these triangulations require ground control data in the initial model as a minimum, some consideration of the quality of these points is necessary. The basic assumption has been that the location errors of control points i.e., photo-identifiable ground points whose positions are known, are uncorrelated, and equal to a spherical error of

±10 meters. This is a typical internal error value that could be encountered in existing high quality geodetic nets. The specific problem of the errors between distinct geodetic systems necessitates that a datum shift for each geodetic net be incorporated into the data reduction scheme. In general, such shifts with respect to a world geodetic system might be expected to be as much as 50 meters. Although the determination of these shifts is the basic objective of the DOD satellite triangulation program (PAGEOS), it is also an incidental accomplishment of the GOPSS program. These aspects are discussed in some detail in this volume and in Volume 4.

3.1.1 Photogrammetric Study Objectives

The basic objective of this photogrammetric study was to evaluate the accuracy of positioning landmarks, well distributed over the earth's surface, with respect to a World Geodetic System.

In order to accomplish this objective, various prerequisite studies were conducted, which permitted the evaluation of some intermediate objectives. These studies showed:

1. That the measured photographic data can be corrected for systematic errors, such that the residual errors in the corrected measurements due to calibration, film distortion, etc., are maintained to a maximum value of ±4 microns at the 1-sigma level. This is predicated on the use of a prescribed 12-inch focal length lens, and the lens design and its performance characteristics that were generated during the program.

2. That the optimum reseau spacing, assisting the suppression of these errors to the ±4-micron level should be determined.

3. That the accuracy can be evaluated with which the camera exposure stations may be photogrammetrically determined with respect to the centroid of five landmarks imaged on three adjacent frames.

Before discussing the specific analyses, a general description of the overall study is given below.

3.1.2 Photogrammetric Study Description

Section 3.2 consists of an examination of the systematic errors affecting the recorded and extracted photographic data, and the corrections necessary for their removal from the measured coordinates. Since it is frequently not possible to exactly define the systematic errors and their corrections, residual errors are expected to exist in the refined coordinates. These residual errors are the basic inaccuracies present in the photogrammetric data input into the computational schemes.

The most significant of the systematic errors, mechanical film distortions, can be reduced by the use of a reseau. The reseau spacing necessary to suppress the effects of the residual errors to a specified tolerance is described in Section 3.6.

Section 3.3 consists of a theoretical photogrammetric analysis in which the mathematical model for the numerical evaluation of the photographic subsystem is developed. This analysis is directed toward the overall data reduction scheme in which auxiliary data, prime orbital data, etc., are simultaneously incorporated.

These two portions of the study were accomplished through an extensive literature search, discussions with several of the authors, and a certain amount of original work.

Section 3.4 consists of a sequence of numerical analyses, utilizing the model developed in the second phase. Basically, the photographs were either statistically constrained to discrete orbital positions, or functionally constrained to orbital positions and utilized stellar orientations.

The numerical analyses that were performed established the following design parameters and attainable accuracies:

1. The optimum overlap between successive photographs, with the incidental determination of the effects of varying the weights assigned to the measured photocoordinates (Section 3.4.1.1)
2. The effects of decreasing the length of the format on the attainable photogrammetric accuracy (Section 3.4.1.2)
3. The determination of the accuracy of locating camera positions with respect to the centroid of five landmarks imaged on three adjacent frames with the incidental determinations of the effects of varying the orbital covariance matrix (Section 3.4.2)
4. The attainable accuracy of strip triangulations, as bridges and extensions, assuming ground control data (Section 3.4.3)
5. The attainable accuracy of positioning landmarks from orbitally constrained photography, with no ground control (Section 3.4.1.1, Table 3-11).

The last three sets of numerical studies were repeated at three different altitudes, namely, at 120, 160, and 200 nautical miles, in order that the effects of increasing the altitude on the system performance could be evaluated.

3.2 RESIDUAL DATA EXTRACTION ERRORS

This section is concerned with examining the fundamental accuracy with which data extracted from the photographic records can be refined through the removal of systematic errors.

The inaccuracy of these refined data is due in part to an inadequate knowledge or expression of the systematic errors and in part to the presence of random errors inherent in the extracted data.

This section considers the various systematic errors and provides estimates of the magnitudes of the residuals errors in the refined data. These estimates lead to the imposition of various conditions on the data extraction equipment, and the refining processes in order that measuring tolerances can be met.

A preliminary objective states that the reduced photo coordinates should be accurate to a 1-sigma level no greater than 4 microns. This is a total error that results from a combination of all the individual contributing errors. For this study, a linear error model is used, such that the residual error, σ_i, at any point, i, is expressed as

$$\sigma_i = [\Sigma \ \sigma_{ij}^2 \ ]^{1/2}$$

where the summation is over j, of the contributing errors at the point i.

The basis for selecting the linear model is based on the hypothesis that the individual errors are independent, and that the residual systematic errors are randomly distributed.

The various contributing residual errors, σ_i, are tabulated

σ_1 = residual film distortion error
σ_2 = residual refraction error
σ_3 = residual camera calibration error
σ_4 = residual aberration error
σ_5 = residual mensuration error
σ_6 = residual comparator calibration error

Each of these component errors is now individually considered.

3.2.1 Residual Film Distortion Errors

Perhaps the most serious problem involved in the reduction of photogrammetric measurements is the adequate removal of systematic film distortions. The usual methods of compensating for these distortions involve the use of either calibrated fiducial markers or a reseau, the images of which are recorded on the photography at the time of exposure.

Film distortions existing in photography cause image points to be displaced from instantaneously imaged locations. These displacements are primarily a function of the inherent characteristics of the film base, and of the developing procedures. Some of the distortions occur as a result of tensile forces applied to the imperfectly elastic roll film during its transport in the camera and in the developing and drying equipment. Other permanent distortions occur as a result of the manner in which the film is handled, developed, and dried. They are primarily caused by the release of stresses in the dry film and emulsion during development and by the compressive forces acting on and between the emulsion and film base during drying. Irregular random distortions are also present, the magnitudes of which determine a noise level or threshold, beyond which the application of adjustment procedures to measure photographic images is pointless.

3.2.1.1 Permanent Film Distortions

The original negatives are considered to have a format size of 9 by 18 inches. The film used is assumed to be an Estar base, 0.0025 inch thick, with a type SO-130 emulsion.

The high stiffness and low flow of the Estar base resist the tensile forces of the camera and processing equipment. Furthermore, the backing of the film causes the unbalance of forces during drying to be very small, so that the elastic compression is frozen in the film. The dimensional changes that can be expected as a result of processing may amount to 0.05 percent and those due to aging may be ignored.

For the selected format, this would cause total shrinkages as large as 228 microns in length and 114 microns in width. In the event that copy positives used in the measuring apparatus are made on a thick (0.007 inch) Estar base, which has a shrinkage factor of 0.02 percent, an additional shrinkage of 92 microns in length and of 46 microns in width will be present. Since these are systematic deformations, they are additive.

3.2.1.2 Nonpermanent Film Distortions

The most important factors causing these temporal variations are changes in the temperature and relative humidity of the film's environment. Although Estar base films possess excellent physical characteristics, only very small changes in temperature and humidity can be neglected. The coefficient of linear thermal expansion is $15 \times 10^{-6}/°F$, and that of linear hygroscopic expansion is $35 \times 10^{-6}/1$ percent relative humidity. Thus, temperature changes of 1 °F during the measuring period will cause a dimensional change of approximately 6 microns over an 18-inch length of film. The corresponding dimensional change for a 1 percent increase in humidity will be approximately 17 microns. Provided that the absolute humidity remains constant, these changes will tend to compensate each other, although the hysteresis of the film expansion with humidity may negate this compensation.

In addition to the dimensional changes induced by changes in the whole environment, local temperature and humidity variations may occur when the film is being measured. These are primarily due to the effect of concentrated light on that portion of the film which is being viewed and the heating effect of other electrical machine components. These local distortions may be difficult to detect and remove from the measurements.

It is often difficult to determine whether image displacements are caused by film distortion or by some other factor unrelated to the dimensional stability of film. Perhaps the most significant source of such displacements is lack of flatness in the camera (partially compensated for by

using a reseau register glass in the focal plane of the camera). It appears to be impossible to separate the errors caused by this source from those caused by dimensional changes. Furthermore, lack of film flatness in reproduction and measuring equipment may occur unless very careful precautions are taken. Environmental conditions must be rigorously stabilized during the processing and measurement of film if accurate results are to be obtained. According to Michener, these environmental conditions should be maintained in the postdevelopment storage areas. The obvious solution would be to store the processed film in the same room that is used for the measuring equipment. This would mean that it would be necessary to environmentally control only one room. The environmental controls which is felt necessary to maintain in order to minimize the effects of atmospheric temperature and humidity changes are listed in Table 3-1.

The alternative to using original film or copy diapositives on a stable film base, is to make reproductions on coated glass plates.

Glass plates are superior to film base in all respects involving stability. Although the former are quite expensive when compared to a film base, an economic advantage is obtained when using glass since the cost of establishing the precise environmental controls for the storage and mensuration of film is not invovled. Furthermore, by selecting the thinnest Grade I plates, substantial savings may be made. It may be argued that the lower flatness tolerance of these plates negates such an advantage. However, it should be noted that such plates are much flatter than a film base can be, and that the lack of flatness is unimportant when using an orthogonal viewing instrument.

Glass plates are easy to handler and rigidly attach to the measuring and reproduction machines. It is extremely difficult to secure film in such apparatus without applying tensile or compressive forces to the film. Such forces produce distortions which may defy evaluation.

It is therefore concluded that glass plates are to be preferred over a film base for use in a precise phtogrammetric data reduction system. Copies of the original exposure should be made onto glass plates, thereby "freezing" the distortions existing at that time onto a permanent record. It has frequently been commented that the bulk of glass plates requires a large storage facility, however, a 9-inch by 18-inch glass plate 1/4 inch thick displaces a volume of 40.5 cubic inches. For 15,000 glass plates, this displacement to 351.5 cubic feet. Assuming that an equal volume is required for the crating and separation of these plates, a storage area of 700 cubic feet is required. This is not a significantly large storage requirement.

3.2.1.3 Calibration Marks

Normally, survey cameras are provided with four fiducial markers. These are located at either the four corners or at the midpoint of each side of the format. By comparing the measured distances between the marker images with their calibrated values, the effect of the systematic film distortion can be reduced to the extent that the standard residual error is about 20 microns (Tewinkel, 1960) to 15 microns (Laurila, 1961) for acetate base films. In the event that a stable Estar base film is used, the standard residual error is reduced to about 5 microns (Tewinkel, 1961; Adelstein, 1962).

A significiant improvement in the compensation for systematic film distortion may be obtained if the survey camera is provided with additional calibrated markers. According to Tewinkel, 1961 and 1962, the use of eight markers, located at the four corners and at the midpoint of each side of the format, forces the discrepancies into smaller bounds so that the standard residual error is decreased by about one half ($2\frac{1}{2}$ microns). If a central mark is included, the effect of the nine marks is to reduce the standard residual error by one quarter (1.25 microns).

Table 3-1 — Recommended Environment Controls

Environment*	Temperature, °F	Humidity, percent
Pre-exposure	70 ± 2	50 ± 5
Development	70 ± 1 to 2	—
Drying	70 ± 1 to 2	50 ± 2
Storage	70 ± 2	50 ± 5
Measuring†	70 ± 1 to 2	50 ± 1

*All environments are assumed to be dust free.
†If storage and measuring environments are difficult, ensure that the film is presoaked in the measuring environment for at least 24 hours. This should then be followed by a 4-hour instrumental soak period.

Substantial analyses by Brock and Faulds, Gimrada, et al., indicate that residual film distortion cannot be expected to be less than 1 to 2 microns. With the exception of some of the Gimrada studies, these analyses pertain to 9- × 9-inch format. Extrapolation to a 9- × 18-inch format is valid, provided that 12 fiducial marks and 3 central marks are imaged onto the film.

To ensure that a precise determination of the systematic film shrinkage is obtained, a calibrated reseau plate which is imaged on the negative at the instant of exposure will be used. It is pointed out that two different philosophies concerning the use of a reseau exist.

The first of these, implied by the preceding comments, is to use measures of the reseau point to determine an analytical expression for the systematic distortions. Since this may be adequately determined by an 8- to 10-parameter equation, a dense reseau spacing is unnecessary.

On the other hand, reseau marks may be considered to have their calibrated "exact" values and coordinates of image points determined by measuring and adjusting the incremental differences from surrounding reseau points. To prevent measuring and interpolating over long distances, a reseau spacing of 1 centimeter is recommended.

3.2.1.4 Recommendations

It is recommended that a reseau plate having a maximum density of 1 centimeter be used, so residual errors in the order of 1 to 2 microns are to be expected. The specific reseau technique to be used will be determined with regard to instrument and data reduction characteristics.

3.2.2 Residual Refraction Errors

The displacement of image rays due to atmospheric refraction may be corrected by applying various well known expressions. Owing to the dependency of most of the usual solutions on an accurate determination of the central angle, θ, and of the astronomic refraction, r_α, the strength of these solutions is somewhat variable.

The geometric situation for photogrammetric refraction, r_p, from a satellite-borne camera is illustrated by Figure 3-1. With reference to Figure 3-1

$$r_p = \alpha - \beta$$

where $\tan \beta = \sin \theta \left[1 + \frac{H}{R} \cos \theta \right]^{-1}$

in which

$$\theta = Z + r_\alpha - \alpha$$

and

$$\sin Z = \left[1 + \frac{H}{R} \right] \frac{\sin \alpha}{\mu_p}$$

μ_p being the index of refraction at the point P, which is appropriately determined from four terms of Garfinkel's model.

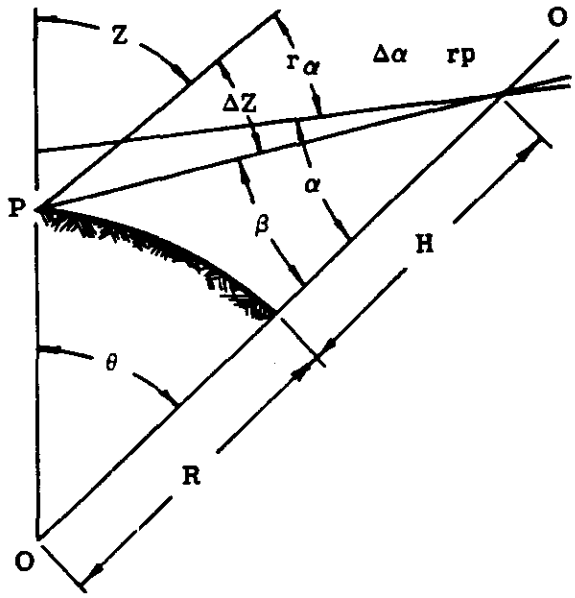

Fig. 3-1 — Geometry of atmospheric refraction

It is seen that the photogrammetric refraction is a function of six dependent variables α, H, R, Z, $r\alpha$, and μ_p. Errors in these variables affect the accuracy of the photogrammetric refraction. Photogrammetric refraction is relatively unaffected by errors in the satellite height, the index of refraction, the zenith distance, and the radius of the earth. This has been discussed by Case, who shows that the sensitivity of photogrammetric refraction to error in the nadir angle, α, satellite height, H, earth radius, R, and index of refraction, μ_p, is so small that it may be considered negligible. However, the sensitivity to errors in astronomic refraction and in zenith distance is extremely high and cannot be ignored. Case recommends the use of the flat earth formula, thereby dispensing with the central angle, θ, which is simple to use but relatively insensitive to errors in all the variables. His implication is that the difficulty lies with the small central angle, θ.

Subsequent work by Schmid discusses the problem of refraction more extensively, and derives the following formula

$$r''_p = \frac{2.330 \tan (180 - \alpha - \theta)\, \rho'' \cdot W}{H}$$

where W is a meteorological correction factor. Schmid presents tabulated data indicating the effects of completely neglecting the refraction problem, from which it is estimated that if the refraction is considered, the maximum residual error will not exceed 0.4 arc second, i.e., 0.6 micron, for the camera under consideration.

3.2.3 Residual Camera Calibration Errors

Advanced camera calibration techniques exist today which utilize photography of control fields made on glass plates and are capable of reducing the errors due to the distortions to the order of 1 to 2 microns. Such calibrations must necessarily be much more sophisticated than the usual consideration of radial lens distortion, and include parameters that account for tangential distortions, asymmetry of the distortions, lens decentering, etc. The most advanced of these calibrations are those of D. Brown, and of the USCGS, due to H. Schmid. Both are similar, being based on stellar photography, but differ in that Schmid's method is somewhat more sophisticated (carrying 23 parameters against Brown's 18). Both authors commendably apply generalized least square techniques in which appropriate weighting functions are applied to the input data, thereby enabling statistically valid estimates of error propagations to be formed. These methods are well documented, and need not be detailed here.

It is of interest to note that these methods are photographic, following the recommended practice of Commission I of the International Society of Photogrammetry. Since these recommendations further state that it is desirable for calibrations to be performed under conditions similar to the working environment of the camera system, it is perhaps worthwhile to consider the possibility of inflight calibration of the airborne cameras. Although preflight calibrations will be performed with the sytem, it is not unlikely that environmental conditions will affect the camera performance in some unknown manner, which can be detected only through inflight calibrations, (discussed in Volume 2). This calibration would require that the vehicle be rotated in such a manner that the terrain and stellar cameras both point into star fields, and that during the exposure time, the vehicles be in free flight. This can reasonably be accomplished during passage through the earth's shadow zone.

The great advantage of this inflight calibration is emphasized by the difficulties that exist in determining the camera constants for a near vacuum, and for recognizing any temporary change

in the relative orientation of the stellar and terrain cameras. The reduction of these calibrations would be performed in the same manner as ground based calibrations.

3.2.4 Residual Aberration Errors

Aberration is the image displacement caused by the (relative) motion of the camera system during the time it takes for the image radiation to reach the recording medium from the receptor.

If the relative vehicle velocity is v, the angular deviation, A, due to aberration is

$$A = \frac{v}{C} \sin \theta$$

where C = velocity of light
θ = angle between the image-object vector and the velocity vector

Since A is a small angle, the image displacement, Δ, may be written as

$$\Delta = S_i A$$

where $S_i = (x_i^2 + y_i^2 + f^2)^{1/2}$

This displacement is parallel to the velocity vector. For a tilted photograph this displacement is reduced to

$$\Delta' = \Delta \cos t$$

provided the resultant tilt is not too large. For a primary rotation of ω and a secondary rotation φ, one obtains t as

$$t = \tan^{-1} [(\tan^2 \omega + \sin^2 \varphi)^{1/2} (\cos \varphi)^{-1}]$$

The resulting displacement of the images is resolved into the components parallel to the photo axes through the swing angle κ as

$$\delta x = \Delta' \cos \kappa$$

$$\delta y = \Delta' \sin \kappa$$

Since it has been assumed that tilts will be small, one may compute

$$\sin \theta = (x_i^2 + y_i^2)^{1/2}/S_i$$

with little significant error, to obtain

$$\delta x = v(x_i^2 + y_i^2)^{1/2} \cos \kappa \cos t/C$$

and

$$\delta y = v(x_i^2 + y_i^2)^{1/2} \sin \kappa \sin t/C$$

Maximizing, i.e., putting $\kappa = t = 0$, one obtains

$$\delta x = v(x_i^2 + y_i^2)^{1/2}/C$$

For a velocity of v = 7 kilometers/second, and C = 299,696 kilometers/second

$$\delta x \sim 0.234\ (x_i^2 + y_i^2)^{1/2} \times 10^{-4}$$

if

$$(x_i^2 + y_i^2)^{1/2} \sim 200 \text{ millimeters}$$

then

$$\delta x \sim 5\mu$$

This is a significant correction and should not be ignored. However, approximate values for all parameters in this correction may be used without causing any significant residual error.

3.2.5 Residual Mensuration Errors

The mensuration equipment used in extracting data from the photographic records must provide for a readout and least count of 1 micron and be calibrated by appropriate methods in order to attain the ultimate accuracy. The calibration of analytical instruments has greatly improved in recent years, as evidenced by the thoroughly documented techniques to be found in the technical literature.

According to Rosenfield, the application of these calibration data reduces the average standard error of the measured coordinates to ± 1.0 micron, which is due to the mensuration equipment alone. This agrees well with Gugel's data, who, using Rosenfield's technique, obtains standard errors in the order of 1.2 to 1.9 microns, and are not too different from those values determined by Hallert (± 2.5 microns) and Brown (± 2.3 microns).

A more sophisticated modification of this technique has been made by the Itek Data Analysis Center, which utilizes appropriate weighting techniques to obtain the variance-covariance matrix of the corrective parameters and enables one to determine the weight matrix of the corrected coordinates. The unit standard deviation of the reduced coordinates is in the order of 0.5 micron, due to the propagation of the errors in the calibration data. This precision is partly illusionary, since it is necessary to assign appropriate weighting functions to measured image coordinates in order to determine the final precision. The basic criterion for these weighting functions is the resolution.

Before discussing these functions, it is appropriate to comment on resolution.

Resolution when expressed in lines per millimeter, has frequently led to erroneous interpretation. The typical test chart consists of a series of equally spaced uniform lines on a contrasting background, in which the spaces between lines are equal to the line width. The minimum resolvable distance is thus equal to the width of a line, or space. For a resolution of n lines per millimeter, this means that (1/2 n) millimeters is the minimum resolvable distance. From a theoretical point, it has been argued that the minimum resolvable distance is 1/(2n-1) millimeters, consisting of n lines separated by n-1 spaces, but here it is elected to use the value 1/2n. In this respect,

frequency spectra and transfer functions, although less easily understood, are less frequently misinterpreted.

Applying the minimum resolvable distance to determine the dimensions of the minimum object on the ground that can be imaged is not fully correct. This has been fully described by G. Brock, who states:

"As the camera moves away from the object, the image on the negative first grows smaller in accordance with the laws of geometrical optics, until its dimensions have reached the critical value below which the taking system cannot deliver a reproduction. As the distance between the camera and object is further increased, the size of the image remains approximately the same, but its contrast against the surrounding background diminishes. The distance at which a given object is still reproduced on the negative depends primarily on the contrast of the object, although the contrast (γ) of the negative material also has a certain influence. In this extreme case of the reproduction mode, the shape of the image produced is determined by the characteristics of the lens and is virtually independent of the object of photography."

The use of resolution as the criterion for weighting photographic coordinates is generally in agreement with current photogrammetric practice and theory. Extensive experiments have been made, and are still being made, to determine the most appropriate function of resolution to use. Unfortunately, no concurrence of opinion as to the best function to use has been reached, essentially due to the variation in contrast between the sets of experimental data and the absence of any thorough theoretical study of this problem. It has been established by Schmid, Blachut, et al., that well defined photo points and targeted stations can be measured with a precision that is in the order of $1/10^{th}$ of the minimum resolvable element. For high contrast point sources, for example stellar plates, it is generally agreed that the pointing may be obtained with a precision approaching $1/20^{th}$ the diameter of the image. However, as pointed out by Charman, no simple relationship exists between resolution and the measuring error.

Gardiner's data and his criterion are based on determining the absolute accuracy of mapping from air photography, in which low contrast imagery and frequently ill-defined images are characteristic.

His values include an inherent identification error that is always present in general mapping, except when well defined points are being measured. Furthermore, this criterion is to be applied to the mapping mode, a continual sequence of single pointings, not multiple independent pointings.

For reference purposes, the various weighting criteria have been listed in Table 3-2, with an attempt to classify them according to image contrast.

From these tabulated data, it is possible to select a standard error that varies between $\pm 0.025/n$ to $\pm 0.34/n$. In order that a reasonable weighting criterion might be used in the calculations, a value given by Ghosh ($\pm 0.075/n$) was selected.

3.2.6 Conclusions

Measured photographic coordinates are subject to two kinds of errors—systematic and random. The systematic errors may be accounted for by applying the appropriate corrections

Table 3-2 — Standard Errors of Photo Measurements, as a Function of Resolution (n) or Image Diameter (d)

Point	Standard Error	Author
High contrast (steller image)	± 0.025/n millimeter (0.05 d)	Eichorn
Well defined photo point (target)	0.05/n millimeter (0.1 d)	Schmid Blachut
Average contrast natural photo points	0.04/n millimeter - 0.07/n (0.08 d - 0.14 d)	Ghosh Hallert
Low contrast photo points	0.06/n - 0.2/n 0.166/n	Lyon, et al. Charman
Average photo detail (mapping)	0.34/n	Gardiner

for instrumental calibration, film shrinkage, camera calibration, refraction, and aberration. However, owing to the imperfect evaluation of these systematic errors, residual effects remain after their application. These are presumed to be accidental in nature.

The mensuration error is random and functionally related to resolution. It is therefore expedient to define a data extraction error that is random in nature and a combination of the effects of resolution, residual image motion, and residual mensuration errors.

According to the preceding sections, the systematic errors may be eliminated to yield residual accidental errors of the magnitudes shown in Table 3-3. To this total residual error of ± 2.7 microns, the residual extraction error, σ_e, must be applied to yield the final expected precision in the photographic coordinates. According to the system specifications that this should be no greater than ± 4 microns, the magnitude of the error, σ_e, cannot attain a value greater than ± 2.9 microns. This value, σ_e, is due to the image alone and is essentially a pointing and identification error. The question that must now be answered is whether this is a value that might reasonably be expected.

The tolerance can be met if one can apply a weighting function that is proportional to 0.09/n millimeter, since the minimum resolution of the camera system is in the order of 30 lines per millimeter.

When multiple readings of each image coordinate are made, the precision of the measurements increases as the square root of the number of pointings. In order to achieve a ± 4-micron tolerance, a minimum of three pointings on each image point is necessary. This is in accordance with the standard operating procedures when making comparator measurements.

It is therefore concluded that the ± 4-micron reduced photo coordinate tolerance can be met, provided that careful mensuration and reduction procedures be used, and that all equipment be associated with valid calibration parameters. However, in the numerical studies described in Section 3.4, it has been elected to use a value that is considerably worse than this 4-micron value, in order that our results should not be too optimistic.

Table 3-3 — Expected Residual Errors After Applying Systematic Corrections

	Residual Error	Magnitude, microns
σ_1	Film distortion	± 1.5
σ_2	Refraction	± 0.6
σ_3	Camera calibration	± 1.5
σ_4	Aberration	± 0.0
σ_6	Comparator calibration	± 0.5
—	Camera mechanisms	± 1.6
	Total residual error (RMS)	± 2.7

3.3 THEORETICAL PHOTOGRAMMETRIC ANALYSIS

3.3.1 Introduction

The objective of this section is to devise an appropriate mathematical model by means of which the photogrammetric aspects of the GOPSS program might be examined. In order that this examination might be efficient, it has been devised to incorporate auxiliary data and to propagate input errors through the computations into the output data. This error propagation is statistically sound, and enables one to perform a systems analysis using covariance methods rather than the laborious Monte Carlo techniques.

The selected error model will consider up to nine consecutive overlapping photographs, although in practice it is doubtful if nine consecutive exposures can be obtained. These nine photographs can be subject to orbital constraints and those imposed by auxiliary data. As a consequence of the limited extent of the orbital arc, a simple Keplerian model is assumed, which corresponds to the osculating ellipse at the midexposure time. It is pointed out that such a simple orbital model will not be used in the final data reduction scheme, but will include an extensive parameterization of the perturbing forces.

The theory presented here is sufficiently general and extensive to perform an analysis of the photogrammetric portion of the GOPSS. However, if long arc reductions are performed, as will be the case in the final data reduction scheme, there is no serious problem in modifying the model that is presented here. The basic theory and concepts remain the same, but some laborious algebraic evaluations will be required.

3.3.1.1 Notation and Definitions

With reference to Figure 3-2, the following notation and definitions will be used in the subsequent development:

- a Semimajor axis of the elliptic orbit
- e Eccentricity of this ellipse
- I Inclination of the orbit, angle YNP
- Ω Longitude of ascending node, angle XSN
- ω Argument of perigee, angle NSA
- f True anomaly, angle ASP
- T Orbital period, the time elapsing between successive passages through the pericenter
- τ Epoch, the time at which the body passes through the pericenter
- t The time at which the body is at some point P
- μ Universal gravitational constant
- η Mean motion of body: $\eta = \mu^{1/2} a^{-3/2}$ rad/sec
- M Mean anomaly: $M = \eta (t - \tau)$
- E Eccentric anomaly, defined by $M = E - e \sin E$
- Φ Celestial longitude of body, angle XZP
- θ Celestial latitude of body, angle CSP

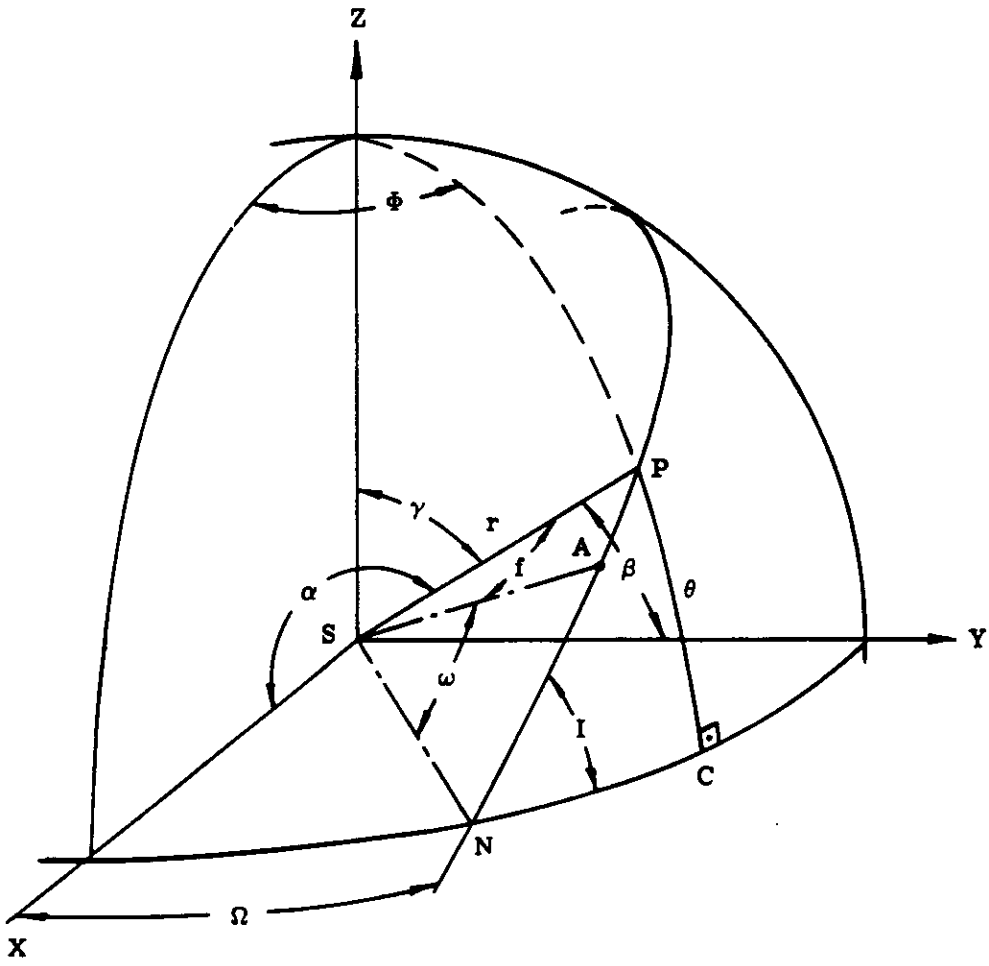

Fig. 3-2 — Orbital elements

3.3.1.2 Rectangular Coordinates (XYZ) of Body

The coordinates of P with respect to the inertial system are given by

$$\begin{bmatrix} X_o \\ Y_o \\ Z_o \end{bmatrix} = \begin{bmatrix} A_x & B_x \\ A_y & B_y \\ A_z & B_z \end{bmatrix} \begin{bmatrix} \cos(E) - e \\ \sin E \end{bmatrix} \tag{3.1}$$

in which the matrix

$$\begin{bmatrix} A_x & B_x \\ A_y & B_y \\ A_z & B_z \end{bmatrix}$$

is given by

$$\begin{bmatrix} A_x & B_x \\ A_y & B_y \\ A_z & B_z \end{bmatrix} = a \begin{bmatrix} \cos\Omega & -\cos I \sin\Omega \\ \sin\Omega & \cos I \cos\Omega \\ 0 & \sin I \end{bmatrix} \begin{bmatrix} \cos\omega & -\sin\omega \\ \sin\omega & \cos\omega \end{bmatrix} \begin{bmatrix} 1 & 0 \\ 0 & (1-e^2)^{1/2} \end{bmatrix} \tag{3.2}$$

The positional coordinates given by Equation 3.2 are in an inertial system with reference to which the orbital elements are given. In order that they may be referred to some other coordinate system, transformations will be necessary. These transformations are specified in Section 3.5.4.

3.3.2 Camera Orientation

Stellar cameras, used in conjunction with the frame camera yield approximate values of the camera roll, pitch, and yaw. At the times of these exposures, the local horizon is equivalent to the tangent plane at the nadir point, which is defined as the point at which the position vector, $\bar{r}$, to the air station intersects the reference ellipsoid. The longitude, Φ_o, and geocentric latitude, λ_o, of the nadir are determined from

$$\begin{bmatrix} X_o \\ Y_o \\ Z_o \end{bmatrix} = r \begin{bmatrix} \cos\Phi_o \cdot \cos\lambda_o \\ \cos\Phi_o \cdot \sin\lambda_o \\ \sin\Phi_o \end{bmatrix} \tag{3.3}$$

according to

$$\lambda_o = \cos^{-1}\left[(X_o)(X_o^2 + Y_o^2)^{-1/2}\right], \text{ for } X_o \geq Y_o \tag{3.4}$$

or

$$\lambda_o = \sin^{-1}\left[(Y_o)(X_o^2 + Y_o^2)^{-1/2}\right], \text{ for } X_o \leq Y_o \tag{3.5}$$

and

$$\Phi_O = \tan^{-1}\left[(Z_O)(X_O^2 + Y_O^2)^{-1/2}\right] \tag{3.6}$$

The orientation matrix rotating the ground coordinates into the photographic system may be expressed as:

$$R_j = \begin{bmatrix} \cos\kappa & \sin\kappa & 0 \\ -\sin\kappa & \cos\kappa & 0 \\ 0 & 0 & 1 \end{bmatrix} \begin{bmatrix} \cos\varphi & 0 & -\sin\varphi \\ 0 & 1 & 0 \\ \sin\varphi & 0 & \cos\varphi \end{bmatrix} \begin{bmatrix} 1 & 0 & 0 \\ 0 & \cos\omega_j & \sin\omega_j \\ 0 & -\sin\omega_j & \cos\omega_j \end{bmatrix} \tag{3.7}$$

The orientation between the local coordinate system and the geocentric terrestrial system is determined as:

$$O_j = \begin{bmatrix} \cos A0 & -\sin A_O & 0 \\ \sin A_O & \cos A_O & 0 \\ 0 & 0 & 1 \end{bmatrix} \begin{bmatrix} \sin\Phi_O & 0 & \cos\Phi_O \\ 0 & 1 & 0 \\ -\cos\Phi_O & 0 & \sin\Phi_O \end{bmatrix} \begin{bmatrix} -\cos\lambda_O & -\sin\lambda_O & 0 \\ \sin\lambda_O & -\cos\lambda_O & 0 \\ 0 & 0 & 1 \end{bmatrix} \tag{3.8}$$

Thus, the relationship between the photo-coordinates and the ground coordinates may be written as:

$$\begin{bmatrix} x_i - x_O \\ y_i - y_O \\ -f \end{bmatrix}_j = k\,(\kappa_j)(\varphi_j)(\omega_j)(A_O)(\Phi_O)(\lambda_O) \begin{bmatrix} X_i - X_O \\ Y_i - Y_O \\ Z_i - Z_O \end{bmatrix}_j \tag{3.9}$$

where k is an undetermined scalar. The values of all terms in Equation 3.9 pertain to a discrete time. For any specific time, t_o, the corresponding terms may be evaluated and held constant in this manner. The dynamic local system may be transformed into a static one with reference to which subsequent computations may be performed for any time, t_i, provided that appropriate variations of $\vec{X}_O$, due to orbital motion of ω_j, ϕ_j, and κ_j (due to capsule tumbling), and of $\vec{X}_i$, due to the earth's rotation, are applied.

This is accomplished through computing in the sidereal system. Denoting the orientation matrix $R_j\ O_j$ as M_j, Equation 3.9 may be rewritten as $\vec{x}_i = M_j\vec{X}_i$ from which the projective relationship

$$x_i = x_O - f\left[\frac{m_{11}(X_i - X_O) + m_{12}(Y_i - Y_O) + m_{13}(Z_i - Z_O)}{m_{31}(X_i - X_O) + m_{32}(Y_i - Y_O) + m_{33}(Z_i - Z_O)}\right] \tag{3.10}$$

and

$$y_i = y_O - f\left[\frac{m_{21}(X_i - X_O) + m_{22}(Y_i - Y_O) + m_{23}(Z_i - Z_O)}{m_{31}(X_i - X_O) + m_{32}(Y_i - Y_O) + m_{33}(Z_i - Z_O)}\right] \tag{3.11}$$

are obtained.

In these expressions, f is the camera focal length, m_{jk} is an element of the orientation matrix M_j, X_O, Y_O, Z_O are the coordinates of the exposure station in the XYZ system, and X_i, Y_i, and Z_i, are the coordinates of the ground point corresponding to the image point x_i, y_i, - f.

These two equations are generalized for convenience into the form

$$F_{ki} = G_{ki} + f\left[\frac{m_{k1}(X_i - X_O) + m_{k2}(Y_i - Y_O) + m_{k3}(Z_i - Z_O)}{m_{31}(X_i - X_O) + m_{32}(Y_i - Y_O) + m_{33}(Z_i - Z_O)}\right] \tag{3.12}$$

where $k = 1, 2$

$G_{1i} = x_i - x_O$

$G_{2i} = y_i - y_O$

These two equations may be expressed in terms of the constituent variables ω_j, ϕ_j, κ_j, $A_O, \ldots Z_O$. It is noted, however, that some of these are functionally related to the orbital parameters and to each other. The constrained solution must utilize independent parameters, as outlined in the subsequent section.

3.3.3 Constrained Solution

The functions given by Equation 3.12 express the relationship between a series of data consisting of observed variables and known and unknown various parameters. Those which are known are derived from observational data and are subject to the errors in these fundamental data.

On substituting the various parameters and data into Equation 3.12 the value of F_{ki} will be zero if, and only if, all entries are exact. The problem is to determine the most probable values for all parameters and variables. This is accomplished through a constrained least squares solution.

3.3.3.1 Least Squares Solution

Equation 3.12 is considered to be a function of the observed variables x_i and y_i, and a function of the parameters x_O, y_O, f, ω_j, ϕ_j, κ_j, Ω, ω, I, e, η, τ, Y_i, X_i, and Z_i.

Consequently, rewrite Equation 3.12 as

$$F_{ki} = f_k(x_i, y_i; x_O, y_O, f; \omega_j, \varphi_j, \kappa_j, \Omega, \omega, I, e, \eta, \tau; X_i, Y_i, Z_i) \tag{3.13}$$

Assuming that approximate values of these parameters are available, designated by a superscript o, an approximate value of Equation 3.13 is obtained as

$$F^o_{ki} = f_k(x^o_i, y^o_i, \ldots X^o_i, Y^o_i, Z^o_i) \tag{3.14}$$

The true values of these items is obtained by applying a correction to these approximate values.

The reduced condition equation may be expressed in the form

$$A_X V_X + B_1 \Delta_1 + B_2 \Delta_2 + E_X = 0 \tag{3.15}$$

where V_x = vector of unknown residuals
Δ_1 = vector of unknown parameter corrections
Δ_2 = vector of unknown parameter corrections
E_x = vector of random variables

and

$$A_x = \frac{\partial\ (F_1,\ F_2)\ ij}{\partial\ (\text{observed variables})} = \frac{\partial\ (F_1,\ F_2)\ ij}{\partial\ (x_i,\ y_i)\ j} \tag{3.16}$$

$$B_1 = \frac{\partial\ (F_1,\ F_2)\ ij}{\partial\ (\text{unknown parameters})} = \frac{\partial\ (F_1,\ F_2)\ ij}{\partial\ (\text{all or none of } x_o, \ldots \tau)} \tag{3.17}$$

$$B_2 = \frac{\partial\ (F_1,\ F_2)\ ij}{\partial\ (\text{parameters to be constrained})} = \frac{\partial\ (F_1,\ F_2)\ ij}{\partial\ (\text{remaining parameters})} \tag{3.18}$$

assuming that a statistical estimate of, for example, q parameters are known, and that we wish to constrain the adjustment to fit these estimates, designate the statistical estimates of the q parameters $\bar{\beta}$ by

$$\bar{\beta}^o = \begin{bmatrix} \beta_1^o \\ \beta_2^o \\ \vdots \\ \beta_q^o \end{bmatrix} \tag{3.19}$$

having an associated covariance matrix σ_β

$$\sigma_\beta = \begin{bmatrix} \sigma^2_{\beta_1} & \sigma_{\beta_1\beta_2} & \cdots & \sigma_{\beta_1\beta_2} \\ \sigma_{\beta_2\beta_1} & \sigma^2_{\beta_2} & \cdots & \sigma_{\beta_2\beta_2} \\ \cdot & \cdot & & \cdot \\ \cdot & \cdot & & \cdot \\ \cdot & \cdot & & \cdot \\ \sigma_{\beta q\beta_1} & \sigma_{\beta q\beta_2} & \cdots & \sigma^2_{\beta q} \end{bmatrix} \tag{3.20}$$

New linear equations may be formed and solved with Equation 3.15, according to

$$\bar{\beta}^o + \bar{V}^o{}_\beta = \bar{\beta}^{oo} + \bar{\Delta}_2 \tag{3.21}$$

where $\bar{\beta}^{oo}$ = a current corrected value of $\bar{\beta}^o$
$\bar{V}^o_\beta$ = an unknown residual vector

This equation is reformed as

$$\bar{\bar{V}}_\beta - \bar{\Delta}_2 + \bar{\bar{G}} = 0 \tag{3.22}$$

where $\bar{\bar{G}} = \bar{\bar{\beta}}^o - \bar{\bar{\beta}}^{oo}$

Whence Equation 3.15 may be written as

$$A\bar{\bar{V}} + B\bar{\Delta} + E = 0 \tag{3.23}$$

where

$$\bar{\bar{V}} = \begin{bmatrix} V_x \\ \hline V_\beta \end{bmatrix} \tag{3.24}$$

$$\bar{\Delta} = \begin{bmatrix} \Delta_2 \\ \hline \Delta_1 \end{bmatrix} \tag{3.25}$$

$$E = \begin{bmatrix} E_x \\ \hline G \end{bmatrix} \tag{3.26}$$

$$A = \left[\begin{array}{c|c} A_x & 0 \\ \hline 0 & I_{qq} \end{array}\right] \tag{3.27}$$

and

$$B = \left[\begin{array}{c|c} B_2 & B_1 \\ \hline -I_{qq} & 0 \end{array}\right] \tag{3.28}$$

The conditioned solution of Equation 3.23 for V and Δ which minimizes

$$S = V^T \sigma^{-1} V \tag{3.29}$$

is required, in which

$$\sigma = \left[\begin{array}{c|c} \sigma_x & 0 \\ \hline 0 & \sigma_\beta \end{array}\right] \tag{3.30}$$

where σ_x = the covariance matrix of the observed variables

The required solution is obtained from

$$S = V^T \sigma^{-1} V - 2\lambda^T (AV + B\Delta + E) \tag{3.31}$$

in which λ is a vector of Lagrangian multipliers, by setting $dS/dV = 0$ and $dS/d\Delta = 0$, to yield

$$V = \sigma A^T \lambda \tag{3.32}$$

and

$$-2B^T\lambda = 0 \tag{3.33}$$

which are combined with Equation 3.23 to yield

$$\lambda = -(A\sigma A^T)^{-1}\,(B\Delta + E) \tag{3.34}$$

and

$$\Delta = -[B^T(A\sigma A^T)^{-1}\,B]^{-1}\,B^T(A\sigma A^T)^{-1}\,E \tag{3.35}$$

This equation is evaluated by partitioning, the partitions being given by the following identities:

$$A\sigma A^T = \left[\begin{array}{c|c} A_X\,\sigma_X\,A_X^T & 0 \\ \hline 0 & \sigma_\beta \end{array}\right] \tag{3.36}$$

$$(A\sigma A^T)^{-1} = \left[\begin{array}{c|c} (A_X\,\sigma_X\,A_X^T)^{-1} & 0 \\ \hline 0 & \sigma_\beta^{-1} \end{array}\right] \tag{3.37}$$

$$B^T(A\sigma A^T)^{-1}B = \left[\begin{array}{c|c} B_2^T\,W_X\,B_2 + \sigma_\beta^{-1} & B_2^T\,W_X\,B_1 \\ \hline B_1^T\,W_X\,B_2 & B_1^T\,W_X\,B_1 \end{array}\right] \tag{3.38}$$

and

$$B^T(A\sigma A^T)^{-1}E = \left[\begin{array}{c} B_2^T\,W_X\,E_X - \sigma_\beta^{-1}\,G \\ \hline B_1^T\,W_X\,E_X \end{array}\right] \tag{3.39}$$

where

$$W_X = (A_X\,\sigma_X\,A_X^T)^{-1}$$

3.3.3.2 Application and Extension

In order to clarify the previous treatment, a descriptive example of applying these formulas to our problem is given.

For each photograph, j, one obtains for each point, i,

$$A_i = \begin{bmatrix} \partial F_1/\partial x_i & \partial F_1/\partial y_i \\ \partial F_2/\partial x_i & \partial F_2/\partial y_i \end{bmatrix} \tag{3.40}$$

To each ground point that is known, a variance-covariance matrix may be assigned. For unknown ground points, coordinate values are estimated, together with large variances for these estimates.

Orbital parameters are estimated from the given ephemeris, and values of rotations ω_j, φ_j, and κ_j are determined from stellar cameras. Values for x_o, y_o, and f are obtained from calibration data.

The end result is that all parameters are to be constrained, dictating that $B_1 = 0$.

Consequently,

$$B_2 = \begin{bmatrix} \partial F_1/\partial x_o & \partial F_2/\partial x_o \\ \partial F_1/\partial y_o & \partial F_2/\partial y_o \\ \partial F_1/\partial f & \partial F_2/\partial f \\ \partial F_1/\partial \omega_j & \partial F_2/\partial \omega_j \\ \partial F_1/\partial \varphi_j & \partial F_2/\partial \varphi_j \\ \partial F_1/\partial \kappa_j & \partial F_2/\partial \kappa_j \\ \partial F_1/\partial \Omega & \partial F_2/\partial \Omega \\ \partial F_1/\partial \omega & \partial F_2/\partial \omega \\ \partial F_1/\partial I & \partial F_2/\partial I \\ \partial F_1/\partial e & \partial F_2/\partial e \\ \partial F_1/\partial n & \partial F_2/\partial n \\ \partial F_1/\partial \tau & \partial F_2/\partial \tau \\ \partial F_1/\partial X_i & \partial F_2/\partial X_i \\ \partial F_1/\partial Y_i & \partial F_2/\partial Y_i \\ \partial F_1/\partial Z_i & \partial F_2/\partial Z_i \end{bmatrix}^T \qquad (3.41)$$

The various covariance matrices are:

σ_{xi} = the measured frame photograph images
σ_{Xi} = the ground coordinates
σ_c = the frame camera constants
σ_α = the camera tilt angles

and

σ_o for the orbital elements

The two condition equations for each ground point image are:

$$A_i V_i + B_i \Delta_i + E_i = 0$$

where

$$A_i = \left[\begin{array}{c|c} A_{xi} & 0 \\ (2 \times 2) & (2 \times 15) \\ \hline 0 & I \\ (15 \times 2) & (15 \times 15) \end{array}\right] \tag{3.42}$$

Now,

$$V_i = (V_{xi}, V_{yi}, \ldots, V_\tau, V_{Xi}, V_{Yi}, V_{Zi})^T \tag{3.43}$$

$$B_i = \left[\begin{array}{c} B_2 \\ (2 \times 15) \\ \hline -I \\ (15 \times 15) \end{array}\right] \tag{3.44}$$

$$\Delta_i = (\delta_{xo}, \delta_{yo}, \delta f, \ldots \delta Z_1)^T \tag{3.45}$$

and

$$E_i = (E_{xi}, E_{yi}, \ldots E_{Zi})^T \tag{3.46}$$

The associated weight matrix is

$$\sigma^{-1} = \text{Diagonal } (\sigma_{xi}, \sigma_c, \sigma_o, \sigma_\alpha, \sigma_{Xi})^{-1} \tag{3.47}$$

On forming the normal equations, rewritten as

$N\Delta = -C$, one obtains

$$N = \sum B_i^T (A_i \sigma A_i^T)^{-1} B_i \tag{3.48}$$

and

$$C = \sum B_i^T (A_i \sigma A_i^T)^{-1} E_i \tag{3.49}$$

from which the solution for Δ is obtained as

$$\Delta = -N^{-1} C \tag{3.50}$$

If one reconsiders the normal equations, it is found that they consist of two parts—one pertaining to the orbital and camera parameter data, and one relating to the ground point data.

Following the notation and derivation of Brown, the observation Equation 3.23 may be rewritten in the form

$$AV + \dot{B}\dot{\delta} + \bar{B}\bar{\delta} + E = 0 \tag{3.51}$$

where $\dot{B}$, $\dot{\delta}$ refer to orbital and camera parameters
$\bar{B}$, $\bar{\delta}$ refer to the ground point data

Equation 3.37 may be rewritten in the form

$$W = (A\sigma A^T)^{-1} = \begin{bmatrix} W_X & 0 & 0 \\ 0 & \dot{W} & 0 \\ 0 & 0 & \bar{W} \end{bmatrix} = \begin{bmatrix} (A_X\sigma_X A_X^T)^{-1} & 0 & 0 \\ 0 & (\dot{\sigma})^{-1} & 0 \\ 0 & 0 & (\bar{\sigma})^{-1} \end{bmatrix} \tag{3.52}$$

where $\dot{\sigma}$ = diagonal $(\sigma_C, \sigma_O, \sigma_\alpha)$
$\bar{\sigma}$ = diagonal $(\sigma_{X_1}, \sigma_{X_2}, \ldots \sigma_{Xi})$

Equation 3.5 is equivalent to

$$W = \begin{bmatrix} A & 0 & 0 \\ 0 & I & 0 \\ 0 & 0 & I \end{bmatrix} \begin{bmatrix} \sigma_X^{-1} & 0 & 0 \\ 0 & \dot{W} & 0 \\ 0 & 0 & \bar{W} \end{bmatrix} \begin{bmatrix} A^T & 0 & 0 \\ 0 & I & 0 \\ 0 & 0 & I \end{bmatrix}$$

Similarly Equation 3.38 may be rewitten as

$$N = B^T W B = \begin{bmatrix} \dot{B}^T & -I & 0 \\ \bar{B}^T & 0 & -I \end{bmatrix} \begin{bmatrix} W_X & 0 & 0 \\ 0 & \dot{W} & 0 \\ 0 & 0 & \bar{W} \end{bmatrix} \begin{bmatrix} \dot{B} & \ddot{B} \\ -I & 0 \\ 0 & I \end{bmatrix}$$

$$= \begin{bmatrix} (\ddot{B}^T W_X \dot{B} + \dot{W}) & (\dot{B}^T W_X \bar{B}) \\ (\bar{B}^T W_X \dot{B}) & (\bar{B}^T W_X \bar{B} - \bar{W}) \end{bmatrix} = \left[\begin{array}{c|c} \dot{N} + \dot{W} & \bar{N} \\ \hline \bar{N}^T & \bar{N} + \bar{W} \end{array}\right] \tag{3.53}$$

Similarly, Equation 3.39 becomes

$$C = B^T W E = \begin{bmatrix} \dot{B}^T & -I & 0 \\ \bar{B}^T & 0 & -I \end{bmatrix} \begin{bmatrix} W_X & 0 & 0 \\ 0 & \dot{W} & 0 \\ 0 & 0 & \bar{W} \end{bmatrix} \begin{bmatrix} E_X \\ \dot{E} \\ \bar{E} \end{bmatrix}$$

or

$$C = \begin{bmatrix} (\dot{B}^T W_X E_X - \dot{W}\dot{E}) \\ (\bar{B}^T W_X E_X - \bar{W}\bar{E}) \end{bmatrix} = \begin{bmatrix} \dot{C} - \dot{W}\dot{E} \\ \bar{C} - \bar{W}\bar{E} \end{bmatrix} \tag{3.54}$$

The normal equations, $N\Delta = -C$ are thus:

$$\begin{bmatrix} \dot{N} + \dot{W} & \bar{N} \\ \bar{N}^T & \bar{\bar{N}} + \bar{\bar{W}} \end{bmatrix} \begin{bmatrix} \dot{\delta} \\ \bar{\delta} \end{bmatrix} = - \begin{bmatrix} \dot{C} - \dot{W}\dot{E} \\ \bar{C} - \bar{W}\bar{E} \end{bmatrix} \tag{3.55}$$

which for computational purposes is partitioned

$$\left[\begin{array}{c|c|c|c|c} \dot{N} + \dot{W} & \bar{N}_1 & \bar{N}_2 & \cdots & \bar{N}_i \\ \hline \bar{N}_1^T & \bar{\bar{N}}_1 + \bar{\bar{W}}_1 & & & \\ \hline \bar{N}_2^T & & \bar{\bar{N}}_2 + \bar{\bar{W}}_2 & & \\ \hline \cdots & \cdots & \cdots & \ddots & \\ \hline \bar{N}_i^T & & & & \bar{\bar{N}}_i + \bar{\bar{W}}_i \end{array}\right] \left[\begin{array}{c} \dot{\delta} \\ \hline \bar{\delta}_1 \\ \hline \bar{\delta}_2 \\ \hline \vdots \\ \hline \bar{\delta}_i \end{array}\right] = \left[\begin{array}{c} \dot{C} - \dot{W}\dot{E} \\ \hline \bar{C}_1 - \bar{W}_1\bar{E}_1 \\ \hline \bar{C}_2 - \bar{W}_2\bar{E}_2 \\ \hline \vdots \\ \hline \bar{C}_i - \bar{W}_i\bar{E}_i \end{array}\right] \tag{3.56}$$

Let $N^{-1} = M$, according to

$$\begin{bmatrix} \dot{N} + \dot{W} & \bar{N} \\ \bar{N}^T & \bar{\bar{N}} + \bar{\bar{W}} \end{bmatrix}^{-1} = \begin{bmatrix} \dot{M} & \bar{M} \\ \bar{M}^T & \bar{\bar{M}} \end{bmatrix} \tag{3.57}$$

Since $NM = I$, then, noting that $M = -\dot{M}\, N\, (\bar{\bar{N}} + \bar{\bar{W}})^{-1}$, one obtains

$$\dot{M} = [(\dot{N} + \dot{W}) - \bar{N}\, (\bar{\bar{N}} + \bar{\bar{W}})^{-1}\, \bar{N}^T]^{-1} \tag{3.58}$$

and

$$\bar{\bar{M}} = [(\bar{\bar{N}} + \bar{\bar{W}})^{-1} + (\bar{\bar{N}} + \bar{\bar{W}})^{-1}\, \bar{N}^T\, \dot{M}\, \bar{N}\, (\bar{\bar{N}} + \bar{\bar{W}})^{-1}] \tag{3.59}$$

In order to determine the corrections $\dot{\delta}$ and $\bar{\delta}$, it is not necessary to solve Equation 3.59. Consider

$$\begin{bmatrix} -\dot{\delta} \\ -\bar{\delta} \end{bmatrix} = \begin{bmatrix} \dot{M} & \bar{M} \\ \bar{M}^T & \bar{\bar{M}} \end{bmatrix} \begin{bmatrix} \dot{C} - \dot{W}\dot{E} \\ \bar{C} - \bar{W}\bar{E} \end{bmatrix} \tag{3.60}$$

from which

$$-\dot{\delta} = [\dot{M}\, (\dot{C} - \dot{W}\dot{E}) + \bar{M}\, (\bar{C} - \bar{W}\bar{E})]$$

and

$$-\bar{\delta} = [\bar{M}^T\, (\dot{C} - \dot{W}\dot{E}) + \bar{\bar{M}}\, (\bar{C} - \bar{W}\bar{E})]$$

Putting

$$Q = (\bar{N} + \bar{W})^{-1} \bar{N}^T \tag{3.61}$$

then

$$\bar{M} = -\dot{M} Q$$

and

$$-\dot{\delta} = \dot{M} [\dot{C} - \dot{W}\dot{E} - Q (\bar{C} - \bar{W}\bar{E})] \tag{3.62}$$

Since

$$-[\bar{N}^T\dot{\delta} + (\bar{N} + \bar{W}) \bar{\delta}] = \bar{C} - \bar{W}\bar{E}$$

then

$$-(\bar{\delta}) = (\bar{N} + \bar{W})^{-1} (\bar{C} - \bar{W}\bar{E}) - Q\dot{\delta} \tag{3.63}$$

It is to be noted that $\bar{N} + \bar{W}$ consists of i diagonally arranged 3×3 matrices, and consequently presents no difficulties.

3.3.3.3 Error Propagation

In the final iteration

$$V_X = E_X - \dot{B}\dot{\delta} - \bar{B}\bar{\delta}$$

$$\dot{V} = \dot{E} - \dot{\delta}$$

and

$$\bar{V} = \bar{E} - \bar{\delta}$$

with $\dot{\delta}$ and $\bar{\delta}$ tending to zero; i.e.,

$$V_X \sim E_X$$
$$\dot{V} \sim \dot{E}$$
$$\bar{V} \sim \bar{E}$$

Now

$$S = V_X^T W_X V + \dot{V}^T \dot{W} \dot{V} + \bar{V}^T \bar{W} \bar{V} \tag{3.64}$$

which when divided by the degrees of freedom gives the unit variance σ_0.

$\dot{M}$ is the covariance matrix of the adjusted camera and orbital parameters, and $\ddot{M}$ is that of the ground points. It is to be noted that $\bar{M} = (\bar{N} + \bar{W})^{-1} + Q\dot{M}Q^T$, so that the covariance matrix of any point g is

$$\bar{M}_g = (\bar{N}_g + \bar{W}_g)^{-1} + Q_g \dot{M}_g Q_g^T \tag{3.65}$$

3.3.3.4 Auxiliary Data

Suppose auxiliary data, independent of the camera system, has been collected, which may be expressed as a function of the various parameters. As an example, a radar altimeter will indicate the value of nadiral distance, which may be expressed in terms of the orbital parameters.

Denote the vector of auxiliary data as Λ, which may be written as

$$\Lambda_h = F_h (\Omega, \omega, \ldots \tau) \tag{3.66}$$

then, as before

$$\Lambda_h = \Lambda_h^\circ + V_{\Lambda h} \tag{3.67}$$

The various parameters $\alpha_p = (\Omega, \omega, \ldots \tau)$ may be expressed as

$$\alpha_p = \alpha_p^\circ + \delta\alpha_p \tag{3.68}$$

so that

$$V_{\Lambda h} - \Lambda_{h1}\, \delta\alpha_1 \ldots \Lambda_{hp}\, \delta\alpha_p = E_{\Lambda h} \tag{3.69}$$

where

$$E_{\Lambda h} = F_h (\alpha_1^\circ, \alpha_2^\circ, \ldots \alpha_p^\circ) \tag{3.70}$$

Consequently, an additional series of equations may be written as follows:

$$V_\Lambda - \Lambda\dot{\delta} = E_\Delta \tag{3.71}$$

which, together with the covariance matrix of Λ, may be incorporated into the previous solution, according to

$$\begin{bmatrix} V_x \\ V_\Lambda \\ \\ \dot{V} \\ \bar{V} \end{bmatrix} + \begin{bmatrix} \dot{B} & \bar{B} \\ -\Lambda & 0 \\ \\ -I & 0 \\ 0 & I \end{bmatrix} \begin{bmatrix} \dot{\delta} \\ \bar{\delta} \end{bmatrix} = \begin{bmatrix} E_x \\ E_\Delta \\ \\ \dot{E} \\ \bar{E} \end{bmatrix} \tag{3.72}$$

to yield

$$N = \left[\begin{array}{c|c} (\dot{B}^T W_x \dot{B} + \dot{W} + \Lambda^T W_\Lambda \Lambda) & \dot{B}^T \tilde{W} \tilde{B} \\ \hline \tilde{B}^T W_x \dot{B} & (\tilde{B}^T W_x \tilde{B} + \tilde{W}) \end{array}\right] = \left[\begin{array}{c|c} \dot{N} + \dot{W} + \Lambda^T W_\Lambda \Lambda^T & \bar{N} \\ \hline \bar{N}^T & \tilde{N} + \tilde{W} \end{array}\right] \quad (3.73)$$

and

$$C = \begin{bmatrix} \dot{C} - \dot{W}\dot{E} - \Lambda W_\Lambda E_\Lambda \\ \\ \tilde{C} - \tilde{W}\tilde{E} \end{bmatrix} \quad (3.74)$$

Similarly, auxiliary data pertaining to ground point data, (X_i, Y_i, Z_i) might be used to exploit the relationship between auxiliary data and the various parameters.

3.3.4 Detailed Formulation

It is considered unnecessary to present the detailed expressions for individual elements of the various matrices and for the partial derivatives. This is due to the means by which these items will be obtained in a computational sequence, namely, by appropriate matrix manipulations. Furthermore, the final mathematical model will not be as simple as that used in this analysis. However, it is considered worthwhile to present the salient formulas, and the expressions from which the complete set of partial derivatives can be obtained.

The orientation matrix $M_j = R_j O_j$ is obtained from the multiplication of six matrices, according to Equations 3.7, 3.8, and 3.9. From Equation 3.12, the partial derivatives are obtained that are defined by Equations 3.16, 3.17, and 3.18 as

$$\left.\begin{array}{ll} \partial F_1/\partial x_i = 1 & \partial F_2/\partial x_i = 0 \\ \partial F_1/\partial y_i = 0 & \partial F_2/\partial y_i = 1 \\ \partial F_1/\partial x_o = -1 & \partial F_2/\partial x_o = 0 \\ \partial F_1/\partial y_o = 0 & \partial F_2/\partial y_o = -1 \\ \partial F_1/\partial f = U_i/W_i & \partial F_2/\partial f = V_i/W \end{array}\right\} \quad (3.75)$$

where

$$\begin{bmatrix} U_i \\ V_i \\ W_i \end{bmatrix} = M \begin{bmatrix} X_i - X_o \\ Y_i - Y_o \\ Z_i - Z_o \end{bmatrix} \quad (3.76)$$

Working in the siderial time system, so that the values of X_i, Y_i, and Z_i are replaced by the value values X_{is}, Y_{is}, and Z_{is} at time t_i according to

$$X_{is} = X_i \cos t_i - Y_i \sin t_i$$
$$Y_{is} = X_i \sin t_i + Y_i \cos t_i \qquad (3.77)$$
$$Z_{is} = Z_i$$

then,

$$\frac{F_1}{\partial X_{is}} = \frac{+f}{W}\left[m_{11} \cos t_i + m_{12} \sin t_i - \frac{U}{W}(m_{21} \cos t_i + m_{32} \sin t_i)\right] \qquad (3.78)$$

$$\frac{\partial F_1}{\partial Y_{is}} = \frac{+f}{W}\left[-m_{11} \sin t_i + m_{12} \cos t_i - \frac{U}{W}(-m_{31} \sin t_i + m_{32} \cos t_i)\right] \qquad (3.79)$$

$$\frac{\partial F_1}{\partial Z_{is}} = \frac{+f}{W}\left[m_{13} - \frac{U}{W} m_{23}\right] \qquad (3.80)$$

$$\frac{\partial F_2}{\partial X_{is}} = \frac{+f}{W}\left[+m_{21} \sin t_i + m_{22} \sin t_i - \frac{V}{W}(+m_{21} \cos t_i + m_{32} \sin t_i)\right] \qquad (3.81)$$

$$\frac{\partial F_2}{\partial Y_{is}} = \frac{+f}{W}\left[-m_{21} \sin t_i + m_{22} \cos t_i - \frac{V}{W}(-m_{31} \sin t_i + m_{32} \cos t_i)\right] \qquad (3.82)$$

$$\frac{\partial F_2}{\partial Z_{is}} = \frac{+f}{W}\left(m_{23} - \frac{V}{W} m_{33}\right) \qquad (3.83)$$

Recalling Equations 3.1 and 3.2, let us denote the component matrices according to

$$[\Omega I] = \begin{bmatrix} \cos \Omega & -\cos I \sin \Omega \\ \sin \Omega & \cos I \cos \Omega \\ 0 & \sin I \end{bmatrix} \qquad (3.84)$$

$$[\omega] = \begin{bmatrix} \cos \omega & -\sin \omega \\ \sin \omega & \cos \omega \end{bmatrix} \qquad (3.85)$$

$$[e] = \begin{bmatrix} 1 & 0 \\ 0 & (1-e^2)^{1/2} \end{bmatrix} \qquad (3.86)$$

$$[E_e] = \begin{bmatrix} \cos E & -e \\ \sin E & \end{bmatrix} \qquad (3.87)$$

Then the partial derivatives of the exposure stations with respect to the orbital elements are obtained from

$$\begin{bmatrix} \partial X^\circ/\partial \Omega \\ \partial Y^\circ/\partial \Omega \\ \partial Z^\circ/\partial \Omega \end{bmatrix} = a\,[\partial(\Omega I)/\partial \Omega]\,(\omega)(e)(E_e) \tag{3.88}$$

$$\begin{bmatrix} \partial X^\circ/\partial I \\ \partial Y^\circ/\partial I \\ \partial Z^\circ/\partial I \end{bmatrix} = a\,[\partial(\Omega I)/\partial I]\,(\omega)(e)(E_e) \tag{3.89}$$

$$\begin{bmatrix} \partial X^\circ/\partial \omega \\ \partial Y^\circ/\partial \omega \\ \partial Z^\circ/\partial \omega \end{bmatrix} = a\,(\Omega I)\,[\partial(\omega)/\partial \omega]\,(e)(E_e) \tag{3.90}$$

$$\begin{bmatrix} \partial X^\circ/\partial e \\ \partial Y^\circ/\partial e \\ \partial Z^\circ/\partial e \end{bmatrix} = a\,(\Omega I)(\omega)\{[(e)/\partial e]\,(E_e) + (e)\,[\partial(E_e)/\partial e]\} \tag{3.91}$$

Since the orbital positions are concerned with the times of observation, t_i, and since the mean anomaly, M, is a function of t_i, the epoch, τ, will be used as an independent variable. The remaining partial derivatives for the orbital parameters are thus with respect to η and τ according to

$$\begin{bmatrix} \partial X^\circ/\partial \eta \\ \partial Y^\circ/\partial \eta \\ \partial Z^\circ/\partial \eta \end{bmatrix} = a(\Omega I)(\omega)(e)\,[\partial(E_e)/\partial e]\cdot(\tau_i - \tau)/(1 - e\cos E) - (X^\circ, Y^\circ, Z^\circ)^T \cdot 2\mu^{1/3}/3a\eta^{5/3} \tag{3.92}$$

and

$$\begin{bmatrix} \partial X^\circ/\partial \tau \\ \partial Y^\circ/\partial \tau \\ \partial Z^\circ/\partial \tau \end{bmatrix} = -\frac{\eta}{\tau_i - \tau} \begin{bmatrix} \partial X^\circ/\partial \eta \\ \partial Y^\circ/\partial \eta \\ \partial Z^\circ/\partial \eta \end{bmatrix} \tag{3.93}$$

In a similar fashion, the partial derivatives of the functions F_{ki}, Equation 3.12, with respect to the orientation angles ω_j, φ_j, and κ_j are obtained according to the general formula

$$\frac{\partial F_{ki}}{\partial \xi} = \frac{-f}{W_i}\left[(X_i - X_o)\left(\frac{\partial m_{ki}}{\partial \xi} - \Gamma_{ki}\frac{\partial m_{31}}{\partial \xi}\right) + (Y_i - Y_o)\left(\frac{\partial m_{k2}}{\partial \xi} - \Gamma_{ki}\frac{\partial m_{32}}{\partial \xi}\right) + (Z_i - Z_o)\left(\frac{\partial m_{k3}}{\partial \xi} - \Gamma_{ki}\frac{\partial m_{33}}{\partial \xi}\right)\right] \tag{3.94}$$

where

$$\Gamma_{ki} = \frac{m_{k_1}(X_i - X_o) + m_{k_2}(Y_i - Y_o) + m_{k_3}(Z_i - Z_o)}{m_{k31}(X_i - X_o) + m_{32}(Y_i - Y_o) + m_{33}(Z_i - Z_o)} \tag{3.95}$$

$k = 1, 2$

and ξ represents the specific orientation angle. The derivatives of the orientation matrix elements are determined from the products

$$[\partial(M)/\partial\omega_j] = (\kappa_j)(\varphi_j)[\partial(\omega_j)/\partial\omega_j](A_o)(\Phi_o)(\lambda_o) \tag{3.96}$$

$$[\partial(M)/\partial\varphi_j] = (\kappa_j)[\partial(\varphi_j)/\partial\varphi_j](\omega_j)(A_o)(\Phi_o)(\lambda_o) \tag{3.97}$$

and

$$[\partial(M)/\partial\kappa_j] = [\partial(\kappa_j)/\partial\kappa_j](\varphi_j)(\omega_j)(A_o)(\Phi_o)(\lambda_o) \tag{3.98}$$

The remaining partial derivatives are those of the matrix M with respect to the six orbital parameters, since the three factors A_o, Φ_o, and λ_o are functions of the camera positions, which are themselves functions of the orbital elements.

The simplest manner of obtaining the required derivatives is again by matrix differentiation according to

$$[\partial(M)/\partial\Omega] = (\kappa_j)(\varphi_j)(\omega_j)\left\{\begin{array}{l}[\partial(A_o)/\partial R_o](\partial R_o/\partial\Omega)(\Phi_o)(\lambda_o) \\ +(A_o)[\partial(\Phi_o)/\partial\Omega_o](\partial R_o/\partial\Omega)(\lambda_o) \\ +(A_o)(\Phi_o)[\partial(\lambda_o)/\partial R_o](\partial R_o/\partial\Omega)\end{array}\right\} \tag{3.99}$$

in which

$$R_o = (X_o, Y_o, Z_o)^T$$

with similar expressions for the remaining elements.

The final result of this procedure is to enable the partial derivatives of F_{ki} to be obtained with respect to the orbtial elements, designated ξ_o, according to

$$\begin{aligned}\frac{\partial F_{ki}}{\partial\xi_o} = \frac{+f}{W}\Bigg[&(X_i - X_o)\left(\frac{\partial m_{k1}}{\partial\xi_o} - \Gamma_{ki}\frac{\partial m_{31}}{\partial\xi_o}\right) + (Y_i - Y_o)\left(\frac{\partial m_{k2}}{\partial\xi_o} - \Gamma_{ki}\frac{\partial m_{32}}{\partial\xi_o}\right) \\ &+ (Z_i - Z_o)\left(\frac{\partial m_{k3}}{\partial\xi_o} - \Gamma_{ki}\frac{\partial m_{33}}{\partial\xi_o}\right) + (\Gamma_{ki}m_{31} - m_{ki})\frac{\partial X_o}{\partial\xi_o} \\ &+ (\Gamma_{ki}m_{32} - m_{k2})\frac{\partial Y_o}{\partial\xi_o} + (\Gamma_{ki}m_{33} - m_{k3})\frac{\partial Z_o}{\partial\xi_o}\Bigg]\end{aligned} \tag{3.100}$$

where Γ_{ki} has been defined previously.

All the terms necessary for the formation of the coefficient matrices have now been defined so that the computational scheme can now be initiated. An identical procedure is available for any type of supporting data.

3.3.5 Weighting Procedures

In order that the analytical solution of photogrammetric problems may be completely general, it is necessary that appropriate weighting factors be applied to the observed data. A basic tenet of error theory is that observed data that are subject only to random errors should be weighted proportionally to the inverse of their variances.

The only consideration of such a weighting procedure that has been revealed by a literature search is that proposed by Hallert. In his original treatment, a near vertical photograph of a signalized test area is measured. From these measurements, the weights of image coordinates are empirically determined from an examination of the residual errors. These weights are then applied to similarly located images on photographs which have been exposed under similar operational conditions.

A theoretically sound attempt is presently being made to develop a generalized weighting system that can be applied to all types of photography. At the moment, it is premature to state any final scheme. The basic development is to consider each of the individual factors that influence the accuracy with which data are photographically recorded and which influence the extraction and refinement of these data.

In the course of combining these individual errors, it was evident that the total effect of these factors on the photographic record was to limit the effectual resolution. That is to say, the weights of the recorded photo data are essentially a function of the resolution after processing.

The influence of measuring errors on the extraction of the data have been considered and it has been found that for accurate and well calibrated instruments, the compounding effects of comparator errors are very small. The same holds true for the residual errors in the refining processes (of which the application of comparator calibration data is one). This is evident if one considers the accuracy of the homogeneous, or refined coordinates, in terms of the covariance matrix

$$C(x,y) = \begin{bmatrix} \sigma_x^2 & \sigma_{xy} \\ \sigma_{yx} & \sigma_y^2 \end{bmatrix}$$

This homogeneous covariance matrix is derived from the covariance matrix of the extracted data and from the refining parameters. Thus, if the extracted data x', y' are transformed according to

$$x = f_1(\alpha_1, \alpha_2, \alpha_3, \ldots \alpha_n; x', y')$$

and

$$y = f_2(\alpha_1, \alpha_2, \alpha_3, \ldots \alpha_n; x', y')$$

then

$$C(x, y) = J(x, y)\begin{bmatrix} C(\alpha) & O \\ O & C(x', y') \end{bmatrix} J^T(x, y)$$

where $J(x, y)$ is the Jacobian of x, y with respect to the variables α, x', y', and $C(\alpha)$, $C(x', y')$ are the corresponding covariance matrices.

For well defined and well determined transformations of the extracted data, $C(\alpha)$ tends towards a null matrix, whence $C(x, y)$ tends towards $C(x', y')$.

The value $C(x', y')$ is a combination of the comparator measuring errors and the inherent data recording errors. Since the latter effectively outweigh the extraction errors, it is reasonable to assign variances to the refined photographic data that are directly dependent on the system resolution. This has been discussed in the previous section and will be the basis of the weighting functions applied in the following section.

3.4 PHOTOGRAMMETRIC COMPUTATIONS AND ANALYSIS

The computations and analyses presented in this section are directed toward demonstrating the accuracy of landmark and camera position determinations. The various computations have been enumerated previously, and each of these will be described in accordance with the following format.

First, a brief description of the computation and its objectives is given; this description includes a minimum of formulation. Second, the calculated data will be summarized. These condensed numerical data will then be used as the basis of the recommendations and conclusions concerning the photographic subsystem.

The first computations described are concerned with the accuracy that might be attained by a resection of the camera station from a single controlled photograph. The subsequent computations are concerned with multiple-photograph considerations, for which the basic program documentation has already been presented in the preceding section.

It must be emphasized that these computations form but a subset of a total data adjustment, and that in the final reduction program they form a subroutine for handling a specific type of data. This is a significant point that should not be overlooked in the detailed photogrammetric considerations which follow.

As a computational convenience, the metric system has been used throughout these numerical studies. This conflicts with the statement of work, and also with the fact that the system design requirements are expressed in feet. Wherever possible, the conclusions and references concerning system performance have been expressed in terms of feet.

Some special terminology has been used in this section. In order to clarify these terms, a glossary has been compiled as Table 3-4.

3.4.1 Operational Design

The first operational consideration necessary for all succeeding computations was that of determining the optimum overlap between consecutive photographs that would provide a solution with a sufficiently high geometric strength to meet the specified accuracy. The program designed to accomplish this was also able to substantiate some other considerations, the most important of which was the selection of the final weighting function applied to the measured photo-coordinates.

The second program was organized to determine whether the increased corner resolution obtained by using a smaller format was sufficient to offset the decrease in accuracy caused by the smaller base/height ratio which may have resulted from using a small format.

Table 3-4 — Glossary of Special Terms

Strip Triangulation. Successive overlapping photographs are analytically connected to form one consistent model of the photographed terrain

Bridge. A strip triangulation in which the consistent terrain model is adjusted to ground control imaged on the terminal photographs

Extension. A strip triangulation in which the consistent terrain model is adjusted to ground control imaged on the initial photograph

Functionally Constrained. The analytical expressions relating sets of data are combined into one analytical expression relating all dependent data sets. Thus, the projective equations relate ground coordinates, image coordinates, and orientations to air station positions; another expression relates air station positions to orbital elements; combining these expressions functionally constrains the photogrammetric solution to an orbit

Statistically Constrained. Same set of data in the least squares solution is permitted freedom to adjust within some limits determined by the assigned covariance matrix

Unconstrained Solution. An unweighted least squares solution which may, however, utilize a functional constraint

Positionally Constrained. Exposure station estimates are statistically constrained to some assigned covariance matrix

Orbitally Constrained. Orbital elements are statistically constrained to the assigned covariance matrix

3.4.1.1 Overlap Program

The basic objective of this program is to determine the optimum percentage overlap between consecutive exposures. This was accomplished by considering five sets of three consecutive photographs in which the percentage overlaps increase by increments of 5 percent from a minimum of 55 percent to a maximum of 75 percent. Computations were performed using two adjacent photographs and three photographs simultaneously. Nine ground control points were selected in the stereo model such that the optimum geometric strength was afforded in each case. In addition, six known points within the model area were suppressed and used as test points. The location of these control data are illustrated in Figure 3-3.

The numerical results obtained from these computations are summarized in Table 3-5, together with one set of data in which no ground control was held. Each number is an average of the standard errors at the suppressed control points which are located at those positions where one might expect the errors to be maximized, according to the Zeller-Brandenberger formulas.

These data do not exhibit any unexpected features. However, it is pointed out that the increase in precision with an increase in the base/height ratio amount to approximately 5 percent as the percentage overlap is decreased by 5 percent. This increased precision is not significant when compared with the considerable improvement obtained with a triplet, which is in the order of 30 percent.

The significant increase in precision resulting from the use of triplets leads to the conclusion that an optimum mission should be planned which utilizes an exposure interval such that all areas of interest are imaged on three consecutive exposures. This dictates that an overlap in the order of 70 percent is necessary—the minimum 67 percent with a 3 percent safety factor. Any overlap range between this and the minimum 50 percent, to achieve complete double coverage, will furnish heterogeneous results. It is suggested, therefore, that either a 55 or a 70 percent overlap be used, but not an intermediate value, with the recommendation that a 70 percent overlap be adopted.

The differences in the ground control errors used on these calculations do no appreciably affect the accuracy of point determination. This is attributed to the uniformity of the control errors and the fact that their projections onto the photographic plate are not greatly different from the size of the resolution elements. It might be argued that datum shifts are considerably larger than the values used for control point errors in these calculations, but it is pointed out that these shifts are uniform and may be determined by other techniques in the overall orbit calculations. As long as no large relative differential errors occur in the ground control, it is not expected that any large decrease in precision will occur.

Since this program is a constrained solution, it was comparatively easy to vary the weights assigned to any input data. This enabled us to determine the individual effects on the output of sets of data processing variable quality, which essentially simulates the designed experiments used by statisticians using analysis of variance techniques. For the purpose of determining the optimum overlap for the GOPSS, the weights that are assigned to the input data are irrelevant, provided they are constant for the set of varying overlaps.

The first set of data to which different weights were assigned in a sequence of parallel but otherwise identical computations were the photo-coordinates. This was made necessary as a result the data handling being considered as an operational task, as opposed to a controlled experiment. There is some doubt as to whether or not the original estimate of the weighting function, namely

(a) Adjacent photographs

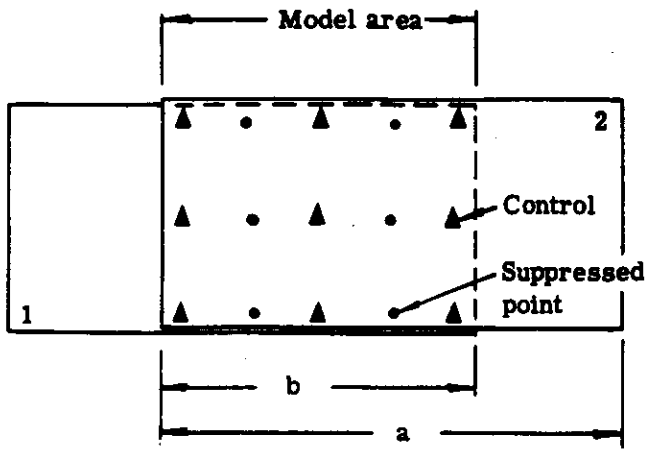

Overlap = a/b

(b) Three photographs

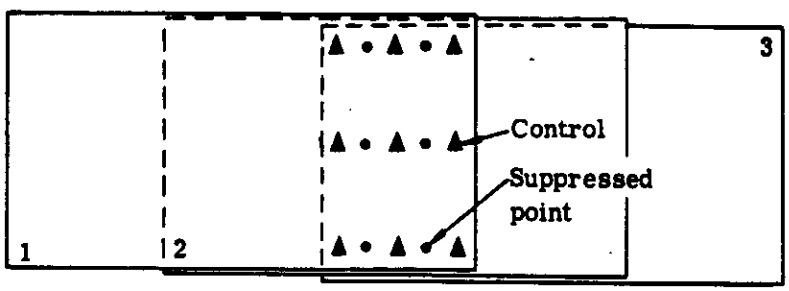

Fig. 3-3 — Control point location

Table 3-5 — Average Standard Errors in Point Determination

Percentage overlap		55		60		65		70		75	
Photo variance		$(0.075/n)^2$	$0.075/n^2$	$(0.075/n)^2$	$0.075/n^2$	$(0.075/n)^2$	$0.075/n^2$	$(0.075/n)^2$	$0.075/n^2$	$(0.075/n)^2$	$0.075/n^2$
Model		meters	meters	meters	meters	meters	meters	meters	meters	meters	meters
Adjacent 2 photo	σ_X	4.3	9.6	4.3	9.9	4.4	10.4	4.4	10.9	4.5	11.3
	σ_Y	2.4	5.6	2.4	5.6	2.4	5.7	2.5	5.9	2.5	6.0
	σ_Z	4.1	8.8	4.1	9.0	4.3	9.9	4.5	10.5	4.5	11.3
Triplet A	σ_X	2.4	5.6	2.4	5.7	2.5	6.0	2.7	6.4	3.5	6.9
	σ_Y	1.6	3.6	1.6	3.7	1.6	3.9	1.7	4.0	2.0	4.7
	σ_Z	2.7	5.7	2.7	5.9	2.7	6.0	2.8	6.3	3.5	6.9
Triplet B	σ_X	2.7	6.1	2.7	6.3	2.8	6.4	2.9	6.9	3.1	7.2
	σ_Y	2.4	5.2	2.4	5.3	2.4	5.3	2.4	5.6	2.4	5.6
	σ_Z	3.5	6.3	3.5	6.4	3.5	6.5	3.5	6.9	3.5	7.2
Triplet C									11.2		
									14.4		
									24.0		

NOTE: Triplet B uses control data errors of ± 10 meters in X, Y, and Z.
Triplet C uses control data errors of ± 1000 meters in X, Y, and Z.
All other models use control data errors of ± 3 meters in X and Y, ± 10 meters in Z.
Orientation angles were held to ± 5.0 arc-seconds.

$(0.075/n)^{+2}mm^2$, is truly applicable in an operational mensuration program. Further discussion of this problem has revealed some sets of data obtained from actual production tasks from which the pessimistic variance of $(0.075/n^2)$ is derived. Consequently, the complete sequence of computations was performed twice, once using the original weighting criterion of $(0.075/n)^{+2}$ and once using the pessimistic value of $(0.075/n^2)^{+1}$.

One other possible variation of input data was performed. This concerned the effects of varying the accuracy of the ground control points on the determination of suppressed points. This was done using the optimum solution, namely, a simultaneous three-photo solution in which the control errors were first ±3 meters in X and Y, and 10 meters in Z; and secondly, ±10 meters in each coordinate.

The tabulated data show that the ground point errors are significantly affected by the weights assigned to the refined photo-coordinates. The initial conclusion that is drawn from these data is that the resulting ground point accuracies are proportional to the square root of the ratio of the normalized standard deviations. This is supported, but not necessarily confirmed, by other numerical data generated in this study.

3.4.1.2 Format and Resolution Program

The objective of this program was to determine the effects on the system accuracy by decreasing the format dimension, thereby causing an increase in the average photographic resolution.

For the same altitude and percentage overlap, a smaller format will yield less accurate results, since the base/height ratio is decreased, all other factors being equal. However, the smaller format decreases the effective angular coverage, and thereby excludes the marginal rays in which the lower resolution degrades the image quality. This means that the accuracy of the measured photographic image coordinates increases, whereas the geometric strength of the solution decreases. These two factors tend to compensate each other. It is emphasized that this was a necessary program for the finalization of the camera design parameters for a specific lens design. Consequently, although a smaller format will produce a photograph with a relatively higher average resolution, the resolution at corresponding off-axis angles is identical.

The program used to determine the total effect of the resolution format compensation was a two-photo solution, functionally constrained to an orbit. In order to remove the effects of errors in the orbital parameters from the program, these elements were assigned extremely high weights.

Parallel computations were performed for two stereo pairs, one for the 9- by 18-inch format and one for 9- by 14-inch format. Both models used a nominal 50 percent overlap and the same geometric distribution of ground control points, which were equally weighted. This ensured that the geometric strength of the solutions differed because of the base/height ratios only, and that no differences could be attributed to ground control data.

Other errors in a photogrammetric model that affect the determination of ground points are those of relative orientation and of the photo-coordinates. The photo-coordinate errors are resolution dependent, so that the relative merits of the two formats may be evaluated by two criteria, namely, the accuracy with which suppressed control points are determined, and the accuracy of the relative orientations. By assigning a large weight to the swing of the initial photograph, and large variances to the remaining angular elements, the relative orientation of each pair is readily determined.

Consequently, the only causes for differences in the computational outputs are due to the resolution effects and the base/height ratios.

The numerical output from the programs consisted of the covariance matrices of the orientation elements and of the suppressed ground points. For brevity, only the diagonal terms are presented.

The tabulated data in Tables 3-6 and 3-7 show that the relative orientation is better determined slightly for the 9- by 18-inch format, and that the volume of the error ellipsoid at determined ground points is also smaller, when compared to the 9- by 14-inch format. It is therefore concluded that the larger format is to be preferred.

3.4.1.3 Summary of Operational Procedures

The preceding computational studies have determined the parameters that are used in all of the succeeding studies. Unless otherwise noted, these will be:

1. The format dimension will be 9 by 18 inches.
2. The sequential adjacent exposures will overlap by 67 percent.
3. Measured photo-coordinates will be weighted according to the lens resolution data tabulated in Table 3-8. The photo-point variance assigned to the image coordinates will be a conservative value of $0.075/n^2$ mm^2.

The relatively large variance for the image coordinates has been selected in order that we might be confident in attaining any predicted system accuracies resulting from these computational studies. It will be noticed that this variance is in conflict with the value used elsewhere in which the criterion of $\pm 0.166/n$ is stated. This value is a result of recently completed studies (May 1966) at the National Research Center, Ottawa and at Delft. The majority of our computational studies had been completed in this data; for consistency, the original calculations have been retained.

3.4.2 Single Model Studies

The prime objective of these single model studies was to evaluate the positioning capability of the photogrammetric sensor with respect to the centroid of five landmarks imaged on three consecutive frames. As in the preceding numerical studies, the use of exact fictitious data in conjunction with associated covariance matrices enabled the effects of various parameters on the end result to be determined.

Essentially, the three consecutive photographs were constrained such that the camera stations lay on an orbit, and that the camera orientations were known to an accuracy of ± 5 arc-seconds, as determined in the photosensor analysis.

The first study determined the purely photogrammetric error in landmark location as a function of altitude by assuming that the orbital elements were exactly known. The second study determined the effect on the landmark location errors by degrading the orbital parameters. The combination of these two systems enables us to estimate the combined effects of an inaccurate orbit at various altitudes on the resulting landmark capability. The third study determined the error in locating the centroid of the five landmarks with respect to the orbit, and the error in locating any other point in the model with respect to this centroid.

Table 3-6 — Variances of Orientation Elements, Radians^2

Format	Photo Number 1			Photo Number 2		
	$\sigma^2\kappa$	$\sigma^2\varphi$	$\sigma^2\omega$	$\sigma^2\kappa$	$\sigma^2\varphi$	$\sigma^2\omega$
9 × 14 inches	1-29*	2.5-11	1.1-10	2.0-10	2.4-11	6.1-11
9 × 18 inches	1-29*	2.5-11	9.9-11	1.7-10	2.5-11	5.6-11

*Enforced variance of 1×10^{-29} radian^2.

Table 3-7 — Standard Errors of Ground Point Determinations, Meters (normalized 160 nautical miles)

Point	1			2			3			4			5			6			7			8			9		
Error	X*	1†	H	X*	1†	H	X*	1†	H	X*	1†	H	X*	1†	H	X*	1†	H	X*	1†	H	X*	1†	H	X*	1†	H
Format																											
9 × 14 inches	1.4	4.1	6.4	1.3	3.3	6.1	1.3	3.2	6.2	1.2	3.2	5.6	1.4	2.5	5.6	1.4	2.4	5.6	1.3	3.8	6.4	1.3	3.3	6.3	1.4	3.4	6.5
9 × 18 inches	1.6	4.0	5.3	1.3	3.1	5.2	1.6	3.1	5.3	1.4	3.2	5.3	1.2	2.5	4.8	1.5	2.5	5.5	1.6	3.9	5.3	1.3	3.3	5.2	1.4	3.5	5.3

X* = Cross-track error
1† = In-track error
H = Elevation error

Table 3-8 — Lens Resolution Data

Radial Distance, millimeter	Resolution, lines per millimeter
0	58
50.8	57
101.6	51
152.4	45
203.2	35
254.0	32

3.4.2.1 Photogrammetric Errors on Landmark Locations

The basic analytical principles underlying this study have been presented in Section 3.3. The essential features of the programmed computation were:

1. Three consecutive 9- by 18-inch photographs, overlapping by 67 percent, were functionally constrained to orbital parameters.

2. The six elements of the orbit were statistically constrained, to exactitude, by assigning to them a covariance matrix that was a six- by six-unit matrix multiplied by a scale factor of 1×10^{-29} units.

3. Within the triple overlap, nine symmetrically arranged ground points were selected. The four corner points and the central point were assigned positional covariance matrices equivalent to positional errors of ±300 meters (±1000 feet). The remaining points were assigned covariance matrices equivalent to positional errors of ±1000 meters.

4. Camera orientations were assumed to be predetermined from stellar indices, with accuracies of ±5 arc-seconds.

5. The inner orientation parameters of the photogrammetric camera were assigned accuracies of $\sigma_{xp} = \sigma_{yp} = \pm 0.01$ mm and of $\sigma_f = \pm 0.015$ mm.

6. The times at which the exposures were made were assigned accuracies of ±0.001 second.

7. The photographic image coordinates were assigned a variance according to the function $0.075/n^2$, using the resolution data listed in Table 3-8.

The calculation of the covariance matrices of all nine ground points, and of the adjusted camera orientations, were performed at three different altitudes, namely 120, 160, and 200 nautical miles.

The data resulting from these calculations (together with a parallel set in which altimeter data were included) are summarized in Table 3-9. It will be noted that an average value of the standard deviations for each set of nine ground points are given, since the range in accuracy was not greatly different between each point in the photograph. The data without any altimeter control do not meet the landmark specification with respect to elevation.

These tabulated data indicate that there is little improvement in the camera orientations. A significant improvement is noticed in the accuracy of the landmarks, and these accuracies are directly proportional to the camera altitude, according to a linear scale factor. It is thus possible to estimate the accuracy attainable from some altitude, H_1, by multiplying H_2 by the scale factor H_1/H_2.

The inclusion of an altimeter in the GOPSS should provide elevation control to the photogrammetric model, along the track of the orbit. In order to determine the effect of such control on the resultant landmark location errors, the central row of ground points was assigned elevation errors of ±15 meters, which is the expected accuracy of the radar altimeter.

A significant increase in the accuracy of the ground point locations results from this constraint. The average standard deviations, for the 160-nautical mile altitude, are ±12.0 meters cross-track, ±12.8 meters in-track, and ±13.0 meters in elevation, indicating that the landmark elevation criterion of ±40 feet can just be met if the system includes an altimeter, and operates at altitudes below 160 nautical miles.

Table 3-9 — Average Photogrammetric Errors on Landmark Location

Altitude, nautical miles	Cross-Track Error Average, meters		In-Track Error Average, meters		Elevation Error Average, meters		Orientation Error	
	Without Altimeter Control	With Altimeter Control	Without Altimeter Control	With Altimeter Control	Without Altimeter Control	With Altimeter Control	Average Error, arc-seconds	Range of Error, arc-seconds
120	±9.1	9.1	±9.9	9.7	±17.2	11.2	±4	2.8 to 4.2
160	±12.1	12.0	±13.1	12.8	±23.4	13.0	±4	2.6 to 4.2
200	±14.9	14.8	±15.7	15.7	±26.7	14.2	±4	2.7 to 4.2

3.4.2.2 Orbital Errors in Landmark Location

This study consisted of a sequence of calculations, for an elevation of 160 nautical miles, which was identical with the preceding numerical study except that the covariance matrix of the orbital parameters was varied. Before discussing the details of this study, it is appropriate to describe the manner in which these covariance matrices were obtained.

The calculation of fictitious data for the three altitudes required that the orbital parameters be known. Those used were derived for a nominal operational altitude of 120 nautical miles and in a roughly polar and circular orbit. These parameters were rigorously scaled to the operational altitudes of 160 and 200 nautical miles. Typical covariance matrices for normally circular and polar orbits at the altitudes of 160 and 200 nautical miles were calculated in the process of the orbital analysis. These calculations were acquired for a simulated orbit reduction that utilized tracking data and Doppler data acquired over a 24-hour period. The simulated data were contaminated by typical errors in the tracking data and in the ground station location. They are, however, unaffected by errors that might be present in the selected geopotential model.

Although several of the harmonic terms of the earth's potential field are fairly well known, the use of such predetermined values might result in large positional errors. This is one of the reasons for redetermining the geodynamic terms, not only to obtain improved values for these parameters, but also to permit a certain amount of the residual errors to be absorbed by them. It is in the basis of such an argument that Kaula, Anderlee, Veis, et al., predict relatively small positioning errors and, furthermore, acquired satellite data in a redetermination of the potential model.

It was reasonably assumed that these covariance matrices would be typical of the scaled orbits that were used in calculating the fictitious data, and could therefore be applied to our cases. The covariance matrices obtained from the orbital studies were expressed with reference to the geocentric radius vector, X, Y, Z, and the velocity components of this vector $\dot{X}$, $\dot{Y}$, $\dot{Z}$, at a specific time. These were subsequently transformed into the covariance matrices corresponding to the six orbital elements used in our solution, according to the rigorous transformation expressed in Section 3.3.5.

The upper triangular portion of the specific covariance matrix obtained from the orbital analysis task described in Vol. IV for the 160-nautical mile altitude is as follows:

	X	Y	Z	$\dot{X}$	$\dot{Y}$	$\dot{Z}$
X (m^2)	8.68+0	4.21-2	2.53-3	3.90-3	6.44-5	-2.80-5
Y (m^2)		8.55-1	2.27+0	2.88-5	-2.59-3	-9.49-4
Z (m^2)			9.25+1	5.53-4	-1.06-1	-1.21-3
X (m^2/s^2)				4.34-5	-6.38-7	-1.17-8
Y (m^2/s^2)					1.22-4	1.36-6
Z (m^2/s^2)						1.08-6

In this matrix, the signed numbers following the numerical value for each element are the exponent of 10 by which each term must be multiplied. Thus, the element XY designated by 4.21-2 is interpreted to be 4.21×10^{-2}. This is in accordance with general computer usage.

The transformed matrix corresponding to the six orbital elements used in our solution is:

		Ω	ω	I	e	η	τ
Ω	(radians^2)	7.25-13	-7.56-11	9.05-13	1.60-13	-2.38-15	-7.64-8
ω	(radians^2)		8.52-9	-9.87-11	-2.32-11	2.62-13	8.58-6
I	(radians^2)			1.17-12	2.28-13	-3.08-15	-9.96-8
e	(unitless)				1.71-12	-3.24-15	-3.59-8
η	(radians^2/sec^2)					1.25-17	2.86-10
τ	(sec^2)						8.75-3

In order that the effects of varying the quality of the orbital covariance matrix on the resultant landmark locations could be determined, the original X, Y, Z, $\dot{X}$, $\dot{Y}$, $\dot{Z}$ was multiplied by scale factors of 10, 100, and 1000, transformed into the corresponding orbital covariance matrices, and applied to the three photo solutions.

As expected, and in accordance with the preceding numerical study, no great improvement in the camera orientations was exhibited. The essential data with respect to the averaged standard errors are listed in Table 3-10, for each case, together with their differences from the case in which no orbital errors are present, as determined in Section 3.4.2.1. The essential conclusion to be drawn from these data is that the photogrammetric and orbital errors should be root mean squared to yield the final total error.

3.4.2.3 Relative Errors in Centroid Location

The basic data used in calculating the accuracy with which the centroid of the five landmarks is determined with respect to the orbit is obtained from the numerical study pertaining to the photogrammetric errors (Section 3.4.2.1).

Since the centroid is the center of gravity of the five landmarks, it is only necessary to determine the standard error of the mean of these coordinates.

The covariance matrix of the centroid, denoted $[C(\bar{X})]$, is obtained from the equation

$$[C(\bar{X})] = [I\ I\ I\ I\ I][C(\bar{X}_i)][I\ I\ I\ I\ I]^T/25$$

in which each I is a 3 by 3 unit matrix, and $[C(\bar{X}_i)]$ is the 15 by 15 covariance matrix of the five points considered. This furnishes the standard errors listed in Table 3-11.

Another numerical study was associated with this calculation. This was the evaluation of the relative accuracy with which any point in the model could be coordinated with respect to some other point located in the model. This was accomplished by considering the covariance matrices of a series of points, at different separations, together with their correlations. The results for the 160-nautical mile altitude are graphically presented in Figure 3-4.

These internal coordinate errors exhibit a remarkable linearity, as a function of distance beyond a 40-nautical mile distance, that was quite unexpected. This is confirmed by those data that were calculated for the 120 and 200-nautical mile altitudes, the values of which are related to the 160-mile altitude produced by, a scale factor that is the ratio of the flying heights. This is in agreement with the results of Section 3.4.2.1. For ranges below 40 nautical miles, additional data have been calculated according to the standard photogrammetric error formulas.

Table 3-10 — Average Landmark Errors With Varying Orbital Covariance Matrix at 160 Nautical Miles

Scale of Orbital Covariance	Cross-Track		In-Track		Elevation	
	Total Error, meters	Orbital Error, meters	Total Error, meters	Orbital Error, meters	Total Error, meters	Orbital Error, meters
0	12.1	-	13.1	-	23.4	-
1	12.1	0	14.3	5.7	23.4	0
10	12.6	3.5	24.7	21.0	31.1	20.4
100	14.9	8.7	53.3	52.2	56.2	51.2
1000	69.0	67.6	115.7	115.0	113.6	111.2

Table 3-11 — Standard Errors Furnished by Covariance Matrix of Centroid

Altitude	Cross-Track Error, meters	In-Track Error, meters	Elevation Error, meters
120	±11.4	±12.6	±10.9
160	±15.1	±17.3	±14.4
200	±17.6	±19.8	±16.9

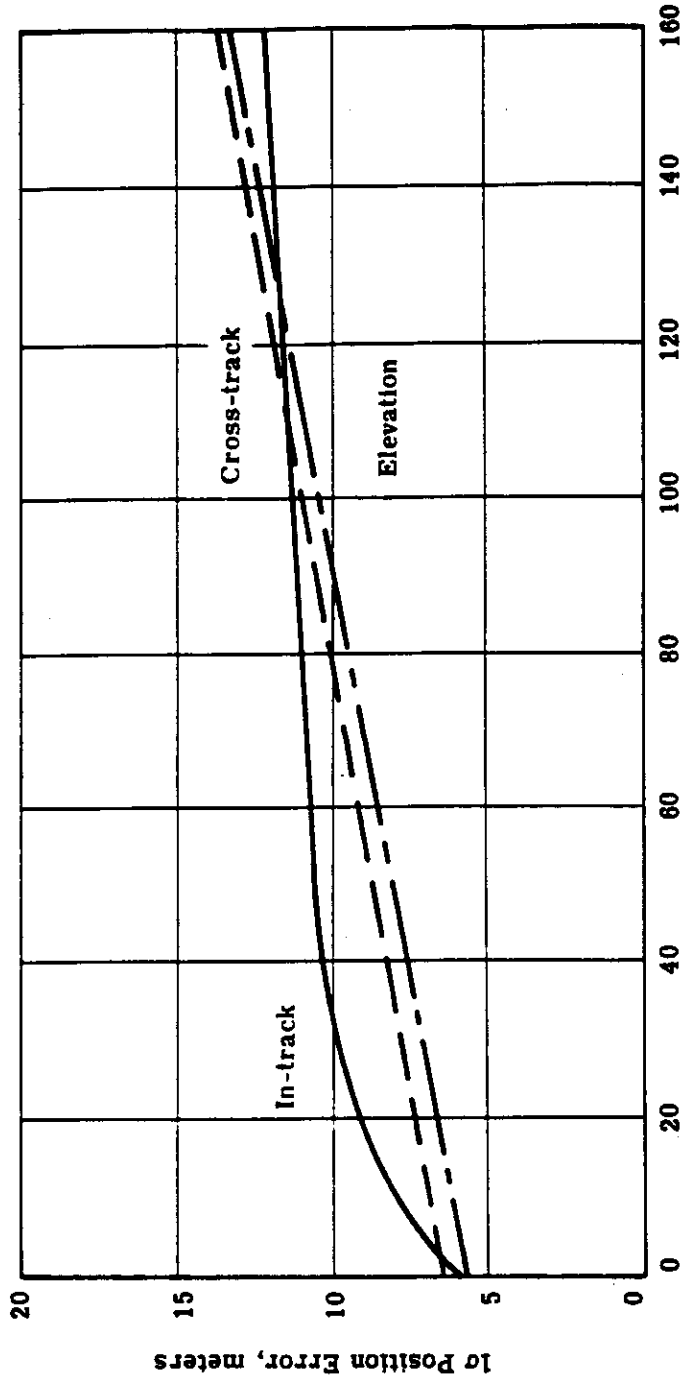

Fig. 3-4 — Internal model coordinate errors at 160-nautical mile altitude

3.4.2.4 Final Analysis and Summary of Single Model Studies

The accuracy of locating the centroid of 5 landmarks in the triple overlap with respect to the orbit has been determined. This could be equally well considered as a determination of an orbital position with respect to accurately known landmarks. Viewed in this manner, it is concluded that the specification for the determination of the camera position to an accuracy better than ±9 meters (±30 feet) is not met, (according to Table 3-12). There are two ways of improving this situation. The first of these is to ensure that elevation control is established in the model by including a radar altimeter in the operational GOPSS. The other is to make extremely precise measurements of the photographic coordinates so that the weighting factor proportional to 0.166/n can be applied to the computational procedure. As mentioned in Section 3.2., this is not an unreasonable factor to use, whereas that which has been incorporated in all the calculations presented here is an overly pessimistic value. The effect of using the better weighting value is to increase the system accuracy to the values listed in Table 3-12, in which all computational data for the centroid calculations are summarized.

These studies have also confirmed that the effect of changing the system's operational altitude corresponds to a scale change, and that the effects of a poor orbit determination do not degrade the results as rapidly as one would expect, owing to the constraint imposed on the orbit by the photogrammetric data.

3.4.3 Strip Triangulation Studies

The strip triangulation studies consist of two sets, namely, those pertaining to control extension and those concerned with photogrammetric bridging. The distinction between bridging and extension is that of interpolation against extrapolation. Bridging is essentially a means of determining the location of ground points between areas of known geodetic control, whereas extensions are used in determining ground point locations by cantilevering from an area of known geodetic control.

The objectives of these triangulation studies were as follows:

1. Determine the accuracy with which landmark locations could be extrapolated from, and interpolated between, geodetic control located on a local reference datum.
2. Determine the accuracy with which either the camera positions or the six parameters of the oscillating ellipse could be obtained from the local geodetic control.

The triangulations may be functionally constrained to an orbit and various statistical restrictions can be imposed on the solution. This is termed the orbital mode. This means that the triangulations can be performed either independently to determine the orbital parameters, or in conjunction with data in an orbit determination. In the second case, the influence of the photogrammetric data will be minimal, but the simultaneous adjustment ensures that the photogrammetric and orbital parameters are consistent with each other. The imposition of statistical restraints on input data, in the form of a weight matrix, means that these data can be adjusted within the bands imposed by the weight matrix. Thus, it is possible to include such parameters as the camera focal length in the solution in order to solve for any bias that might exist in the calibrated value, or to enforce such data as orientation angles determined from stellar cameras.

The triangulations may also be calculated without the functional orbit constraint. However, orbital parameters may be indirectly enforced on the solution by restricting the lens position by the covariance matrices of the orbital radii vectors of the times of exposure. This is termed the positional mode.

Table 3-12 — Accuracy of Camera Station Determinations*

Conditions		120 Nautical Miles			160 Nautical Miles			200 Nautical Miles		
Weight	Altimeter	Cross Track	In Track	Elevation	Cross Track	In Track	Elevation	Cross Track	In Track	Elevation
$0.075/n^2$	No	11.4	12.6	10.9	15.1	17.3	14.4	17.6	19.8	16.9
$0.075/n^2$	Yes	11.4	12.5	7.1	15.0	17.2	8.2	17.5	19.6	9.0
$(0.166/n)^2$	No	7.4	8.2	7.1	9.8	11.2	9.6	11.3	12.9	11.0
$(0.166/n)^2$	Yes	7.4	8.2	4.7	9.8	11.2	5.4	11.2	12.7	6.0

*Considered as the centroid of five landmarks known to ± 1000 feet. Angular orientations known to ± 5 arc-seconds.
All errors given in meters.

Both computational sequences in the orbital and positional modes consist of three phases, which are as follows:

1. Phase I considers all input data as exactly known except photographic coordinates and ground point coordinates. A weighted, least-squares solution yields the best fit of photographic and ground coordinate data to camera orientation parameters.
2. In Phase II the adjusted values resulting from Phase I are used in a weighted, least-squares solution to determine the values of the remaining parameters within the tolerances assigned to their initial estimates.
3. In Phase III the adjusted values from Phase II are then used to re-adjust the ground point and photographic coordinate data.

Each of these phases is an iterative procedure, requiring initial estimates of unknowns as an input to the program. Initially, each phase as well as the complete sequence was iterated. It was discovered, however, that one iteration sufficed. Small differences between iterations did result, but these differences were below the noise level of the computer. It should be noted that, in an operational system which uses real and not fictitious data, several iterations may be necessary to achieve convergence.

The typical strip contained three parallel rows of control data located along the strip's longitudinal axis and the strip edges. Various combinations of these control data were used, and are described in the following sections. Also included is a brief description of the salient program features, and an analysis of the computational results.

Both modes have been used in the following computations, which consist of two parallel sets. The first of these considers the orbital parameters and lens positions as unknowns, so that the use of controlled strip triangulations for determining either lens positions or orbital parameters could be evaluated in addition to the position of landmark location. The second set of data enforced positional or orbital covariance matrices that were obtained from a typical orbital solution using ground tracking data. Both sets of computations were repeated with the inclusion of simulated altimeter data.

In this way, the efficiency of the photogrammetric method as a means of orbit determination was obtained, and the value of altimeter data in the orbital calculations established.

The essential computations are specified in Tables 3-13 and 3-14.

3.4.3.1 Triangulation Study Description

Strip triangulations were performed in both the orbital and positional modes for operational altitudes of 120, 160, and 200 nautical miles. Of these calculations, the positional mode is of limited value, being virtually identical to a standard photogrammetric case.

With regard to the ground control data used in these triangulations, errors have been assumed with respect to a localized survey datum. As such, the discrepancies between separate datums have not been considered. It is possible to determine these datum shifts, with respect to some defined world wide geodetic system, by including a bias parameter, or even a set of bias parameters, for each of the separate geodetic systems that are utilized.

Table 3-13 — Computational Scheme

Orbital Mode	Positional Mode
Bridges and Extensions	**Bridges and Extensions**
1. Determines accuracy of calculating orbit parameters and landmark locations, using stellar orientation and minimum ground control (Table 3-20).	1. Determines accuracy of calculating orbital positions and landmark locations, using stellar orientations and minimum ground control (Tables 3-18, 3-19, and 3-22.)
2. As above, but adds altimetric control.	2. As above, but adds altimetric control (Table 3-25).
3. Determines improvement in orbital parameters, and the accuracy of landmark location, using orbital parameters and stellar orientations (Tables 3-21 and 3-22).	3. Determines improvement in orbital positions, and the accuracy of landmark location, using positions and stellar orientations (Tables 3-23 and 3-24).
4. As in 3, but adds altimetric control (Tables 3-21 and 3-22).	4. As in 3, but adds altimetric control (Tables 3-23 and 3-24).
Single Model	**Single Model**
5. Determines accuracy of calculating landmark locations, enforcing orbital parameters and stellar orientation only, without any ground control (Table 3-26).	5. Determines accuracy of calculating landmark location, enforcing orbital parameter and stellar orientation only, without any ground control (Table 3-27).

Table 3-14 - Computational Scheme

Item	Table Number	Computations	Constraints	Ground Control Reference
1	3-18	Strip triangulation (extension) in positional mode. Lists accuracy of camera station locations, with and without altimeter control.	1. Camera orientations held to ± 5 arc-seconds 2. Camera positions unknown	1. Six points in initial model held to ± 10 meters 2. For altimeter control, 15 additional central points held to ± 15 meters
2	3-19	Strip triangulations (bridge) in positional mode. Lists accuracy of camera station locations, with and without altimeter control.	1. Camera orientations held to ± 5 arc-seconds 2. Camera positions unknown	1. Six points in initial model held to ± 10 meters, 3 points in final model held to ± 10 meters 2. For altimeter control, 14 additional central points held to ± 15 meters
3	3-20	Strip triangulations (bridges and extensions) in orbital mode, with and without altimeter control. Lists determined covariance matrices of orbital elements.	1. Camera orientations held to ± 5 arc-seconds 2. Functionally constrained to orbit; orbital parameters unknown	1. Extensions: according to item 1 (3-18) 2. Bridges: according to item 2 (3-19)
4	3-21	Strip triangulation (extension) in orbital mode. Lists accuracy of landmark locations.	1. Camera orientations held to ± 5 arc-seconds 2. Statistically constrained to orbit. Orbital parameters held according to data in Section 3.4.2.2	As in item 1 (3-18)
5	3-22	Strip triangulation (bridge) in orbital mode. Lists accuracy of landmark locations.	1. Camera orientations held to ± 5 arc-seconds 2. Statistically constrained to orbit. Orbital parameters held according to Section 3.4.2.2	As in item 2 (3-19)
6	3-23	Strip triangulation (extension) in positional mode. Lists accuracy of landmark locations.	1. Camera orientations held to ± 5 arc-seconds 2. Statistically constrained to uncorrelated positions according to Section 3.4.2.2	As in item 1 (3-18)
7	3-24	Strip triangulation (bridge) in positional mode. Lists accuracy of landmark locations.	1. Camera orientations held to ± 5 arc-seconds 2. Statistically constrained to uncorrelated positions according to Section 3.4.2.2	As in item 2 (3-19)
8	3-25	Strip triangulation (bridge) in positional mode. Lists accuracy of landmark locations.	1. Camera orientations held to ± 5 arc-seconds 2. Camera positions unknown	As in item 2 (3-19)
9	3-26	Three-photo model in orbital mode. Lists accuracy of landmark locations.	1. Camera orientations held to ± 5 arc-seconds 2. Statistically constrained to orbital parameters according to Section 3.4.2.2	No ground control points
10	3-27	Three-photo model in positional mode. Lists accuracy of landmark locations.	1. Camera orientations held to ± 5 arc-seconds 2. Statistically constrained to uncorrelated positions according to Section 3.4.2.2	No ground control points

NOTE: All photocoordinates weighted according to $0.075/n^2$, using data listed in Table 3-8.
All times were held to ± 0.001 second.

The objective of the first set of computations, in which either the orbital parameters or camera positions were virtually unknown, was to determine the accuracies with which either orbital parameters or camera positions could be calculated, while simultaneously evaluating the accuracy of landmark location.

A duplicate set of calculations was performed, in which simulated radar altimeter data was incorporated into the solution, in order that the value of including an altimeter into the GOPSS could be evaluated.

The specific restrictions imposed on these calculations were as follows:

1. Ground control points located in the first model were assigned spherical position errors of ±10 meters. All unknown ground points were assigned spherical position errors of ±1000 meters. These errors are considered to be with respect to a local geodetic datum.
2. Simulated altimeter control was assigned a planimetric circular error of ±1000 meters, and an elevation error of ±15 meters.
3. Timing accuracies were assumed to be ±0.001 second.
4. Camera orientations were assumed to be predetermined from stellar indices, with accuracies of ±5 arc-seconds.
5. Inner orientation parameters of the terrain camera were assigned accuracies of $\sigma_{xp} = \sigma_{yp} = \pm 0.01$ mm and of $\sigma_f = \pm 0.015$ mm.
6. For the orbital mode, the six elements were assigned a covariance matrix that was a six by six unit matrix multiplied by a scale factor of 1×10^{29} units, causing them to be unknown.
7. For the positional mode, the lens positions were assigned a covariance matrix that was a three by three unit matrix multiplied by a scalar of 1×10^{29} mm^2, causing them to be unknown.
8. Photo coordinates were assigned variances according to $\pm 0.075/n^2$ mm^2.

A second set of triangulations was also performed (Tables 3-21 to 3-24), in which typical orbital or positional covariance matrices were imposed on the solutions. The source, and the actual values of these covariance matrices, are described in Section 3.4.2.2; otherwise, the same restrictions listed above were maintained.

3.4.3.2 Analysis of Triangulational Data

3.4.3.2.1 Orbital Elements and Camera Positions

The tabulated covariance matrices for the unconstrained solution of the orbital extensions and bridges indicate the accuracy with which these short photogrammetric arcs can be used to determine the six elements of the osculating ellipse. With the exception of the eccentricity and the mean motion, all elements exhibit almost perfect correlation. This indicates that although a solution has been obtained from the short arc, it can be improved by holding certain elements as known values and solving for the three less dependent elements. Essentially, it is necessary to utilize the photographic bridge in conjunction with other data that furnishes an orbital solution; alternatively, the nine exposures should be widely distributed over the mission arc, since in their present configuration they form little more than a single data point. For convenience, the standard errors

of each element for the operational modes has been extracted from the tables located at the end of this section, and are compared in Table 3-15 with the corresponding data obtained from the orbital analysis as described in Section 3.4.2.2. These data indicate that the orbital elements are determined from two to three times better in the case of triangulated bridges. Surprisingly, the inclusion of altimeter data has little effect on the accuracy of the orbital elements.

The most significant factor is obtained by examining the pertinent covariance matrices. Although the elements Ω, I, e, and η, appear to be well determined, in contrast to the determinations of ω, and τ, these accuracies may be more apparent than real.

The solution for these elements, using the photogrammetric approach, is extremely weak for short strip triangulations. This is evidenced by the high correlations existing between various elements that is essentially due to the photogrammetric approach. As a typical example, the cavariance matrix of the elements for the altimetric controlled bridge has been transformed into the corresponding correlation matrix, and is presented:

Ω	ω	I	e	η	τ
1	-.940	+.972	+.132	-.718	-.935
	1	-.982	-.194	+.739	+.990
		1	+.154	-.740	-.975
			1	-.762	-.321
				1	+.824

In the case of the constrained modes, there is a small but significant improvement of the imposed orbital covariance matrix. These data are not tabulated, but it is considered desirable to present the transformed correlation matrix to demonstrate the increased strength of solution in these constrained calculations (the matrix corresponding to the previous example):

Ω	ω	I	e	η	τ
1	-.6	+.8	+.05	-.5	-.6
	1	-.8	-.05	+.9	+.9
		1	+.1	-.7	-.8
			1	-.6	-.6
				1	+.9

The location of camera stations, when operating in the positional mode, exhibit virtually the same general characteristics as obtained in the orbital constrained calculations. That is, there is little or no improvement in the case of constrained bridges and extensions whereas the unconstrained solutions provide the expected conclusion that bridges are more accurate than extensions, and that both are improved by the inclusion of altimetric data. This is due to the high accuracy of the imposed constraints, Section 3.4.2.2. The maximum geocentric positional errors for the 160-nautical mile solutions in which the camera stations are assumed to be unknown are given in Table 3-16. These data lead to the obvious conclusion that photogrammetrically determined air stations are not sufficiently accurate to form the basis of an orbit determination, unless those stations are located over well controlled areas.

Table 3-15 — Comparison of Standard Errors of Orbital Elements

Mode	Ω radians	ω radians	I radians	e	η rad/sec	τ seconds
Extension	6.3-6	8.9-3	7.5-6	5.6-5	1.0-7	1.2
Extension with altimetry	6.3-6	8.2-3	7.5-6	5.4-5	1.0-7	1.1
Bridge	3.4-6	3.3-3	3.3-6	1.6-5	3.0-8	0.4
Bridge with altimetry	3.4-6	3.2-3	3.2-6	1.6-5	3.0-8	0.4
Orbital analysis (Section 3.4.2.2)	8.5-7	9.2-5	1.1-6	1.3-6	3.5-9	9.3-2

Table 3-16 — Maximum Camera Station Location Errors for 160-Nautical Mile Altitude

Positional Mode	σ_X	σ_Y	σ_Z
Extension	99m	35m	111m
Extension with altitude	42m	24m	72m
Bridge	33m	18m	34m
Bridge with altitude	18m	14m	19m

3.4.3.2.2 Landmark Locations

Let us now consider the accuracy of landmark location for each of the triangulation programs. The maximum errors in point locations for each computation of the nine photo strip programs have been extracted and incorporated in Table 3-17; detailed data are listed in Tables 3-18 to 3-27.

With regard to these extracted data, it is to be noticed that there are two sets of data which have been derived from a single photographic model. These computations were made by constraining either the positional or orbital parameters to the previously defined covariance matrices together with the orientation covariance matrices, in order to determine the accuracy with which landmark locations could be hung on to an orbit. In essence, the model is without any ground control and indicates the magnitude of the maximum errors that can occur for points imaged on 3 photos or in a bridge triangulation, provided enforced covariance matrices are realistic. These calculations are similar to those performed in Section 3.4.2.1, except that all ground points were assigned standard errors of ±1000 meters.

It also should be noted that there are some numerical values in the extracted data that exceed those listed in Table 3-17. These data, however, do not occur in the area of trilap, and in the case of the bridges, are beyond the control areas; consequently, they are excluded from the selective tabulation.

The first point that is evident from the detailed tabulations is that the results obtained from the orbital mode are of a far greater accuracy than those resulting from the positional. This points out that the imposition of functional orbital constraints on a solution enhances the targeting capability to such an extent that it is pointless to use the other computational method if optimum results are desired. This concurs with the recommendation that the final data reduction scheme should incorporate all data simultaneously.

These data indicate that both the orbital extension and bridge can meet the specified landmark location tolerances over a nine photo strip. It should be mentioned that these accuracies are with respect to the local geodetic network, so that it is necessary to determine the relationship of the various nets to a world geodetic system. This is a task that can be accomplished by the orbital reduction, and in reality the referencing of the various geodetic datums to a fundamental system should not compound these results seriously. This is basically confirmed by the analyses of the single model studies, Section 3.4.2.

Some comments concerning the detailed tabulations are in order. The first column consists of the point identification number. These points have been selected, in groups of three, normal to the flight direction, such that one point is at the extreme port side, one is on the flight track, and the other at the extreme aft side of the strip swath. There are seventeen groups of these points, sequentially arranged along the strip as shown in Figure 3-5.

As an illustrative example, consider Table 3-21. The first three points numerated, 1a, 1b, and 1c, correspond to the first column of the preceding scheme; the points, 2a, 2b, and 2c, correspond to the second column, etc.

Table 3-17 — Maximum Errors in Landmark Location at an Altitude of 160 Nautical Miles
(Imaged on Three Photographs)

Calculation	Unconstrained Solution Orbital Elements or Positions Assumed to be Unknown			Constrained Solution Orbital Elements or Positions Enforced by Covariance Matrix		
	Cross-Track Error, meters	In-Track Error, meters	Elevation Error, meters	Cross-Track Error, meters	In-Track Error, meters	Elevation Error, meters
Positional bridge*	35	24	26	16	6	14
Positional bridge with altimeter control†	16	17	12	16	6	12
Positional extension*†	71	151	70	34	9	16
Positional extension with altimeter control*†	38	80	24	34	9	11
Orbital bridge*	10	8	14	7	6	13
Orbital bridge with altimeter control*	10	7	12	7	6	12
Orbital extension*	28	18	18	8	9	15
Orbital extension with altimetry*	24	18	13	8	9	11
Uncontrolled positional model†				31	13	24
Uncontrolled orbital model†				12	15	25

*Unconstrained tabulations not included in report.
†Solutions are of academic but not practical interest.

Table 3-18 — Positional Mode, Camera Station Errors in Geocentric Coordinates (H = 160 Nautical Miles)

Camera Station	Unconstrained Extension						Orientation Errors					
	No Altitude Control			With Altitude Control			No Altitude Control arc-sec			With Altitude Control arc-sec		
	σ_x	σ_y	σ_z	σ_x	σ_y	σ_z	σ_κ	σ_φ	σ_ω	σ_κ	σ_φ	σ_ω
1	17.8	13.9	16.8	17.4	13.7	16.3	3	4	4	3	3	4
2	16.6	14.7	17.8	16.5	14.2	17.7	3	3	3	3	3	3
3	16.6	18.4	29.1	16.1	15.3	23.0	3	3	2	3	3	2
4	21.1	21.1	40.7	16.6	16.4	28.9	3	3	2	3	3	2
5	27.6	21.8	52.8	18.5	17.5	35.5	3	3	2	3	3	2
6	43.2	23.9	61.8	22.0	18.8	43.0	3	3	2	3	3	2
7	58.9	25.7	81.7	27.1	20.1	51.6	3	3	2	3	3	2
8	74.3	27.8	94.7	33.9	21.7	61.3	3	3	2	3	3	2
9	99.0	34.8	111.4	42.7	23.7	72.5	4	4	2	4	3	3

Units : Meters

Table 3-19 — Positional Mode, Camera Station Errors in Geocentric Coordinates (H = 160 Nautical Miles)

Camera Station	Unconstrained Bridge						Orientation Angles					
	No Altitude Control			With Altitude Control			No Altitude Control arc-sec			With Altitude Control arc-sec		
	σ_x	σ_y	σ_z	σ_x	σ_y	σ_z	σ_κ	σ_φ	σ_ω	σ_κ	σ_φ	σ_ω
1	17.5	13.5	18.7	17.2	13.4	18.7	3	3	3	3	3	3
2	16.2	14.0	17.4	15.6	13.7	17.1	3	3	2	3	3	3
3	16.4	16.1	25.9	15.6	13.4	18.7	3	3	2	3	3	2
4	20.6	17.7	33.7	16.3	14.2	19.4	3	3	2	3	3	2
5	25.3	16.3	31.8	17.6	13.5	18.2	3	3	2	3	3	2
6	33.1	16.4	29.4	18.2	13.2	18.4	3	3	2	3	3	2
7	29.6	17.6	14.4	17.2	12.9	13.4	3	3	2	3	3	2
8	14.3	12.5	14.2	13.5	12.1	13.4	3	3	2	3	3	2
9	12.9	12.2	17.6	12.9	12.1	12.9	4	3	2	4	3	2

Units : Meters

Table 3-20 — Covariance Matrices of Orbital Elements Determined From Strip Triangulations

Elements	Ω	ω	I	e	η	τ
Model						
Extension	4.0825-11	-4.8867-10	4.6093-11	3.9537-11	-7.1468-14	-7.4855-07
		7.8616-07	-5.4179-10	-4.1386-08	7.6695-11	1.0279-03
			5.5816-11	4.4233-11	-7.9931-14	-8.3236-07
				3.1874-09	-5.7887-12	-6.2485-05
					1.0531-14	1.1485-07
						1.4140-00
Extension with altimetry	4.0737-11	-4.8795-09	4.5993-11	3.5045-11	-6.3844-14	-7.1130-07
		6.7067-07	-5.4897-10	-3.9186-08	7.2075-11	9.0885-04
			5.5701-11	3.9132-11	-7.1293-14	-7.0239-07
				2.9082-09	-5.2990-12	-5.8379-05
					9.6659-15	1.0698-07
						1.2763-00
Bridge	1.1401-11	-1.3254-11	9.8409-11	1.8566-12	-3.2663-15	-2.5446-08
		1.0817-07	-8.5613-12	-2.2789-09	4.5486-12	1.1252-04
			1.1103-11	1.8581-12	-3.2468-15	-2.1589-08
				2.7177-10	-4.9548-13	-4.2792-06
					9.1314-16	8.1779-09
						1.3352-01
Bridge with altimetry	1.1397-11	1.2193-11	9.8375-12	1.8409-12	-3.2505-15	-2.4477-08
		1.0550-07	-7.7804-12	-2.2599-09	4.5058-12	1.1007-04
			1.1099-11	1.8391-12	-3.2272-15	-2.0805-08
				2.6964-10	-4.9218-13	-4.2435-06
					9.0781-16	8.1092-09
						1.3114-01

Table 3-21 — Constrained Extension in Orbital Mode at 160 Nautical Miles

Ground control points located on initial model; uses orbital parameters obtained from long arc solution

	No Radar Altimeter			With Radar Altimeter		
Point	Cross-Track Error, meters	In-Track Error, meters	Elevation Error, meters	Cross-Track Error, meters	In-Track Error, meters	Elevation Error, meters
1a	6.1	6.1	8.6	5.9	6.1	8.5
1b	6.0	7.4	8.4	5.9	7.4	8.2
1c	5.7	6.4	8.6	5.6	6.2	8.5
2a	5.4	5.2	7.6	5.2	5.2	7.4
2b	4.7	5.0	7.5	4.6	4.9	7.2
2c	5.5	5.5	7.7	5.3	5.2	7.3
3a	6.3	6.3	10.1	6.2	5.7	8.6
3b	5.4	6.0	9.8	5.3	5.4	7.3
3c	6.3	6.2	10.0	6.1	5.7	8.5
4a	7.1	7.3	13.5	7.0	6.4	11.7
4b	5.8	6.8	12.3	5.7	5.9	8.6
4c	7.4	7.1	13.3	7.2	6.3	11.7
5a	6.7	7.4	11.3	6.6	6.2	8.6
5b	5.9	7.1	11.1	5.8	6.0	7.4
5c	6.8	7.2	11.3	6.6	6.2	8.6
6a	7.3	8.2	13.9	7.2	6.7	11.5
6b	6.2	7.8	13.1	6.1	6.4	8.6
6c	7.6	8.0	14.1	7.4	6.8	11.7
7a	6.9	8.3	12.1	6.9	7.0	8.7
7b	6.3	8.1	12.0	6.1	6.6	7.4
7c	7.1	8.2	12.1	6.9	10.7	8.6
8a	7.6	8.9	14.5	7.5	7.5	11.7
8b	6.5	8.6	13.6	6.4	7.0	8.6
8c	7.8	8.9	14.5	7.6	7.3	11.6
9a	7.1	8.9	12.4	7.0	7.5	8.6
9b	6.5	8.8	12.3	6.4	7.3	7.4
9c	7.2	8.9	12.4	7.1	7.3	8.6
10a	7.9	9.3	14.7	7.7	7.8	11.6
10b	6.7	9.0	13.8	6.6	7.6	8.6
10c	7.9	9.2	14.7	7.8	7.8	11.6
11a	7.4	9.2	12.7	7.2	8.0	8.6
11b	6.7	9.0	12.6	6.6	7.8	7.4
11c	7.4	9.2	12.7	7.3	6.5	8.5
12a	8.2	9.4	15.0	8.0	8.5	11.6
12b	6.9	9.2	14.1	7.2	8.2	8.6
12c	8.0	9.4	14.8	7.9	8.5	11.3
13a	7.7	9.2	13.3	7.5	8.7	8.6
13b	6.9	9.0	13.2	6.8	7.4	8.5
13c	7.5	9.2	13.3	7.5	8.5	8.6
14a	8.6	9.5	15.5	8.3	9.2	11.7
14b	7.1	9.2	14.7	7.1	8.8	8.6
14c	8.2	9.4	15.3	8.6	9.0	11.3
15a	8.6	9.9	15.3	8.3	9.7	11.3
15b	7.3	9.4	14.9	7.2	9.2	8.5
15c	8.4	9.5	15.3	8.1	9.3	11.1

Adjusted camera stations consistantly accurate to ± 1 meter cross track, ± 5 meters in track, ± 5 meters elevation.

Adjusted camera orientations consistantly accurate to ±3 arc-seconds for each orientation angle.

Table 3-22 — Constrained Bridge in Orbital Mode at 160 Nautical Miles

Ground control points located on terminal models; uses orbital parameters obtained from long arc solution

	No Radar Altimer			With Radar Altimeter		
Point	Cross-Track Error, meters	In-Track Error, meters	Elevation Error, meters	Cross-Track Error, meters	In-Track Error, meters	Elevation Error, meters
1a	5.8	6.0	8.5	5.7	6.1	8.5
1b	5.7	7.0	8.5	5.7	7.5	8.3
1c	5.4	6.2	8.5	5.5	6.2	8.5
2a	4.9	5.0	7.5	4.9	5.0	7.4
2b	4.2	4.7	7.5	4.3	4.7	7.2
2c	4.9	5.0	7.5	5.0	4.9	7.3
3a	5.6	5.4	9.7	5.7	5.2	8.6
3b	4.7	5.1	9.4	4.7	5.0	7.3
3c	5.5	5.3	9.6	5.6	5.3	8.5
4a	6.4	6.1	12.9	6.5	5.8	11.7
4b	5.0	5.5	11.7	5.1	5.2	8.6
4c	6.6	5.9	12.8	6.6	5.7	11.7
5a	5.8	5.7	10.5	5.9	5.4	8.6
5b	5.0	5.5	10.3	5.1	5.2	7.4
5c	5.9	5.7	10.5	5.9	5.4	8.6
6a	6.6	6.2	13.2	6.6	5.8	11.4
6b	5.3	5.8	12.2	5.3	5.4	8.6
6c	6.7	6.2	13.4	6.7	5.8	11.7
7a	6.0	5.9	11.0	6.1	5.6	8.6
7b	5.2	5.8	10.9	5.3	5.4	7.4
7c	6.1	5.9	11.0	6.1	5.6	8.6
8a	6.7	6.3	13.4	6.8	5.9	11.6
8b	5.4	6.0	12.4	5.4	5.6	8.6
8c	6.8	6.4	13.5	6.8	5.9	11.6
9a	6.1	5.9	10.7	6.1	5.6	8.6
9b	5.3	5.8	10.6	5.4	5.4	7.4
9c	6.1	5.9	10.7	6.1	5.6	8.5
10a	6.8	6.2	13.0	6.9	5.9	11.6
10b	5.4	5.8	11.9	5.5	5.5	8.6
10c	6.7	6.3	13.0	6.8	5.9	11.5
11a	6.0	5.7	9.9	6.1	5.6	8.5
11b	5.2	5.6	9.8	5.3	5.4	7.3
11c	5.9	5.8	9.9	6.0	5.6	8.4
12a	6.8	5.9	12.2	6.9	5.9	11.4
12b	5.2	5.6	11.0	5.4	5.5	8.4
12c	6.5	5.9	11.9	6.6	5.8	11.1
13a	5.2	5.0	6.8	5.2	5.2	6.3
13b	5.1	5.3	8.9	5.3	5.4	7.1
13c	5.0	5.0	6.8	5.2	5.1	6.3
14a	7.0	5.8	11.8	7.0	6.0	11.4
14b	5.2	5.4	10.7	5.4	5.6	8.4
14c	6.4	5.7	11.6	6.6	5.9	11.6
15a	5.5	5.4	7.4	5.6	5.6	7.2
15b	5.5	5.7	9.8	5.7	5.9	8.6
15c	5.4	5.2	7.5	5.5	5.5	7.2

Adjusted camera station consistantly accurate to ± 1 meter cross track, ± 5 meters in track, and ± 5 meters elevation.

Adjusted camera orientations consistantly accurate to ± 3 arc-seconds for each orientation angle.

Table 3-23 — Ground Point Location Errors Constrained Extension in Positional Mode at 160 Nautical Miles

Ground control points located on initial model; uses orbital parameters obtained from long arc solution

	No Radar Altimeter			With Radar Altimeter		
Points	Cross-Track Error, meters	In-Track Error, meters	Elevation Error, meters	Cross-Track Error, meters	In-Track Error, meters	Elevation Error, meters
1a	10.4	6.1	9.1	9.9	6.0	8.8
1b	12.5	6.0	8.8	12.2	5.8	8.7
1c	15.8	6.6	9.1	15.7	6.4	9.1
2a	10.7	5.3	7.9	10.2	5.2	7.6
2b	12.8	4.9	7.6	12.3	4.8	7.3
2c	16.9	5.4	8.1	16.9	5.2	7.9
3a	12.9	6.2	10.4	12.3	5.8	8.8
3b	14.4	5.8	10.1	14.5	5.4	7.5
3c	20.3	6.0	10.3	20.2	5.7	8.8
4a	13.9	7.2	13.8	13.7	6.4	12.0
4b	15.6	6.6	12.6	15.6	5.9	8.7
4c	21.9	6.9	13.6	21.7	6.3	11.9
5a	14.1	7.2	11.8	13.8	6.3	8.9
5b	16.3	6.9	11.5	16.2	6.0	7.6
5c	22.4	7.0	11.7	22.1	6.2	8.9
6a	15.0	7.9	14.3	15.0	6.8	11.7
6b	17.0	7.5	13.5	17.0	6.4	8.8
6c	23.9	7.8	14.4	23.5	6.7	12.0
7a	15.6	8.0	12.5	15.6	6.8	8.9
7b	18.1	7.7	12.2	17.6	6.4	7.6
7c	24.5	7.9	12.4	24.3	6.7	9.0
8a	16.9	8.6	14.9	16.7	7.2	11.9
8b	19.0	8.2	13.9	19.0	6.8	8.8
8c	26.1	8.5	14.8	25.9	7.1	11.9
9a	16.9	8.7	12.9	17.2	7.1	8.9
9b	19.9	8.4	12.7	19.9	6.9	7.6
9c	26.8	8.5	12.8	26.7	7.0	8.9
10a	18.3	9.1	15.1	18.5	7.5	11.9
10b	20.8	8.7	14.1	20.9	7.1	8.8
10c	28.3	8.9	15.0	28.2	7.4	11.9
11a	18.9	9.0	13.1	18.9	7.5	8.9
11b	21.7	8.0	12.9	21.7	7.3	7.6
11c	29.2	8.9	13.0	29.0	7.4	8.9
12a	20.2	9.3	15.4	20.1	8.0	11.8
12b	23.1	8.9	14.4	23.0	7.6	8.7
12c	30.7	9.1	15.1	30.6	7.8	11.6
13a	20.7	9.1	13.7	20.5	8.2	8.9
13b	23.9	8.8	13.5	23.3	7.8	7.5
13c	31.5	9.0	13.6	31.3	8.0	8.9
14a	21.7	9.4	16.1	21.7	8.9	11.9
14b	24.9	9.0	15.2	24.8	8.4	7.3
14c	32.9	9.2	15.8	32.8	8.6	11.6
15a	22.7	9.9	16.3	22.4	9.7	11.4
15b	25.7	9.3	15.7	25.6	9.0	8.7
15c	33.9	9.5	16.1	33.7	9.2	11.3

Adjusted camera stations consistantly accurate to ± 1 meter cross track, ± 5 meters in track, ± 5 meters elevation.

Adjusted camera orientations consistantly accurate to ±3 arc-seconds for each orientation angle.

Table 3-24 — Ground Point Location Errors Constrained Bridge in Positional Mode at 160 Nautical Miles

Ground control points located on terminal models; uses orbital parameters obtained from long arc solution

	No Radar Altimeter			With Radar Altimeter		
Point	Cross-Track Error, meters	In-Track Error, meters	Elevation Error, meters	Cross-Track Error, meters	In-Track Error, meters	Elevation Error, meters
1a	9.0	5.9	8.8	9.1	6.0	8.7
1b	10.4	5.8	8.7	10.9	5.8	8.7
1c	13.1	6.3	8.9	13.9	6.3	8.8
2a	8.6	5.0	7.6	8.9	5.0	7.4
2b	10.0	4.6	7.4	10.7	4.7	7.3
2c	13.1	5.0	7.7	13.9	5.0	7.6
3a	9.9	5.5	9.9	10.4	5.4	8.8
3b	10.9	5.2	9.6	11.7	5.1	7.4
3c	15.2	5.4	9.7	16.1	5.4	8.8
4a	10.6	6.3	13.2	11.1	6.0	11.9
4b	11.4	5.8	12.1	12.0	5.4	8.7
4c	16.1	6.1	13.1	16.9	5.9	11.8
5a	10.1	6.1	11.0	10.6	5.7	8.9
5b	11.4	5.8	10.7	12.0	5.5	7.5
5c	15.8	6.0	10.9	16.5	5.7	8.8
6a	10.8	6.6	13.6	11.3	6.1	11.6
6b	11.8	6.2	12.7	12.3	5.7	8.7
6c	16.6	6.5	13.7	17.1	6.1	11.9
7a	10.4	6.3	11.6	10.8	5.9	8.9
7b	11.7	6.1	11.3	12.1	5.6	7.5
7c	16.1	6.2	11.5	16.6	5.9	8.9
8a	11.1	6.6	13.9	11.4	6.2	11.9
8b	12.0	6.2	12.8	12.4	5.8	8.7
8c	16.8	6.6	13.8	17.1	6.1	11.9
9a	10.6	6.2	11.4	10.8	5.9	8.9
9b	11.9	6.0	11.2	12.2	5.6	7.6
9c	16.4	6.2	11.3	16.6	5.8	8.9
10a	11.3	6.3	13.6	11.4	6.0	11.8
10b	12.1	6.0	12.5	12.3	5.5	8.7
10c	16.9	6.4	13.6	17.0	6.0	11.8
11a	10.8	5.9	10.5	10.9	5.6	8.7
11b	12.0	5.6	10.3	12.3	5.4	7.4
11c	16.5	5.9	10.5	16.6	5.5	8.7
12a	11.5	5.9	12.5	11.6	5.8	11.6
12b	12.4	5.5	11.4	12.5	5.4	8.6
12c	17.1	5.8	12.3	17.2	5.7	11.3
13a	9.7	5.0	6.9	9.6	5.1	6.5
13b	12.5	5.2	8.9	12.7	5.2	7.2
13c	14.6	5.0	7.1	14.8	5.0	6.6
14a	12.5	5.9	11.9	12.3	6.0	11.5
14b	11.7	4.8	7.3	13.2	5.5	8.4
14c	17.9	5.7	11.6	18.0	5.9	11.2
15a	10.4	5.5	7.6	10.3	5.7	7.3
15b	13.8	5.7	9.8	13.8	5.9	8.4
15c	15.2	5.4	7.8	15.3	5.5	7.5

Adjusted camera stations consistantly accurate to ± 1 meter across track, ± 5 meters in track, ± 5 meters elevation.

Adjusted camera orientations consistantly accurate to ± 3 arc-seconds for each orientation angle.

Table 3-25 — Ground Point Location Errors Unconstrained Bridge in Positional Mode
(H = 160 Nautical Miles)

	No Elevation Control			With Elevation Control		
Point	Cross-Track Error, meters	In-Track Error, meters	Elevation Error, meters	Cross-Track Error, meters	In-Track Error, meters	Elevation Error, meters
1a	6.9	9.5	8.6	6.8	9.4	8.5
1b	6.9	9.9	7.7	6.9	9.7	7.6
1c	6.4	14.2	8.9	6.7	14.1	8.8
2a	7.2	9.5	7.7	7.2	9.4	7.6
2b	6.4	11.4	8.7	6.4	11.3	8.7
2c	7.2	14.2	7.9	7.2	14.1	7.8
3a	7.9	10.6	7.0	7.7	9.4	6.8
3b	7.5	11.5	7.0	7.4	10.9	6.9
3c	7.5	14.8	7.2	7.4	13.9	7.1
4a	15.0	12.9	11.0	12.2	10.8	10.9
4b	12.9	13.0	12.4	9.1	12.2	8.0
4c	11.7	16.9	12.0	10.2	16.3	10.8
	13.8	13.7	18.3	13.5	10.6	10.3
5b	22.6	13.1	18.4	11.5	12.1	8.8
5c	20.1	14.7	18.4	11.2	13.4	10.3
6a	31.1	11.7	19.6	15.7	9.1	12.0
6b	27.8	14.3	19.8	12.5	13.2	8.5
6c	26.2	15.5	19.5	13.3	14.9	11.7
7a	35.0	10.8	21.6	15.2	8.0	10.1
7b	34.2	12.6	22.4	13.9	11.0	9.3
7c	30.8	19.8	23.4	13.8	14.9	11.4
8a	33.6	14.9	17.5	15.8	10.7	11.5
8b	33.8	15.3	19.3	13.7	12.3	8.5
8c	32.1	20.8	20.2	14.8	16.3	12.4
9a	32.4	18.0	23.0	14.5	11.1	10.8
9b	32.1	18.6	23.4	13.6	16.1	11.4
9c	30.1	22.8	23.9	13.6	12.7	9.4
10a	29.8	21.9	20.2	14.8	12.3	11.6
10b	29.6	22.3	20.6	12.8	15.4	8.6
10c	29.1	23.1	22.4	14.1	16.8	12.4
11a	26.6	21.5	24.3	13.2	11.9	11.2
11b	25.6	22.4	25.2	11.9	14.8	9.7
11c	25.3	23.2	25.6	12.3	16.2	11.5
12a	20.2	24.0	20.4	12.9	12.7	11.7
12b	20.9	22.2	21.2	10.8	13.7	8.6
12c	20.7	23.1	22.6	12.0	16.9	12.5
13a	16.9	18.6	25.8	9.6	11.3	10.9
13b	15.5	17.2	26.8	8.3	12.4	9.5
13c	12.5	15.9	27.0	8.6	14.8	11.4
14a	17.7	17.6	19.2	10.8	11.5	11.4
14b	17.4	16.5	21.2	8.3	12.7	8.6
14c	15.3	16.3	23.8	9.4	15.4	12.6
15a	6.8	10.5	8.3	6.3	8.8	6.8
15b	6.7	11.4	7.6	6.1	10.4	7.0
15c	6.8	12.8	7.8	6.0	12.3	7.3

Table 3-27 — Uncontrolled Positionally Constrained Three Photo Model at 160 Nautical Miles

No ground control; uses stellar orientations and long arc positions.

Point	Photos	Cross-Track Error, meters	In-Track Error, meters	Elevation Error, meters
1a	1-2	21.9	16.6	29.8
1b	1-2	22-6	16.7	29.4
1c	1-2	25.9	17.1	29.8
1d	1-2	29-8	18.2	30.6
2a	1-2	21.1	14.1	27.4
2b	1-2	22.6	13.8	25.1
2c	1-2	26.0	13.8	25.2
2d	1-2	30.1	14.4	27.3
3a	1-2-3	20.4	13.1	22.7
3b	1-2-3	22.8	12.9	22.2
3c	1-2-3	26.8	12.9	22.2
3d	1-2-3	30.1	13.1	22.6
4a	1-2-3	21.1	12.9	23.2
4b	1-2-3	23.6	12.5	22.7
4c	1-2-3	27.1	12.5	22.7
4d	1-2-3	31.1	12.6	23.2
5a	1-2-3	21.7	13.4	23.6
5b	1-2-3	23.8	12.8	23.2
5c	1-2-3	27.8	12.7	23.2
5d	1-2-3	31.8	12.8	23.6
6a	2-3	23.4	16.3	29.7
6b	2-3	25.3	15.0	28.6
6c	2-3	29.0	14.9	28.6
6d	2-3	33.6	15.0	29.8
7a	2-3	24.2	20.6	31.2
7b	2-3	26.2	18.9	31.7
7c	2-3	29.9	18.7	31.6
7d	2-3	34.7	18.3	32.2

Adjusted camera orientations consistently ±3 to 4 arc-seconds for each angle.

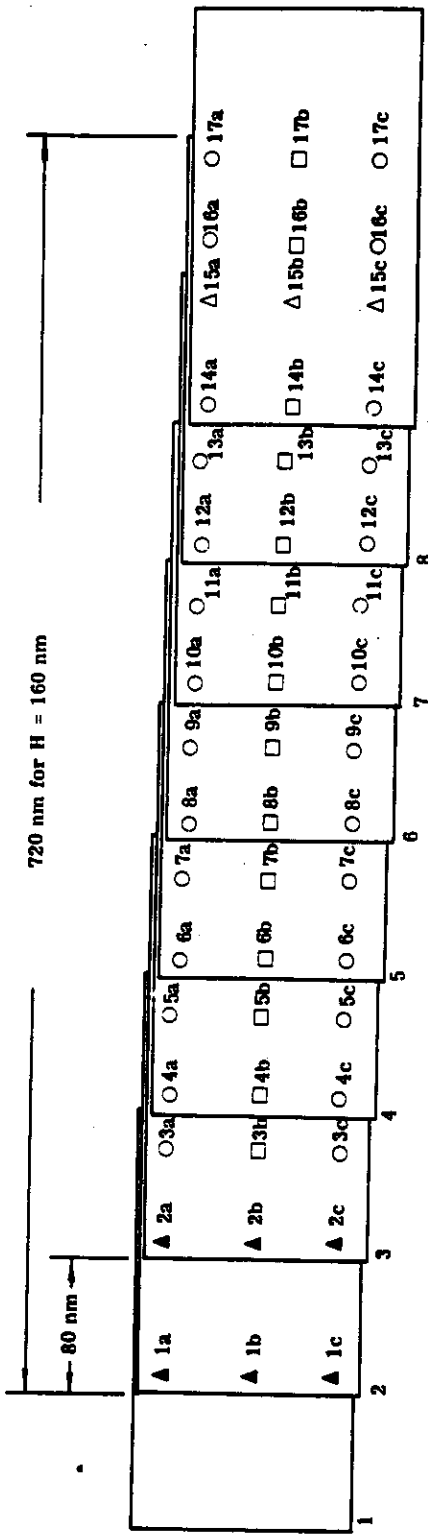

Fig. 3-5 — Location of ground points for strip triangulations

3.5 SUBSTANTIATING STUDIES

Many different types of data, in addition to those specifically collected by the GOPSS, will be used in the envisioned reduction scheme to calculate orbital parameters, orbital positions, and the location of ground points. Both the input data and the computed outputs will be metrically represented in different reference frames characteristic of their differing nature. It is considered necessary to describe the basic coordinate reference systems that will be utilized in the GOPSS, together with the transformations that relate them to each other.

The description of these basic systems forms the first part of this study. This necessarily means that some consideration of "time" is made within this section, since time is the metric quantity that is common to all dynamic systems. Time will be considered in detail in the second portion of this study, which means that a certain amount of duplication exists.

The third section considers the accuracy of a specific type of coordinate data, namely stellar positions. This investigation of the accuracy of stellar catalogs is vital to the understanding of the errors that might be incurred through the use of satellite-borne stellar photography.

3.5.1 Coordinate Systems

3.5.1.1 Introduction

Owing to the varied nature of the system inputs, various coordinate systems will be required in the data reduction scheme. For geodetic purposes, three distinct systems are necessary. These will be expressed in terms of rectangular Cartesian coordinates, since they are easily managed and readily transformed into other Cartesian systems. The three basic systems are:

1. Terrestrial reference system
2. Celestial reference system
3. Orbital reference system

Although the terrestrial system is defined by the mean terrestrial pole and mean Greenwich meridian of a certain date, and the celestial system by the mean equator and ecliptic of a certain date, in practice both systems are actually defined by the coordinates of physical points.

Thus, the terrestrial system consists of a number of distinct geodetic systems; the celestial being defined by the mean places and proper motion of the reference stars in a catalog. These two systems are related by a knowledge of the instantaneous pole, Greenwich sidereal time, and the constants of precession and nutation.

3.5.1.2 Terrestrial Systems

An ideal terrestrial coordinate system has been defined by Veis such that the origin is located at the center of gravity of the earth, the Z-axis directed to the mean north pole, and the

X-Z plane parallel to the meridian of Greenwich. This fixed system requires that the center of gravity of the earth be known and, therefore, is replaced, in practice, by a number of geodetic systems (X_g, Y_g, Z_g) defined by the geodetic coordinates (Φ_o, λ_o, H_o) of the origin of each geodetic datum. The origin of such a system may be transformed into the ideal terrestrial system, and is a function of the absolute deflections of the vertical, ξ, ν, ζ, (expressed in linear units) at the datum origin according to

$$\bar{X}_o = \begin{bmatrix} X_o \\ Y \\ Z_o \end{bmatrix} = \begin{bmatrix} \sin\Phi_o \cos\lambda_o & \sin\lambda_o & -\cos\Phi_o \cos\lambda_o \\ \sin\Phi_o \sin\lambda_o & \cos\lambda_o & -\cos\Phi_o \sin\lambda_o \\ -\cos\Phi_o & 0 & -\sin\Phi_o \end{bmatrix} \begin{bmatrix} \xi \\ \eta \\ \zeta \end{bmatrix}$$

Provided that the geodetic systems are correctly oriented by astronomic methods, each system is paralled to the ideal terrestrial system. In practice, however, small errors in azimuth (dA), meridian tilt ($d\xi$), prime vertical tilt ($d\eta$), and scale (dE) exist at the origin of the datum (since these are all determined by observational methods).

Transformation of a geodetic system into the idealized terrestrial system is obtained from

$$\bar{X}_i = (\bar{X}_i)_g + \bar{X}_o + M_A\, M_\xi\, M_\eta\, (\bar{X}_i - \bar{X}_o)_g + E\, (\bar{X}_i - \bar{X}_o)_g$$

where

$$M_A = \begin{bmatrix} 1 & +dA \sin\Phi_o & -dA \cos\Phi_o \sin\lambda_o \\ -dA \sin\Phi_o & 1 & +dA \cos\Phi_o \cos\lambda_o \\ +dA \cos\Phi_o \sin\lambda_o & -dA \cos\Phi_o \cos\lambda_o & 1 \end{bmatrix}$$

$$M\xi = \begin{bmatrix} 1 & 0 & -d\xi \cos\lambda_o \\ 0 & 1 & +d\xi \sin\lambda_o \\ d\xi \cos\lambda_o & d\xi \sin\lambda_o & 1 \end{bmatrix}$$

$$M_\eta = \begin{bmatrix} 1 & -d\eta \cos\Phi_o & -d\eta \sin\Phi_o \sin\lambda_o \\ d\eta \cos\Phi_o & 1 & d\eta \sin\Phi_o \cos\lambda_o \\ d\eta \sin\Phi_o \sin\lambda_o & -d\eta \sin\Phi_o \cos\lambda_o & 1 \end{bmatrix}$$

Despite the internal consistency that exists within geodetic nets (about 10^{-5}), nonconnected triangulations may be at different scales, which is why the scale error, E, has been included above.

3.5.1.3 Celestial Systems

For points that do not rotate with the earth, for example stellar bodies, it is desirable to define a coordinate system that is independent of the Earth's rotation. The true pole is in motion, and defined by the instantaneous axis of rotation of the Earth. This is determined by the International Latitude Service, in terms of the angular coordinates of the instantaneous pole with respect to the mean pole, used to define the terrestrial system. The rotation around this instantaneous axis is measured by sidereal time—the Greenwich hour angle of the vernal equinox.

It should be noted that the equinox is in motion due to the precession and nutation. Both of these effects are dependent on the orbital configuration of the solar system and, being functions of ephemeris time, may be predicted in advance. In addition, there are variations in the rotation of the Earth which cannot be predicted and must be measured.

Both mean and true sidereal time (referrring to mean and true equinoxes respectively) are given as functions of universal time, which is defined from actually observed sidereal time, according to analytical expression. This time, corrected for motion of the pole is UT-1, which is further corrected for seasonal variation in the Earth's rotation to yield UT-2. Since this seasonal variation is extrapolated from past observational data, UT-2 is not exactly uniform time.

This mean sidereal time is defined as

$$\bar{\theta} = 100^\circ .075542 + 360^\circ .985647348\ (\text{MJD}-33282.0) + 0^\circ .2900\ (\text{MJD}=33282.0)^2 \times 10^{-12}$$

and the true sidereal time by

$$\begin{aligned}\theta = \bar{\theta} &- 4.392 \times 10^{-3} \sin (12^\circ .1128 - 0^\circ .52954T) \\ &+ 0^\circ .053 \times 10^{-3} \sin 2\,(12^\circ .1128 - 0^\circ .52954T) \\ &- 0^\circ .325 \times 10^{-3} \sin 2\,(280^\circ .0812 - 0^\circ .985647T) \\ &- 0^\circ .050 \times 10^{-3} \sin 2\,(64^\circ .3824 + 13.176398T)\end{aligned}$$

where the modified Julian Date, MJD, = JD - 2400000.5 and T = MJD - 33282.0. This value of θ is accurate to better than 0.2 inch. For higher accuracies, additional terms for the nutation in RA will be required. The independent variable, T, has to be expressed in UT-1.

If the observations are made with respect to a clock keeping UT-2C as given by WWV or VLF radio transmissions, this time must be converted to UT-1 by use of the corrections published by the U.S. Naval Observatory. The application of the preliminary corrections to convert UT-2C to UT-1 results in a standard error of sidereal time of about 5 milliseconds. For orbital work, ephemeris time is ideal. This is not available until several years after the necessary data has been collected, but may be adequately substituted for by Atomic Time A-1. Since UT-2C is at a constant offset rate from A.1, A.2 could be computed from the known value of UT-2C. However, it is recommended that the corrections published by the U.S. Naval Observatory be used if available.

The true sidereal system, $\bar{X}_S$, is related to the terrestrial system according to

$$\bar{X} = S_\theta X_S$$

where

$$S_\theta = \begin{bmatrix} \cos\theta & \sin\theta & x \\ -\sin\theta & \cos\theta & -y \\ -x\cos\theta - y\sin\theta & -x\sin\theta + y\cos\theta & 1 \end{bmatrix}$$

and x, y are the coordinates of the instantaneous pole (radians).

The axes of the system defined above are not fixed with respect to the star background, owing to the luni-solar gravitational attraction on the Earth's equatorial bulge. The effect of nutation may be removed to yield a system, $\bar{X}_p$, that has only a long term periodic motion according to

$$\bar{X}_s = M_\Delta \bar{X}_p,$$

where

$$M_\Delta = \begin{bmatrix} 1 & -\Delta\mu & -\Delta\nu \\ \Delta\mu & 1 & -\Delta\epsilon \\ \Delta\nu & \Delta\epsilon & 1 \end{bmatrix}$$

$\Delta\mu$, $\Delta\nu$, $\Delta\epsilon$, being the nutation in right ascension, declination, and obliquity, according to

$$\begin{aligned}
\Delta\mu = {} & -76.7 \times 10^{-6} \sin (12^\circ.1128 - 0^\circ.0529539T) \\
& +0.9 \times 10^{-6} \sin 2 (12^\circ.1128 - 0^\circ.0529539T) \\
& -5.7 \times 10^{-6} \sin 2 (280^\circ.0812 + 0^\circ.9856473T) \\
& -0.9 \times 10^{-6} \sin 2 (64^\circ.3824 + 13^\circ.176396T)
\end{aligned}$$

$$\begin{aligned}
\Delta\nu = {} & -33.3 \times 10^{-6} \sin (12^\circ.1128 - 0^\circ.0529539T) \\
& +0.4 \times 10^{-6} \sin 2 (12^\circ.1128 - 0^\circ.0529539T) \\
& -2.5 \times 10^{-6} \sin 2 (280^\circ.0812 + 0^\circ.9856473T) \\
& -0.4 \times 10^{-6} \sin 2 (64^\circ.3824 + 13^\circ.176396T)
\end{aligned}$$

$$\begin{aligned}
\Delta\epsilon = {} & 44.7 \times 10^{-6} \cos (12^\circ.1128 - 0^\circ.529539T) \\
& -0.4 \times 10^{-6} \cos 2 (12^\circ.1128 - 0^\circ.529539T) \\
& +2.7 \times 10^{-6} \cos 2 (280^\circ.0812 + 0^\circ.9856473T)
\end{aligned}$$

This instantaneous mean system may be referenced to a mean system of standard epoch (1950.0) and, by eliminating the precession effects, yields a fixed celestial system, $\bar{W}$, related to the $\bar{X}_p$ system according to

$$\bar{X}_p = P \bar{W}$$

where the matrix, P, is given by

$$P = \begin{bmatrix} \cos\omega & -\sin\omega & 0 \\ \sin\omega & \cos\omega & 0 \\ 0 & 0 & 1 \end{bmatrix} \begin{bmatrix} \cos\nu & 0 & -\sin\nu \\ 0 & 1 & 0 \\ \sin\nu & 0 & \cos\nu \end{bmatrix} \begin{bmatrix} \cos\kappa & -\sin\kappa & 0 \\ \sin\kappa & \cos\kappa & 0 \\ 0 & 0 & 1 \end{bmatrix}$$

where $\kappa = 23''.0495.t + 0''.30 \times 10^{-4} \cdot t^2$

$\omega = 23''.0495.t + 1''.09 \times 10^{-4} \cdot t^2$

$\nu = 20''.0426.t + 0''.43 \times 10^{-4} \cdot t^2$

t being the epoch in tropical years since 1950.0. The terrestrial system is related to this inertial celestial system, $\bar{\bar{W}}$, according to

$$\bar{\bar{X}} = S_\theta \, M_\Delta \, P \, \bar{\bar{W}}$$

At this point it is to be noticed that the ideal celestial system can be replaced by a number of systems, as the terrestrial systems are replaced by several geodetic systems. Each of these astrometric systems is associated with a star catalog that gives the mean positions and proper motions of the stars, which are not always referred to the same equator and equinox. Transformations may be made between the existing catalogs by applying the appropriate systematic and periodic corrections.

3.5.1.4 Orbital Systems

Desirably, orbital reference systems should be inertial, and preferably use the midepoch of the interval for which the orbit is computed. Owing to the motion of the Earth in such a system, due to precession and nutation, a periodic perturbation occurs. For an inertial system, only the effect caused by the equatorial bulge, J_2 , needs to be considered.

If reference is made to the sidereal system, all zonal harmonics are fixed, the tesseral and sectorial harmonics rotating with the earth. Perturbations will occur however, since the sidereal system is not inertial, but a combined system that minimizes the perturbations has been devised.

Veis' combined system for minimizing the perturbations has been proved to be the least influenced by precession and nutation. This modified sidereal system ($\bar{\bar{X}}_m$) is related to the true sidereal system ($\bar{\bar{X}}_s$) according to

$$\bar{\bar{X}}_m = R\bar{\bar{X}}_s$$

where

$$R = \begin{bmatrix} \cos(\mu + \Delta\mu) & \sin(\mu + \Delta\mu) & 0 \\ -\sin(\mu + \Delta\mu) & \cos(\mu + \Delta\mu) & 0 \\ 0 & 0 & 1 \end{bmatrix}$$

μ being the precession in R.A. since 1950.0. The modified sidereal time (angle), $\dot{\theta}$, between the X_m - axis and the Greenwich meridian is

$$\dot{\theta} = \theta - (\mu + \Delta\mu) = \bar{\theta} - \Delta\mu$$

The transformation that relates these modified coordinates to the celestial ones is

$$\bar{\bar{X}}_m = R.M.\Delta P \, W$$

and that between the terrestrial and modified system

$$\bar{\bar{X}} = M_m \, \bar{\bar{X}}_m$$

where

$$M_m = \begin{bmatrix} \cos\dot{\theta} & \sin\dot{\theta} & x \\ -\sin\dot{\theta} & \cos\dot{\theta} & -y \\ -x\cos\dot{\theta} - y\sin\dot{\theta} & -x\sin\dot{\theta} + y\cos\dot{\theta} & 1 \end{bmatrix}$$

so that

$$\vec{X} = M_m \text{ R.M. } \Delta P\, \vec{W}$$

This reference system, devised by Veis, eliminates the use of the ecliptic. In order to determine the relation between the celestial and terrestrial systems, the sidereal system is used as an intermediary only, for which the equator is a necessary reference plane, affected by precession and nutation. The x axis, being selected as the mean equinox of a standard epoch (1950.0), is also the x axis of the celestial system. However, it does not lie on the true equator of the same date, so that a reduction for the nutation is applied.

This system has been used as a reference frame for satellite orbits computed at the Smithsonian Astrophysical Laboratory since 1959.

3.5.1.5 Conclusion

The selection of an appropriate terrestrial coordinate system for use in the data reduction scheme may be completely arbitrary, since it is possible to transform between each system.

It is suggested, in view of the parallelism between different geodetic systems and the miniscule errors dA, $d\xi$, $d\eta$, and dE, that terrestrial coordinates be expressed in the ideal terrestrial systems. This implies that the value of such points are approximated by the local geodetic coordinates, and a solution for the absolute deflection components at the origin of each geodetic system is obtained. This is one of the objectives of the program.

There is no reason why the celestial and orbital coordinate systems should not be one and the same. Desirably, this should be inertial, so that the absolute values of the harmonics of the Earth's potential can be determined without being influenced by precession and nutation effects. As pointed out, the various celestial systems are subject to inaccuracies. The discussion of the sources of these errors and the recommendation for the system to be used is the content of Section 3.5.5.

3.5.2 Time Systems

Three basic systems of time that are important in geodetic observations are ephemeris, atomic, and astronomical. A brief description of these three systems is given in the following paragraphs.

3.5.2.1 Ephemeris Time

Ephemeris time is the independent variable in the solar, lunar, and planetary theories. It is a uniform time which is defined so that the length of the day in ephemeris time is equal to the average length of the day in universal time over the last three centuries. Ephemeris time is theoretically defined by the orbit of the Earth about the sun alone, but it is necessarily determined

from observations of the moon. Ephemeris time is not available until the reduction of the moon observations is obtained, but this causes no practical problem as atomic time can be substituted for ephemeris time.

3.5.2.2 Atomic Time

Atomic time, A-1, is derived from atomic frequency standards. These are based upon the frequency, γ, corresponding to a transition between two atomic states separated in energy by ΔE, according to the Bohr relation

$$h\gamma = \Delta E$$

where h is Planck's constant. There is no proven difference between atomic time and ephemeris time, although integration over an extremely long period of time may show slight differences. Since ephemeris time is not available until the moon observations are reduced, atomic time is substituted for ephemeris time for the accurate determination of interval and frequency.

Systems of atomic time are set up by averaging a number of atomic resonators and defining the mean as atomic time. The system in most common use is A-1, set up by the U.S. Naval Observatory using the weighted mean of a number of atomic resonators tied together by VLF transmissions.

3.5.2.3 Astronomical Time

Astronomical time (as either sidereal or universal time) is a measure of the rotation of the earth. The Earth is subject to changes in rotation which can be classified as secular retardation, irregular variations, and periodic variations, in the order of a year or less.

The secular retardation, which is attributed to tidal friction, causes an increase in the difference between astronomical time and ephemeris time which can be predicted and is so small as to be of no practical importance in astronomical observations.

The irregular variation, which has not been completely explained but is thought to be due to changes in the Earth's core, cannot be predicted and causes an important discrepancy between astronomical and ephemeris or atomic time. This difference must be accounted for in astronomical and geodetic observations.

The periodic variations are probably due to changing meteorological conditions throughout the year. The effect on time, however, is suprisingly uniform from one year to the next.

In addition to the periodic variations in the rotation of the Earth, there are variations in the position of the instantaneous pole of rotation of the earth that produce an apparent variation in time. This variation of latitude places a limitation upon the accuracy to which astronomic time can be determined. An error of 0.01 second in the latitude produces an error of about one millisecond in time. Although the position of the pole is immediately known to 0.03 second, the accurate determination of astronomical time must wait for the reduction of the latitude data by the International Latitude Service. In retrospect, astronomical time can be determined to about one millisecond from the average of all PZT's and astrolabe sights for one day.

Astronomical time is determined by measuring the transits of stars. This is given in sidereal time to an instantaneous pole which can be changed to universal time by a rigorous formula. When corrections are applied to bring this to the mean pole, the transformed time is UT-1. The national time services further transform UT-1, which is the time that must be used

for geodetic and astronomical measurements, to UT-2. UT-2 can be compared more easily with E.T. and UT-2C. The system UT-2C is broadcast by WWV, and meets the requirements for modern day timekeeping systems. These requirements are:

1. The phase angle of the Earth must be available, since this is needed for astronomical observations and for the purposes of geodetic measurements.
2. The time must have an invariant rate, in order to meet the demands for physical measurements and frequency control.

The UT-2C system meets the second requirement by offsetting the rate from atomic time, A-1, by $50 \times n$ parts in 10^{10} where, n, is an integer. This rate is only changed at the first of the year. The requirement that UT-2C gives a good value for the phase angle of the Earth is accomplished by changing the clock by 100 milliseconds at the first of a month, if UT-2C differs from UT-2 by more than 100 milliseconds. If the offset rate of UT-2C from A-1 is a good choice as to the variation between atomic time and the rotation of the Earth, then it should not be necessary to change UT-2C by 100-millisecond jumps for that year. In actual practice it is extremely difficult to determine when the irregular variation will change direction, so that for the past several years it has been necessary to introduce 100-millisecond jumps in the broadcasts for UT-2C. Thus, UT-2C is a combination of universal time and atomic time, giving approximately the epoch of universal time and the frequency of atomic time plus a known offset rate.

The radio time signals broadcast by WWV give UT-2C. These can be reduced to a preliminary value to UT-1 using the predicted position of the pole as given by the International Time Service. The final accuracy of the difference between UT-2C and UT-1 is determined by the International Time Service using data from the complete system of latitude stations.

3.5.3 Frequency Standards

The basis of any modern timing system is a stable frequency source. Great strides have been made in recent years in improving frequency standards. The clock associated with the frequency standard counts the number of cycles elapsed between the epoch of the clock and the event to be timed.

Of prime importance is the stability of the oscillator driving the clock. Oscillator stability is usually expressed in terms of $\Delta F/F$ per unit time, where ΔF is the change in frequency per unit time and F is the nominal value of the frequency. For example, short term stability may be expressed as one part in 10^{13} per second, or longer term stability as one part in 10^{10} per day.

Let us consider the effect of oscillator drift on time. If the drift rate is one part in 10^8 per day, then each day as given by a clock driven by this oscillator is one part in 10^8 shorter (or longer) than the true length of the day. If LOD (length of day) we have, after ten days,

$$\Delta \text{ (LOD)} = \Delta F/F \text{ (10 days)} = 8.64 \times 10^{-3} \text{ second}$$

The average amount by which each day is short is 1/2 (8.64×10^{-3}) seconds or 4.32×10^{-3} second. Then the accumulated time difference, ΔT, will be the average amount by which each day is short times the number of days.

$$\Delta T = (4.32 \times 10^{-3} \text{ second/day})(10 \text{ days})$$

$$\Delta T = 4.32 \times 10^{-2} \text{ second} \quad \text{or } 43.2 \text{ milliseconds}$$

In general, we have

$$\Delta T = 8.64\ CT + 4.32\ KT$$

where ΔT is the time in microseconds, C is the initial frequency offset in parts in 10^{10}, K is the drift rate in parts in 10^{10} per 24 hours, and T is the time in days.

In terms of stability and reproducibility, the best frequency sources are atomic resonators. These devices depend upon an atomic transition to provide the frequency either by absorption at resonance by gas, the atomic beam method, the maser principle, or the optical microwave double resonance technique.

The rubidium frequency standard, unlike the cesium beam, is not a primary reference standard because the rubidium gas cell must be adjusted, using a cesium or other suitable reference source to give the correct frequency. Once this adjustment has been performed, the rubidium can serve as a frequency standard. The performance of rubidium is far superior to that of quartz oscillators.

Other atomic frequency standards such as the hydrogen maser and NH_3 maser are not suitable for airborne applications. Very good results have been obtained by thallium beam standards, but the equipment has not been designed into a small package as in the case of cesium and rubidium.

For reliability of operation and minimum volumetric and power requirements, the quartz crystal oscillator is unexcelled as a frequency source. Quartz oscillators have very good short term stability but over long periods they tend to drift badly. At the U.S. Naval Observatory, quartz oscillators have been used to drive the clocks on a continuous basis with periodic comparisons with cesium standards to correct long term drift.

Quartz crystals tend to age and change frequency after a number of years, but the best frequency stability is attained after the oscillator has been in operation for at least a month.

Where the clock can be calibrated occasionally or is not required to operate for long periods of time, quartz oscillators offer considerable savings in weight and power requirements over atomic frequency standards.

Quartz frequency standards are entirely suitable for millisecond timing accuracy if it is not required that they operate for longer than about 20 days without calibration or time checks. If periodic time checks are available as in the Navy Navigational Satellite System, and a method is provided either to adjust the oscillator or change the counting rate of the clock, then the quartz crystal oscillator has sufficient short term stability to operate a clock for the life of the system. It is pointed out that it is not necessary to adjust the oscillator physically, provided that a record of the calibration checks is made and subsequently imposed analytically.

3.5.4 Accuracies of Star Catalogs

The users of stellar photography frequently ask for the accuracy with which star positions can be obtained. This is rarely answered satisfactorily, owing to the long lead time and voluminous amount of work required in order to determine specific accuracies. However, valid estimates of mean catalog errors are available, which are of great value to the engineer who uses stellar positions as a tool, not requiring an ultimate limiting accuracy. Although a comprehensive

analysis of the accuracy of stellar positions is academically desirable, and serves to indicate the future of stellar mapping programs, the systems engineer cannot afford, nor requires, to wait the years necessary to complete such a program.

In the course of this analysis, it has been found that in the material that has been published, many misleading statements have been made. The significant work consulted, apart from the introductory material included in the catalogs themselves, are due to Scott, Eichorn, the Franklin Institude, and the great Russian work "Fundamental Astronomy" of the Pulkovo observatory.

In regard to this discussion, it becomes obvious that the consideration cannot be completely divorced from the studies of coordinate systems and time determinations. Consequently, although this is at present an independent study, it will not be treated as such in the final system integration.

In order that the ensuing sections might be appropriately considered, let us consider the general philosophy of catalog errors, with special reference to the Washington N 30 catalog, the internal precision of which approaches 0.1 second. However, this was published in 1952 using observations relating to a mean epoch of 1930. Consequently, any errors in the proper m motions must be propagated over a 35-year period, and although the proper motions of the N 30 stars are among the most accurately known, average standard errors accumulate at the rate of 0".006 per annum. In addition systematic errors also exist, and contribute in an unknown way to the end result. The subsequent sections will consider:

1. Systematic errors of catalogs
2. The derivation of a general system
3. Technique for comparing catalogs
4. An evaluation of the various catalogs

Systematic Errors of Catalogs

Systematic errors of stellar catalogs in right ascension α, declination δ, and proper motions μ are usually expressed in the form:

$$\Delta\alpha = \Delta E + \Delta\alpha_{\alpha} + \Delta\alpha_{\delta} + \Delta\alpha_{m}$$

$$\Delta\delta = \Delta\delta_{\alpha} + \Delta\delta_{\delta}$$

$$\Delta\mu = \Delta\mu_{\alpha} + \Delta\mu_{\delta} + \Delta\mu_{m}$$

$$\Delta\mu = \Delta\mu'_{\alpha} + \Delta\mu'_{\delta}$$

where ΔE = zero point correction to true equinox
$\Delta\alpha_\alpha$ = error in α, as a function of α
$\Delta\alpha_\delta$ = error in α, as a function of δ
$\Delta\alpha_m$ = error in α, as a function of magnitude
$\Delta\delta_\alpha$ = error in δ, as a function of α
$\Delta\delta_\delta$ = error in δ, as a function of δ
$\Delta\mu_\alpha$ = error in μ, as a function of α
$\Delta\mu'_\delta$ = error in μ, as a function of δ
$\Delta\mu_m$ = error in μ, as a function of magnitude
$\Delta\mu'_\alpha$ = error in μ', as a function of α
$\Delta\mu'_\delta$ = error in μ', as a function of δ

The above equations are approximate. The systematic errors are functions of all parameters simultaneously. The $\Delta\alpha_\delta$, $\Delta\delta_\delta$, $\Delta\mu_\delta$, $\Delta\mu'_\delta$ are usually considered constant for the entire catalog, whereas the other terms are examined individually for zones of declinations. Let these errors be considered:

1. ΔE is the adjustment to the catalog coordinate system needed to have the origin of the right ascension catalog system coincide with the equinox at epoch. Even the absolute catalogs of most observatories are dependent upon a correction to the true equinox for the catalog construction normally uses the origins of coordinates of the fundamental catalogs.

2. $\Delta\alpha_\alpha$ is a periodic error which can be expressed as:

$$\Delta\alpha_\alpha = a \sin \alpha + b \cos \alpha + c \sin 2\alpha + d \cos 2\alpha$$

The $\Delta\alpha_\alpha$ term is also a function of declination if the observatory clock is at the wrong rate; however, most modern observatories do not have this problem. Other than clock errors, the $\Delta\alpha_\alpha$ error is the result of diurnal influences, instrument variations, seasonal variations, personal responses, and refractional variation.

3. $\Delta\alpha_\delta$ is mainly due to instrumental effects, personal errors of a systematic nature, refraction anomalies. One form of $\Delta\alpha_\delta$ is the discontinuity at the zenith which results in a personal error as the observer is forced into a new position. This systematic error is determined by comparing different declination zones: for zones far from the equator $\Delta\alpha_\delta \cos \delta$ is compared.

4. $\Delta\alpha_m$ is essentially a personal error. All observers record the transit of bright stars early when compared to the transit of faint stars. The errors vary from observer to observer, from magnitude to magnitude. The older catalogs list coordinates of faint stars that were determined by correlation with bright stars (as in the AG zone catalog). The errors in such an approach are substantial and are presently undertermined. The modern catalog does not have this particular error in position; however, there are statistical discrepancies between the proper motions of bright and faint stars that have not been eliminated.

5. $\Delta\delta_\alpha$ errors are periodic and their major causes are seasonal instrumental effects and refractional changes. The equation

$$\Delta\delta_\alpha = a \sin \alpha + b \cos \alpha$$

adequately expresses this term; however, in some of the older catalogs the wrong nutation correction was applied, and this produced an effect that was incorporated into the $\Delta\delta_\alpha$.

In the case of absolute observations, the wandering of the pole and the variations in latitude are additional sources of error. If the period of observation is many years, the 14-month (Chandler) period can be excluded, but latitude variation, composed of two components (a polar motion, and a local component or "Z" term) have an additional annual component. Corrections, in accordance with the data from the International Latitude Service for polar motion is not sufficient; all absolute observations must be correlated to the local variations of latitude at epoch.

The $\Delta\delta_\alpha$ of the catalogs seldom exceeds 0".2, and are commonly less than 0".1.

6. $\Delta\delta_\delta$ are the most complicated and largest systematic errors of catalogs. The greatest contributions are instrumental, personal, and refractional. The personal contribution at the discontinuity at the zenith can develop systematic differences at either side of the zenith as great as 0".4 (Pulkovo Declination Catalogs of 1845). The $\Delta\delta_\delta$ of the catalogs are independent if the latitude variation and refraction determination are carried independently. The error is at its largest near the equator and is one of the serious problems in astronometry.

The systematic errors in proper motion are completely analagous with those in right ascension and declination, and need no further consideration here.

Derivation of a Fundamental System

The objective of a Fundamental System, such as the F.K. 4, is to represent the true system of spherical coordinates as accurately as possible, from all available independent fundamental positions of stars. The basic principles outlined below may also be used in a more restricted sense, in converting stellar positions from one catalog to another. The essential steps are stated below.

First, the systematic differences of all contributing catalogs must be removed (personal, instrumental, refractional, etc.). These purified data serve as the basis of the new system. Let $a_1, a_2, a_3, \ldots a_n$ be the coordinates in right ascension of N catalogs of various observatories at corresponding epochs $t_1, t_2, t_3, \ldots t_n$; let K be the star in the existing fundamental system.

Second, reduce $a_1, a_2, a_3, \ldots a_n$ and K to a common equinox and epoch, t_0. A new star system is generated by calculating the systematic corrections to the coordinates and proper motions of the stars in the existing fundamental and to each, and all, of the observatories' catalogs. Let the corrections to a particular star be

ΔK = correction to the star's position in α in the fundamental system

$\Delta\mu$ = correction to the star's proper motion

a_1 = correction to the star's position in α in the observatory

"i" catalog and let the true position in the new system be K' at epoch t_0.

Apart from random errors,

$$\left.\begin{aligned} K' &= K_1 + \Delta K_1 = a_1 + \Delta\mu\ (t_o - t_1) \\ K' &= K_2 + \Delta K_2 = a_2 + \Delta\mu\ (t_o - t_2) \\ K' &= K_3 + \Delta K_3 = a_3 + \Delta\mu\ (t_o - t_3) \\ &\cdot \\ &\cdot \\ &\cdot \\ K' &= K_N + \Delta K_N = a_N + \Delta\mu\ (t_o - t_N) \end{aligned}\right\} \qquad (3.1)$$

Now, expand this scheme to include all stars in a region of sky with the star in question as for example, a zone of declination or right ascension. The ΔK, $\Delta\mu$, a_i are treated as systematic corrections of a particular nature, such as $\Delta\alpha_\alpha$, $\Delta\delta_\delta$, or $\Delta\alpha_m$. The N catalogs differ in the individual systematic errors which are intrinsic to each catalog, and furnish N condition equations containing N+2 unknowns, so that two additional conditions are needed. One of the two additional conditions can be that the fundamental system has been derived as a weighted mean of the observational catalogs, thus:

$$\sum_N W_i\ \Delta a_i = 0 \qquad (3.2)$$

However, there is good reason to regard the M most recent catalogs, which have been compiled by modern methods, with special attention. A second equation analogous to Equation 3.2 for all the M catalogs may then be:

$$\sum_M W_i\ \Delta a_i = 0 \qquad (3.3)$$

At this point let t_o be defined as the weighted mean epoch of the M most recent catalogs:

$$t_o = \left(\sum_M W_i\ t_i\right)\ \left(\sum_M W_i\right)^{-1} \qquad (3.4)$$

This can be done if the corrections for the mean proper motions are included in $(K_i - a_i)$ of (1).

Now, each condition equation of the form 3.1 is multiplied by the appropriate catalog weight, and then combined in conjunction with Equation 3.2, and similarly treated with Equations 3.3 and 3.4. The following two equations result:

$$\Delta K \sum_M W_i + \Delta\mu \sum W_i\ (t_i - t_o) = -\sum_N W_i\ (K_i - a_i) \qquad (3.5)$$

$$\Delta K \sum_M W_i = \sum_M W_i\ (K_i - a_i) \qquad (3.6)$$

Equation 3.6 yields ΔK directly, and Equation 3.5 gives $\Delta\mu$. Substituting, the results into Equation 3.1, a_1 can be determined.

Technique of Comparing Catalogs

In order that data from various catalogs might be compared the following steps are necessary.

1. The two catalogs to be compared are referred to one epoch by means of the proper motions of FK4.

2. The $\Delta\alpha$ (catalog minus FK4) are formed for all stars in common, which are grouped into 5-degree zones in δ in the range -80 to +80 degrees, the limits being 0, 5, 10, . . . up to 80 degrees (the polar stars are examined separately) and are formed into means. Adjustment in threes give the final $\Delta\alpha_\delta$, which are subtracted from all $\Delta\alpha$.

3. The residuals ($\Delta\alpha - \Delta\alpha_\delta$) for the equatorial zone (from -25 to +40 degrees for the northern catalog) are divided into groups with limits 0h, 1h, 2h, and so on. Averages within the groups are adjusted in threes to give the final $\Delta\alpha_\alpha$ for this zone, which is denoted by $(\Delta\alpha_\alpha)_1$; they are subtracted from the residuals for stars of all zones.

4. The $\Delta\alpha_\alpha$ for the stars in the other zones (+40 to +60 degrees and +60 to +80 for the northern catalogs) are found by combining the residuals $\Delta\alpha - \Delta\alpha_\delta - \Delta\alpha_\alpha$ into three-hour groups twice, (the first with limits of 0h, 3h, 6h, etc., and the second with limits of 1.5h, 4.5h, etc.). Those for the northern (+60 to +80 degrees) zone are multiplied by the corresponding cos δ; the means are combined with the $(\Delta\alpha_\alpha)_1$ to give (without further smoothing) the final values.

5. The $\Delta\alpha_m$ (brightness effects) are deduced by arranging the $\Delta\alpha - \Delta\alpha_\delta - \Delta\alpha_\alpha$ in order of increasing m, the values being formed into groups covering 15 to 25 stars. The mean is calculated for each group, as is the mean m, and these are adjusted by mean of $\Delta\alpha - x + (m - 4.0)\, y$. All differences are freed from $\Delta\alpha_m$ if significant results are obtained.

6. The systematic differences are checked for completeness by averaging the $\Delta\alpha - \Delta\alpha_\delta - \Delta\alpha_\alpha - \Delta\alpha_m$ over areas of dimensions 2h in α and 10 degrees in δ, the results being examined for any residual trend with Δ and δ.

Various Catalog Accuracies

Each star catalog refers to a specific epoch, and the accuracy of star positions at some other epoch depends on the accuracy of the star's proper motion. Thus, if the mean errors of proper motion at the epochs t_1 and t_2 are known to be ϵ_1 and ϵ_2, the mean error ϵ of an extrapolated position at time t is obtained as

$$\epsilon = |\epsilon_1^2 (t - t_2)^2 + \epsilon_2^2 (t - t_1)^2|^{1/2} \quad (t_2 - t_1)^{-1}$$

This is the basic equation from which the tabulated mean errors of the various catalogs can be projected.

The following catalogs are in general use, and are briefly described:

1. Boss (GC): The GC was compiled from over 50 different catalogs during the years 1905 to 1937, and lists the coordinates and proper motion of 33,342 stars. The probable error of the standard stars (1900) is 0.1", but the probable error of over 2/3 of the stars exceeds 0.3".

The errors in proper motions have a greater dispersion. The GC has a degree of completeness through the seventh magnitude, although many eighth and ninth magnitude stars are included. It should be pointed out that the probable error of the faint stars in position and motion are always of less accuracy than those of bright stars in any system, and as a consequence the fainter stars of the GC have errors far worse than those quoted.

"Modern positions derived from the GC are so far in error that the expression, 'GC system,' has no meaning when applied to them" — F. P. Scott, Accuracy of Star Positions, U.S. Naval Observatory. The GC was quite accurate at the time of its mean epoch, and the main problem in using the GC for current times is the proper motions. Approximately eight or nine stars brighter than seventh magnitude from the GC would be required to give the same accuracy as the N 30. Stars fainter than the seventh magnitude in the GC have a range of errors from 0.6" to 1.0" at epoch 1965.0, and the errors are unquestionably systematic.

2. N 30: The N 30 appeared in 1952, and has 5,268 stars well distributed over the entire sky. It has a mean epoch of 1930, and at this current epoch (1965) two N 30 stars give the same accuracy as one FK4 star (the two N 30 stars must be seventh magnitude or brighter). The probable error of the N 30 is of the order 0.1" to 0.2". The N 30 is perhaps the best system of its size, for accurate astronometry having well distributed stars; however, evidence is available which suggests that the system is not completely homogenous. The FK4 and the N 30 systems are departing from one another in quite a pronounced manner. By 1975, the two right ascension systems will have deviated from each other by approximately 0.80" at -60 degrees declination.

3. Yale Zones: The AGK1 (Astronomische Gesellschaft Katalog) was completed at the turn of the century. For its development zones of declination were set up, in which visual observations were undertaken. These same declination zones were employed in the construction of the Yale Catalog. The Yale Zone Catalog included the proper motion of the AGK1 which are poor. As a result, the Yale System is not homogenous, but it does contain a large number of coordinates and motions of fair quality. The Yale System is composed of 22 catalogs, contains 145,000 stars, and covers from 90 to -30 degrees in declination. This system would not suffice for detailed position programs. Estimated mean errors are in the order of 0.3" to 1.4".

4. AGK2: The AGK2 was developed at the same time as the Yale, using the same declination zones. There was one difference between the two approaches. The makers of the AGK2 considered the AGK1 too inhomogenous, and thus did not use the AGK1 proper motions. The AGK2, integrated into FK3 system, yields a completely homogenous picture of the northern sky.

5. FK3: The FK3 is a network of 1535 stars, which was used as the ultimate fundamental system for nearly all differential positional work prior to the advent of the FK4. The mean positions of this catalog were published yearly to 0.01", but the probable errors of position were of the order of 0.2". Systematic corrections have been uncovered in recent years with an order of magnitude of 0.2". A revision of the FK3 has resulted in the FK4. These data have been derived from the mean error at epoch and an annual proper motion, which are in the order of 0.042" and 0.0024" respectively.

6. FK4: The FK4 represents at this time (1965) the most homogenous system available. Each of 1535, well distributed over the entire sky, have been observed in absolute and differential series. (The FK4 stars are those of the FK3.) The epoch and equinox is of 1950.0, the mean error at epoch and in annual proper motion being 0.033" and 0.0016" respectively.

7. S.A.O. Star Catalog: The S.A.O. is a reduction of all available stellar catalogs to a homogenous frame of reference—the FK4. The total number of stars is 258,997, covering the entire sphere, having a star density of 6 stars per square degree.

The catalog is available in three formats: magnetic IBM-729 tapes; printed book form; and a set of 156 star charts. The average error of the S.A.O. catalog is a little better than that of the GC. A more detailed representation of the errors is given in the histogram shown in Figure 3-6.

Perhaps the most significant attribute of the S.A.O. catalog is the extensive data available for each star. The most pertinent information, for the purposes of error analyses, that are listed with each star position are:

1. The right ascension and declination for the equator, equinox, epoch 1950.
2. The standard deviation of position at epoch.
3. The right ascension and declination for the equator and equinox of 1950 at the mean epoch of the original observations.
4. The standard deviations of 3.
5. The mean epochs for the original observations.
6. The proper motions in right ascension and declination.
7. The standard deviations of 6.

It would appear that this monumental work will not be surpassed until observational data are available for a revision of the fundamental system.

The distribution of stars and their positional accuracies for the catalogs that have been described are summarized by Table 3-28.

Concluding Remarks

From the survey that has been made, it is apparent that one can apply appropriate weights to the positions of stars that might be used in a data reduction shceme. It appears obvious that the S.A.O. catalog is the most appropriate to use in a data reduction scheme, although the average standard error is greater than that of the FK4. Essentially, it maintains the accuracy that could be obtained from the FK4 catalog, if only the FK4 stars are used, and cannot be much worse than the accuracies that are obtainable through using any other catalog. Although it may never provide better results than the separate catalogs, since this is a transformation of all cataloged data to the most modern fundamental reference frame, thereby containing unknown and undeterminable systematic errors, it is the most extensive and homogenous catalog that exists.

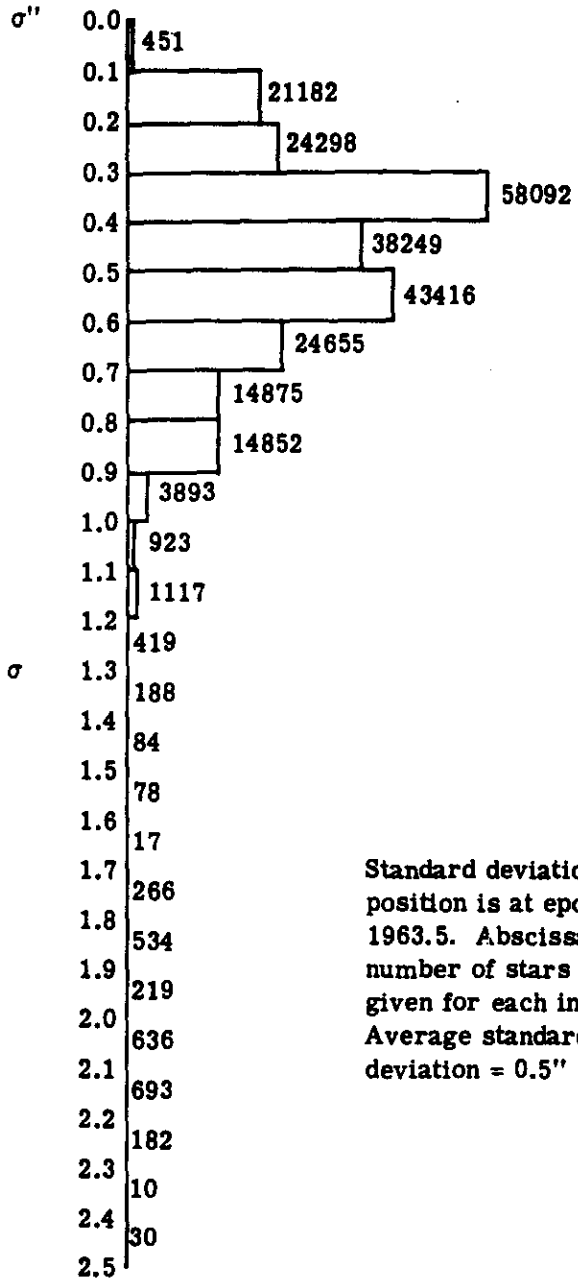

Fig. 3-6 — Frequency diagram of SAO position errors

Table 3-28 — Stellar Distribution Accuracies of Major Star Catalogs

Catalog	Mean Epoch 1900+	Number of Stars	Number per Degree	Mean Error (1965) α, δ	Mean Error (1965) μ	Zones
Yale 26	51	1,031		0.22	0.6	90 to 85
Yale 27	47	8,164		0.24	0.6	60 to 55
Yale 26	47	8,380		0.24	0.6	55 to 50
Yale 24	23	10,358		0.51	0.9	30 to 25
Yale 25	28	8,703		0.43	0.7	25 to 20
Yale 18	40	9,092		0.37	0.8	20 to 15
Yale 19	40	8,967		0.46	1.1	15 to 10
Yale 22	40	1,904		0.46	1.1	10 to 9
Yale 22	37	9,060		0.50	1.1	9 to 5
Yale 20	37	7,996		0.46	1.0	5 to 1
Yale 21	37	5,583		0.50	1.1	1 to -2
Yale 17	34	8,108		0.61	1.3	-2 to -6
Yale 16	34	8,248		0.57	1.2	-6 to -10
Yale 11	34	8,101		0.78	1.7	-10 to -14
Yale 12	34	8,563		0.82	1.8	-14 to -18
Yale 12	34	4,553		0.74	1.6	-18 to -20
Yale 13	34	4,292		0.74	1.6	-20 to -22
Yale 14	34	15,110		0.82	1.8	-27 to -30
Cape 17	32	12,864		1.03	2.1	-30 to -35
Cape 18	36	12,115		0.80	1.8	-35 to -40
Cape ZC	00	20,843		0.96	1.0	-40 to -52*
Cape 19	38	9,215		0.52	1.2	-52 to -56
Cape 20	46	14,710		0.80	1.2	-56 to -64
GC (Boss)	00	33,342	0.8	0.66		90 to -90
Cape	32	80,000	9.5	0.55		-30 to -64
Yale	36	145,000	6.9	0.45		30 to -30
N30	30	5,268	0.13	0.21		90 to -90
AGK2	30	180,000	8.3	0.21		90 to -2
FK3	12-15	1,535	0.04	0.2		90 to -90
FK4	50	1,535	0.04	0.12		90 to -90
SAO	50	258,997	6.0			90 to -90

*No proper motions.

3.6 RESEAU SPACING

The appropriate spacing of reseau crosses, as implied previously, is largely dependent on the method of applying reseau data. One may either use the measured and calibrated reseau data to determine the parameters of an analytical function that appropriately expresses the film distortion or use these data for interpolation of the distortion.

In either case, the supposition is that the systematic film distortions can be expressed as a continuous function of the measured coordinates. Let the distortion be symbolized as

$$\Delta x = f_1(x^0, y^0)$$

and

$$\Delta y = f_2(x^0, y^0)$$

where x^0, y^0 denote the measured film coordinates. Furthermore, let the interval between reseau crosses be denoted h. Within this interval, linear interpolation may be performed such that the interpolation error E, is never greater than a value

$$E \leq M_2 h^2/8$$

where M_2 is the maximum absolute value of the second derivative of the function over the range h; i.e.,

$$M_2 = |f^{ii}(x^0, y^0)|$$

Hence, in order to make the value of E less than some desired magnitude, say e, the maximum interpolating interval is given by

$$h \leq (8e\ M_2)^{1/2}$$

Similarly, second order interpolation yields a maximum error of

$$E = M_3 h^3/9\sqrt{3}$$

where $M_3 = |f^{iii}(x^0, y^0)|$

Over the range 2h. For third order interpolation, the maximum error is

$$E \leq 3M_4 h^4/128$$

where $M_4 = |f^{iv}(x^0, y^0)|$

over the range 3h.

These formulas are easily rearranged to determine the maximum value of h.

The problem of finding the maximum value of $|M_k|$ consists of determining whether the value M_{k+1} becomes zero within the interval under consideration. However, if a maximum does not exist within this interval, then, since the function is continuous, it must be either increasing or decreasing. By applying Rolle's Theorem, the maximum must lie at either the upper or lower bound of the interval.

Let us consider a specific example, using actual measured data. These data were obtained by multiple measurements of a 9- by 18-inch grid, at 1/4-inch intervals and of contact prints onto a thin base Estar film. The variances of the calibrated grid coordinates was determined as 2.4×10^{-6} mm^2, and that of the measured film as 4.56×10^{-6} mm^2.

These data were used to determine the coefficients of a complete cubic transformation, suppressing all but the major 2" intersections. Using the computed parameters, the suppressed film data were transformed. The results indicated that no significant difference between the 2" fit and the transformation of suppressed data existed. This meant that the selected cubic model was a valid model, and that a reseau spacing closer than 2 inches was unnecessary. The specific computational output on which these conclusions are based, and the substantiation that the expression for systematic film shrinkage was indeed valid, are now summarized.

Data for corresponding film and reseau measurements, at 2-inch intervals, were used to determine the 20 coefficients expressing the film shrinkage. The standard deviation of these film measurements, after adjustment was ±0.98 micron. These parameters were then used to determine the residual error at every point that had been measured, resulting in a standard deviation of ±1.06 microns. Subsequent computations with the original data have been performed to determine the cubic model to which all data is fitted. This gives a closer estimate of the parameters of the equations

$$x = A + Bx^0 + Cy^0 + Dx^{0^2} + Ex^0y^0 + Fy^{0^2} + Gx^{0^3} + Hx^{0^2}y^0 + Ix^0y^{0^2} + Jy^{0^3}$$

and

$$y = A' + B'x^0 + C'y^0 + \quad \ldots + I'x^0y^{0^2} + J'y^{0^2}$$

in addition to enabling the independence of the distortions in x and y to be confirmed.

This means that

$$f_1^{ii}(x^0, y^0) = 2D + 6Gx^0 + 2Hy^0$$

and

$$f_2^{ii}(x^0, y^0) = 2F' + 2I'x^0 + 6J'y^0$$

which are maximized to yield the appropriate values of $|M_2|$. On evaluating the various values of E, for various values of h, the errors in linear interpolation are:

h	Ex, microns	Ey, microns
1"	0.11	0.04
2"	0.44	0.17
$2\frac{1}{2}$"	0.69	0.26
3"	0.99	0.37
4"	1.76	0.67

The interpretation of these results is that for the thin based Estar film that was measured in reseau spacing closed than 5 cms is unnecessary, provided that a valid expression for the systematic film shringkage is obtained, if one uses linear interpolation. Naturally, for quadratic or higher interpolation, the errors are considerably reduced.

3.7 CONCLUSIONS

The conclusions resulting from the numerical studies conducted during the photogrammetric task of the feasibility study are as follows:

1. The positional error of a point on the orbit (Table 3-11), with respect to the centroid of five landmarks common to three consecutive photographs, can be determined to better than ± 65 feet at 200 nautical miles, ± 58 feet at 160 nautical miles (with accuracy), and ± 41 feet at 120 nautical miles. These values are the maximum axial dimensions of the bounding error ellipsoid, and were derived using a pessimistic weighting factor without altimetric control.

2. The location of landmarks with respect to the orbit can meet the specified horizontal accuracy of ± 200 feet for altitudes equal to or less than 200 nautical miles, and the specified elevation accuracy of ± 40 feet for altitudes equal to or less than 160 nautical miles, provided altimetric control is available in each frame or if careful mensuration techniques are used. Without altimeter data, elevation errors in the order of 75 feet are to be expected at the 160-nautical mile altitude.

This section reviews some of the computational results obtained in this study, and examines the conditions under which the specified landmark accuracies can be met.

One group of studies, Section 3.4.2, assumes that landmark locations are known to ± 1000 feet. Using this information, and varying the accuracy of the orbital positions, it will be possible to furnish ground positioning data with respect to a world geodetic system; this information also defines the satellite's orbit.

Another group of studies, Sections 3.4.1 and 3.4.3, examine the accuracy of positioning camera stations and landmarks with respect to a local geodetic survey network. The datum errors in the local system must be applied to these results if the absolute accuracy of these studies is to be evaluated. It should be emphasized that the residual error in the determination of the datum shifts should be applied, and not the datum shifts themselves, in estimating this absolute accuracy.

Next consider the three photo models, constrained to the orbital parameters and stellar orientations, in which no ground controls are assumed to be known to better than 1 kilometer. The results, listed in Tables 3-26 and 3-27 (the so-called uncontrolled constrained models) indicate that the horizontal positional accuracy of landmarks with respect to the orbit can be readily attained. The essential data extracted from these calculations are as follows:

Altitude, nautical miles	Cross-Track Errors, feet	In-Track Errors, feet	Specifications, feet
160	33 - 46	43 - 61	200
200	43 - 54	82 - 110	200

The conclusion that the horizontal accuracies for landmark location can be met is confirmed by similar calculations in Section 3.4.2.1, provided that the orbital constraints and weighting factors applied to the reduced photographic coordinates are valid, or provided that the degradation of these factors does not decrease the accuracy of landmarking beyond the specified tolerances.

The effects of degrading the quality of the orbital covariance matrix, according to scalar multiplications of 10, 100, and 1000 is examined in Section 3.4.2.2. From the results listed in Table 3-10, it can be seen that the specified horizontal accuracies of landmark determination are met when the orbital parameters are degraded ten times (covariance matrix multiplied by a scalar of 100) from those applied in the remaining photogrammetric studies.

Meeting the elevation accuracy specification of 40 feet requires some means of establishing supplemetary elevation control. Such data is available from the radar altimeter which is incorporated into the total GOPSS instrument package. In addition to providing a sufficiency of ground elevation data, the radar altimeter also furnishes data that is of value in the determination of the earth's potential field.

The basic information furnished by the altimeter is a series of distances between the orbiting vehicle and the earth's surface. These vertical distances can be imposed on the photogrammetric solution according to the principles outlined for auxiliary data in Section 3.3. These altimeter data can also be used to provide absolute elevations to numerous points imaged on the photography.

There are two basic problems involved in such a use of the altimeter. The first of these is to determine the points from which the radar returns are obtained; the second is the provision for some reference datum for the reduced elevations.

In conventional aerial photography which uses a radar altimeter, the directional antenna is boresighted with a spotting camera to facilitate identification of the points of radar returns. This is not an absolute necessity since the metric camera itself can be considered a spotting camera. Provided that the vehicle ground track can be determined from the metric camera photographs, the points from which radar returns are obtained can be readily identified. By selecting returns from large flat areas such as lake surfaces that lie along the vehicle track, great precision may be obtained. In this manner, it is envisioned that a large number of scale distances for each mission can be obtained. If the orbit determination is sufficiently accurate, as concluded in Volume 4, the orbit forms a good datum from which the absolute elevations of identified points can be obtained. Alternatively, many of these points, such as lake surfaces, already have well known elevations, and can be used as the basis of further orbital constraints, or as prior elevation control points. For example, Lake Baykal, near the northern Mongolian border is of considerable geographic interest and is known to lie at an altitude of 1500 feet.

The radar altimeter provides elevation control along the vehicle ground track for each photograph. For controlling photogrammetric models, it is desirable that elevations are located at the lateral margins of the photographs as well. In this regard, it has been shown in Section 3.4.2.1 that the central elevation control is sufficient to suppress the elevation errors close to the system requirements. For a multimission system, such as the GOPSS, marginal elevation control points should be readily available by transferring data points between mission photography. In an operational GOPSS, it is envisioned that elevation control points will be adequate to meet the system's specified elevation accuracies. This conclusion is predicated on the use of the radar altimeter and the determinations of the geodynamic terms, and, in this regard, the radar altimeter data can be of considerable value.

The following data, obtained from Table 3-9, summarize the effect of additional data on the minimization of positional errors at the anticipated 160-nautical mile orbit with the orbit constrained to parameters given in Section 3.4.2.2.

	No Control, feet	Plus Altimeter, feet
Across track	39	39
Along track	43	42
Elevation	77	43

This would enhance the system capability and provide for adequate constraints to the determination of shifts between independent geodetic datums. In this regard, it is considered desirable to summarize the significant cases of strip triangulations that have been performed in which the specified horizontal and elevation accuracies have been simultaneously met.

Table 3-29 shows that some of the constrained triangulations exceed the nine-photo strip length. These extrapolations are obtained by considering the maximum errors in an extension, which are certainly larger than the maximum errors of a bridge that is twice as long.

Note that these data are restricted because of the high accuracy required of the ground elevations and that the ground control errors are assumed to be known to within ± 10 meters. If, as is expected and has been verified by the orbital studies, the datum shifts between various geodetic nets can be determined with an accuracy of ± 10 meters, these tabulated data can be applied to landmark positioning with respect to a fundamental geodetic system.

With regard to the ground handling of mission photography, present techniques and equipment can be used, and should be within the capability of any large photographic laboratory; however, a realistic and efficient data handling flow must be established to process the large amount of film that will result from system photography.

Table 3-29 — Maximum Number of Model Triangulations Meeting Landmark Specifications

	Altitude 120 nautical miles		Altitude 160 nautical miles		Altitude 200 nautical miles	
Case	No radar altimeter	With radar altimeter	No radar altimeter	With radar altimeter	No radar altimeter	With radar altimeter
Positional extension	3 models	5-6 models	2 models	4 models	1 model	2 models
Orbital extension	8-9 models	9 models	4 models	7 models	1 model	4 models
Positional bridge	5 models	8-9 models	7 models	8 models	2 models	5 models
Orbital bridge	16-18 models	18 models	8 models	8-14 models	2 models	8 models

3.8 BIBLIOGRAPHY

3.8.1 Film Distortion

Adelstein, P., and Leister, D., Nonuniform Dimensional Changes in Topographic Aerial Film, Photogram. Eng., XXIX: (1) (1963).

Brock, R., and Faulds, R., Film Stability Investigation, Photogram. Eng., XXIX: (5). 1963.

Eastman Kodak Company, Manual of Physical Properties of Kodak Aerial Films and Special Sensitized Materials, (1963).

Hothmer, J., Possibilities and Limitations for Elimination of Distortion in Aerial Photography Photogram. Record, II: (2) (1958); III:(13).

Lampton, B., Film Distortion Compensation, Photogram. Eng., XXXI:(5) (1965).

Laurila, S., Some Aspects of Systematic Distortion for Photographic Image Points, O.S.U.R.F.. T.R. (595)-12-197 (1955).

Takeda, M., Experimentation With Polyester Film T-008 Japan Soc. of Photogram. 1 (1964).

Talts, J., Various Transformation for Correction of Errors Caused by Film Deformation, Sartryck ur Svensk Lantmateritidskrift, 3, (1964).

Tewinkel, G., Film Distortion Compensation for Photogrammetric Use, U.S.C.G.S. Tech. Bull. 14 (1966).

Trachsel, A., Reseau Techniques, Photogram. Eng., XXXI (5) (1965).

3.8.2 Instrument Calibration and Errors

Bennet, J., Method of Determining Comparator Screw Errors With Precision, Opt. Soc. Am.. 51: (10) (1961).

Gugel, R., Comparator Calibration, Photogram. Eng., XXI: (5) (1965).

Hallert, B., Fundamental Probelms in Photogrammetry, Report of Study Group Commission II, I.S.P. (1964).

Hallert, B., Determination of Precision and Accuracy of a Stereo comparator, Fotogrammetriska Meddelanden IV: (4) (1964).

Hallert, B., Accuracy and Precision in Photogrammetry, Photogram. Eng., XXIX (1) (1963).

Hallert, B., Determination of Geometrical Quality of Comparators for Image Coordinates, Gimrada Research Note 3 (1962).

Hoewen, E., Coordinate Measurement, Photogram. Eng., XXX: (6) (1964).

Lyon, D., Let's Optimize Stereoplotting, Photogram. XXX: (6),(1964).

Rosenfield, G., Calibration of Precision Coordinate Comparator, Photogram. Eng., XXIX: (1) (1962).

Schmid, H., Analytical Photogrammetric Instruments, Photogram. Eng., XXX: (4) (1964).

3.8.3 Aberration

Merritt, E., Image Aberration, Photogram. Eng., XXIX: (1) (1963).

Veis, G., Geodetic Applications of Observations of the Moon, Artificial Earth, Satellites and Rockets, Dissertation, Ohio State University, (1958).

Veis, G., Geodetic Uses of Artificial Earth Satellites, Smithsonian Contributions to Astrophysics, 3: (9) (1959).

3.8.4 Camera Calibration Techniques

Brown, D. C., Advanced Reduction and Calibration for Photogrammetric Cameras, AFCRL-64-40 (1964).

Brown, D. C., A Treatment Analytical With Emphasis on Ballistic Cameras, R.C.A., T.R. 39 (1957).

Brown, D. C., Decentering Distortion and Definitive Calibration of Metric Cameras, Presented Paper, A.S.P. (1965).

Schmid, H., General Analytical Solution to the Problem of Photogrammetry, B.R.L. Report 1065 (1959).

Washer, F. E., Calibration of Photogrammetric Lenses and Cameras at the National Bureau of Standards, Photogram. Eng., XXIX: (1) (1963).

3.8.5 Refraction

Case, J. B., Atmospheric Refraction for Satellite Photography, Autometric Corporation Report 56-8B-1 (1962).

Chatfield, A., Influence of Atmospheric Refraction on Positions Obtained From High Oblique Photography, O.S.U.R.F., T.R. (485)-14-174 (1953).

DuFour, H. M., Selection of Formulae of Atmospheric Refraction for Ballistic Camera Observations (In French), Bulletin Geodesique, (Sept. 1964).

Garcia, H., Atmospheric Refraction, Autometric Corporation Technical Report 61-505 (1961).

Holland, A., The Effects of Amostpheric Refraction on Angles Measured From a Satellite, Gephys. Res., 66: (12) (1961).

Jones, B., Photogrammetric Refraction Angle: Satellite Viewed From Earth, Geophys. Res. 66: (4) (1961).

Schmid, H., Influence of Atmospheric Refraction on Directions Measured to and from a Satellite, Gimrada Research Note 10 (1963).

3.8.6 Analytical Photogrammetry and Miscellaneous

American Society of Photogrammetry, Manual of Photogrammetry, Third ed., 1966.

Anderson, J. M., Analytical Aerotriangulation Using Triplets International Archives of Photogrammetry, XV, Lisbon (1965).

Arthur D.W.G. Analytical Aerial Triangulation at the Ordinance Survey, Photogram. Record (1959).

Bachmann, W. K., Theorie des Erreurs et Compensation des Triangulations Aeriennes, Lausanne, 1946.

Brock, G. C., The Status of Image Elevation in Aerial Photogrammetry, International Archives of Photogrammetry, XV, Lisbon (1965).

Brown, D. C., Matrix Treatment of the Method of Least Squares Considering Correlated Observations, BRL Report 937 (1955).

Brown, D. C., Solution to the General Problem of Multiple Station Analytical Stereotriangulation, R.C.A. Data Reduction, Technical Report 43 (1959).

Brown, D. C., Results in Geodetic Photogrammetry I, R.C.A. T.R. 54 (1959).

Brown, D. C., Introduction of Orbital Constraints into Adjustment of a Satellite Photogrammetric Net, 1960, unpublished.

Brown, D. C., Results in Geodetic Photogrammetry II, R.C.A. T.R. 65 (1960).

Brown, D. C., Results in Geodetic Photogrammetry III, I.C.F. Scientific Report 2 (1961).

Brown, D. C., Bush, N., and Sibol, J., "Study of the Feasibility of Rocket and Satellite Approaches to the Calibration of Tracking Systems," (AFCRL, 63-789), D. Brown Associates Inc., 1963.

Brown, D. C., Bush, N., and Sibol, J., "Investigation of the Feasibility of Self Calibration of Tracking Systems," (AFCRL 64-441), D. Brown Associates Inc., 1963.

Eichorn, H. K., Modern Developments and Problems in Photometric Astrometry, Photogram. Eng., (1964).

Ghosh, S. K., Determination of the Weights of Parallax Observations for Numerical Relative Orientation, Photogram. Eng., (1963).

Groves, G. and Owen, G., Camera Plate Reduction by Means of Star Field Reference, Photogram. Record, (1960).

Hallert, B., Investigation of the Weights of Image Coordinates in Aerial Photographs, Photogram. Eng., (1961).

Hallert, B., Fundamental Problems in Photogrammetry, International Archives of Photogrammetry, XV, Lisbon (1965).

Mason d'Autume Le Traitement Numerique des Blocs D'aerotriangulation. S.F.P., Bull. Number 18 (1965).

Mikhail, E. M., Analytical Aerotriangulation: Two Directional Triplets in Subblocks, International Archives of Photogrammetry, XV, Lisbon, (1965).

Miles, M. J., Methods of Solution of the Adjustment of a Block of Aerial Triangulation, Photogram. Record (1963).

Molnar, L., The Measurability and Legibility of Aerial Photographs, Geodezia ES Kartografia, (1963).

Osborne, E. E., On Least Squares Solutions of Linear Equations, Assoc. for Computing Machinery, (1961).

Schmid, H. H., and Schmid, E., A generalized Least Squares Solution for Hybrid Measuring Systems, U.S.X.G.S. (1964).

Schmid, H. H., Basic Considerations for the Future Development of Computational Photogrammetric Methods at the Coast and Geodetic Survey, U.N. Cartographic Conference, Manila (1964).

Schmid, H. H., Geodetic Measurements from Satellites, A.G.U. Symposium Washington, D. C. (1966).

S.F.P. Special Bulletin Number 14, devoted to Aerotriangulation (1964).

Singleton, Notes on Matrix Notation for Performing Statistical Manipulation, M.C.R.L. Tech. Memo. Number 8 (1956).

Tienstra, J. M., Theory of the Adjustment of Normally Disturbed Observations, ARGUS, Amsterdam (1956).

Schemerhorn, W., "Collected Essays on Photogrammetry," Jubilee Volume, I.T.C., Delft, (1965).

Thompson, E. H., Analytical Aerial Triangulation, Societe Francaise de Photogrammetry, Bulletin Number 18 (1965).

Togliatti, G., Experimental Research of Several Types of Analytical Bridging: Statistical Analysis of Model Errors, International Archives of Photogrammetry, XV, Lisbon (1965).

Weightman, J. A., Analytical Procedures in Photogrammetry, Photogram. Record, (1961).

Von Gruber, " Photogrammetry," English Ed., London, 1931.

Zeller, M., "Lehrbuch der Photogrammetrie," Zurich, 1947.

3.9 MAPPING CAPABILITIES

While satisfying the GOPSS objectives, the data collection system will provide data usable for mapping purposes. These data are the photographs themselves and the coordinates of imaged landmarks that can be used to control photogrammetric mapping. It is the purpose of this section to evaluate the potential of these data in producing maps on the scale of 1:50,000, 1:200,000, and 1:250,000.

This will be done by examining the accuracy requirements for these maps with regard to the quality of the GOPSS data as determined by the photogrammetric analysis.

3.9.1 General Mapping Requirements

The accuracy requirements of maps are usually separated into considerations of horizontal and vertical accuracy, and are functionally related to the map publication scale. According to the National Map Accuracy Standards, the evaluation of horizontal accuracy is made as follows:

"For maps on publication scales larger than 1:20,000 not more than 10 percent of the points tested shall be in error more than 1/30 inch, measured in the publication scale; for maps on publication scales of 1:20,000 or smaller, 1/50 inch. These limits of accuracy shall apply in all cases to well defined points only."

The corresponding statement concerning vertical accuracy, extracted from the National Map Accuracy Standards, is:

"Vertical accuracy as applied to contour maps on all publications shall be such that no more than 10 percent of the elevations tested shall be in error more than one half the contour interval. In checking elevations taken from the map, the apparent vertical error may be decreased by assuming a horizontal displacement within the permissible horizontal error for a map of that scale."

These quotations establish the elevation accuracy as a function of slope (and scale), so that the 90 percent limit, for a 1:50,000 map, in an area where the ground slope is α, is obtained by adding to one half the contour interval (in feet) the value $(0.02 \times 50{,}000 \times \tan \alpha)/12$ feet. In the following considerations, the effect of slopes will be ignored, so that in the event that marginal elevation accuracies are achieved in mapping, it may be safely assumed that the elevation tolerances can be met if a complete consideration is made.

The stipulation of a 90 percent assurance implies that the elevation standard error is defined by σ_h = (contour interval)/1.645. Positional errors, on the other hand, are considered to be composed of two horizontal components, so that the horizontal standard error should be calculated as for a bivariate distribution, namely, σ_p = (0.02 × Scale factor)/2.146.

In past considerations by Hallert and Thompson, the standard errors of horizontal positions have been calculated as if they were members of a univariate population according to the 1.645 factor. This is incorrect, and it is theorectically undesirable to consider map errors as belonging to two separate distributions. Ideally, these should be considered as belonging to a trivariate population and map quality should be tested according to a total spherical (or ellipsiodal) error.

Such a treatment, however, has not been fully expounded in the technical literature, and since it is in conflict with the map accuracy standards definitions, vertical errors will be considered as being independent (i.e., belonging to a univariate distribution) and horizontal errors as being members of a bivariate distribution.

In addition to the internal cartographic accuracy, the maps should be associated with a geodetic accuracy, which enables the compiled map sheet to be absolutely positioned to certain accuracies with respect to a world geodetic system. The specific requirements that must be satisfied to generate maps of scales 1:50,000, 1:200,000 and 1:250,000 are listed in Table 3-30.

3.9.2 Mapping Specifications

3.9.2.1 Vertical Accuracies

The contour intervals and relative vertical accuracies listed in Table 3-30 have been derived from document SH-65-8, dated 30 March 1966. The relevant quotation is:

"... a contour accuracy of 5-10 meters per 10-20 miles for 1:50,000 topographic maps, 25 meters per 20 miles for 1:250,000 topographic maps, 50-75 feet per 20-30 miles for 1:200,000 aeronautical charts, where contour accuracy is one-half the contour interval, ..., all accuracies are at 90 percent assurance,..."

For the 1:50,000 maps, the 10-meter limit has been divided by 1.645 and converted to feet to furnish the standard error of 20 feet. Corresponding values have been calculated for the small scale maps.

The contour interval corresponding to these standard errors is consistent with the map accuracy specification were then computed.

3.9.2.2 Horizontal Accuracies

Horizontal accuracies have been calculated by multiplying the value 0.2 mile by the scale factor, converting to feet, and dividing by 2.146.

3.9.3 Geodetic Accuracy

The geodetic accuracy with which the maps can be positioned with respect to an earth-centered world geodetic system is the same as the accuracy with which the individual landmarks can be located in this system.

According to Section 3.4.2.2, Table 3-11, the worst horizontal positional errors for altitude of 120, 160, and 200 nautical miles, are ± 41 feet, ± 58 feet, and ± 65 feet respectively, with respect to the orbit. The orbital errors have been shown to combine with these errors in a root-sum-squares manner, so that the geodetic horizontal accuracy requirement is attained provided that the orbital positions can be determined with an accuracy of ± 200 feet with respect to the world geodetic system. According to the results of the orbital studies, this is a feasible accuracy.

Table 3-30 — Mapping Specification

	Map scale		
Cartographic Requirements	1:50,000	1:200,000	1:250,000
Contour interval	65 feet	150 feet	164 feet
Horizontal standard error	38 feet	168 feet	192 feet
Vertical standard error	20 feet	45 feet	50 feet
Relative vertical accuracy	20 feet/20 miles	45 feet/60 miles	50 feet/20 miles
Spot heighting accuracy	-	15 feet/10 miles	-
Geodetic Requirements			
Horizontal accuracy	210 feet	210 feet	210 feet
Relative horizontal accuracy	24 feet/50 miles	24 feet/50 miles	24 feet/50 miles
Vertical accuracy	182 feet	182 feet	182 feet
Relative vertical accuracy	9 feet/50 miles	9 feet/50 miles	9 feet/50 miles

The absolute vertical positioning of the map in the world geodetic system, with specified accuracy of ± 182 feet, (Table 3-30), can be attained if the orbital errors are less than ± 172 feet. Again, this is feasible.

It is therefore concluded that the absolute geodetic positioning of maps can be fulfilled by the GOPSS landmark data.

The relative geodetic horizontal and vertical accuracies that should be attained using the GOPSS landmark data may be obtained from Figure 3-4, Section 3.4.2.3. For an operational altitude of 160 nautical miles, the relative horizontal accuracy in 50 miles is ± 34 feet across-track, and ± 26 feet in-track. These data do not meet the specification of a ± 24-foot circular error as listed in Table 3-30. It is pointed out that the data obtained from Figure 3-4 is based on our pessimistic weighting factor, and that under good conditions in which a better image weight can be validly applied, relative horizontal accuracies of ±24 and ±17 feet, would be furnished, thus indicating that the relative geodetic horizontal accuracy might be marginally attained.

In the case of the relative vertical accuracy, the GOPSS data, under the best conditions, is approximately twice as bad as the specified 9-foot accuracy, so that this requirement cannot be met by the GOPSS photography.

3.9.4 Cartographic Accuracy

The cartographic accuracies listed in Table 3-30, refer to the relationship of specific features on the graphic representation to the basic control net.

Tests conducted at Gimrada indicate that well adjusted first order plotting instruments introduce a standard error of 0.1 millimeter into the map making processes. An additional graphical error due to the instrumental coordinatograph introduces an additional standard error of 0.1 millimeter. Utilizing the 0.5/2.146 standard error on the map, the permissible standard error due to the photogrammetric data alone must not exceed the value

$$E = [(0.5/2.146)^2 - 0.1^2 - 0.1^2]^{1/2} \times S \text{ mm} = 0.184\ S \text{ mm}$$

where S = the map scale

Referring to the map accuracy standards, these errors should be applied to well defined points. This implies that the landmarking accuracy of the GOPSS, determined by using a high weighting, can be validly applied to this evaluation. These data according to Table 3-9 are:

Altitude, nautical miles	Maximum Horizontal Error, feet	Expected Horizontal Error (Using High Weight), feet
120	33	22
160	43	28
200	52	33

These data indicate that the planimetric mapping accuracies for all cases may be met for operational altitudes less than 160 nautical miles, and that even in the event that one uses ill-defined image points in testing map accuracy, planimetric tolerances for a map at the scale of 1:72,000 for the 160-nautical miles altitude may be met.

The vertical accuracy of contouring is basically related to the relative accuracy where elevation differences can be detected. With regard to Figure 3-4, the relative accuracy of elevation determination is applicable to well defined points, i.e., it illustrates the expected spot heighting accuracy. Contour lines, however, are not a sequence of discrete pointings on well defined points, but consist of a continous traversing of the sterescopic model in which photographic information is of variable content and contrast. This decreased sensitivity and selectivity has been discussed by Hallert, who uses the spot heighting accuracy to determine the minimum contour interval that can validly be used. This is twice the spot heighting accuracy and is in agreement with the contour intervals that most government agencies estimate they can attain. This is also in close agreement with the larger interval quoted in the older photogrammetric texts, namely three times the spot heighting accuracy.

Using the maximum relative spot heighting error or 40 feet at a 140-nautical mile horizontal distance, and the three times criterion, the contour interval that might be applied to GOPSS photography acquired at 160 nautical miles is 120 feet. This is certainly sufficient for mapping at the 1:200,000 to 1:250,000 scales. However, it appears that a more consistent approach is to convert the spot heighting accuracy into 90 percent assurance limits, which, when doubled, furnish the minimum contouring interval that satisfies the map accuracy standards. The 40-foot value leads to a contour interval of 131 feet, which is less than the intervals required for the small scale maps.

For the mapping of a small area, say 80 miles square, we may use the relative accuracy of 24 feet at a distance of 40 miles, from which a contour interval of 80 feet is derived. This is the interval usually associated with mapping at a scale of 1:100,000, but is certainly not sufficient for the larger scale maps of 1:50,000.

In order that mapping at a scale of 1:50,000 might be performed to map accuracy standards, the GOPSS photography must be supplemented by additional data. These data can be supplied by the addition of a high resolution panoramic camera to the GOPSS. The panoramic camera must be capable of providing elevation data with a minimum accuracy of 20 feet. Using the standard parallax formula, this is equivalent to a horizontal ground error of ± 10 feet. This is the specification of the worst ground resolution for the panoramic camera that is necessary to support the GOPSS camera in order to attain the 1:50,000 mapping specifications.

3.9.5 Map Information Content

To fulfill the information requirements of the generated maps, the imagery must provide sufficient detail to interpret and relatively measure cultural objects such as large buildings, suburban areas, roads and road classifications, hydrology, vegetation, and details of hills and mountains.

These examples of landmarks to be interpreted, although most pertinent to the 1:50,000 scale maps, are scalable to the 1:200,000 and 1:250,000 scale maps. The approximate ground resolved distances to satisfy the identification requirements are 8 feet for the 1:50,000 scale and 40 feet for the smaller scales. Also important in the process is the location of this detailed data in the generated maps.

An experimental program conducted during Phase I has evaluated the positioning errors associated with the registratation of high and low contrast edges of varying image quality. Complex targets which were not considered possess an averaging phenomenon, since gradients in intensity occur in all directions and throughout the format; the edges simulate the worst case possible with no compensation in a single edge.

The results of the program indicate the probable error to be 1/6 of the difference between the ground resolved distances of the two images.

In the case of 8-foot high resolution panoramic photography, metric photography, and 108-foot resolution, the probable error is 15 feet, well within the positioning requirement of 50 feet for 1:50,000 scale maps. Also critical to the map-making process is the identification of detail information in the areas being mapped, and the capabilities for transferring the location of this detailed information into the created maps.

In the case of a low-altitude mapping mission, the metric photography provides sufficient detail for the map-making function; in the case of the GOPSS program with its original metric records of scale 1:1,000,000, ground resolved distances for 1:50,000 scale maps will be provided. The high resolution panoramic photography fulfills a dual need in the 1:50,000 scale map-making process, i.e., contouring and detail identification.

3.10 GROUND HANDLING OF MISSION PHOTOGRAPHY

There will be two sets of photographic data recovered from each successful mission. These are:

1. Approximately 22,000 feet of 9½-inch film exposed by the terrestrial camera
2. Approximately 10,000 feet or 70-millimeter film exposed by the stellar cameras

The processing of this film does not require any special techniques or equipment and should be well within the capability of any reasonably sized photographic laboratory. However, owing to the large amount of film that must be processed, a realistic and efficient data handling flow must be realized.

The overall scheme of the film handling is summarized by the following chart (Figure 3-7), with specific reference to the terrain records. This chart is not to be construed as a final description of the data handling, although each of the significant operations is described and associated with specific instrumentation. This hardware represents the selection of currently available equipment that can fulfill the data handling task.

A brief description of the sequential steps in the film handling will now be given to point out some of the anticipated problems.

For each mission, the tasks performed by the photographic laboratory are included in blocks 1 through 7 of Figure 3-7, starting with the original undeveloped film and ending with the production of diapositives for the succeeding mensuration tasks.

The first problem encountered in the processing of the original negatives is due to the limited capacity of the developing equipment. This means that the unprocessed film rolls must be cut into manageable lengths that are compatible with the processor. Since it is not envisioned that equipment having a greatly increased film capacity will be developed, it is expected that the original film will be cut into 1500-foot rolls, compatible with the suggested Houston Fearless HTA/3C processor.

One HTA/3C, operating at 21 feet per second, will process a total mission output (terrestrial) in approximately 20 running hours.

The inspection, editing, and splicing of the processed negatives is a considerably time-consuming task. Despite the possibility that a significant portion of terrain photography will be useless, owing to cloud cover and other detrimental effects, each of the usable records must be inspected to ensure that the data blocks contain all the necessary information, and possibly that their correlation with the stellar records is performed.

A similar problem is encountered with the stellar photography in that it is desirable to edit all exposures, whether or not they correspond to usable terrain records. There are several reasons for this, one of which is the possibility that camera orientations can be determined with

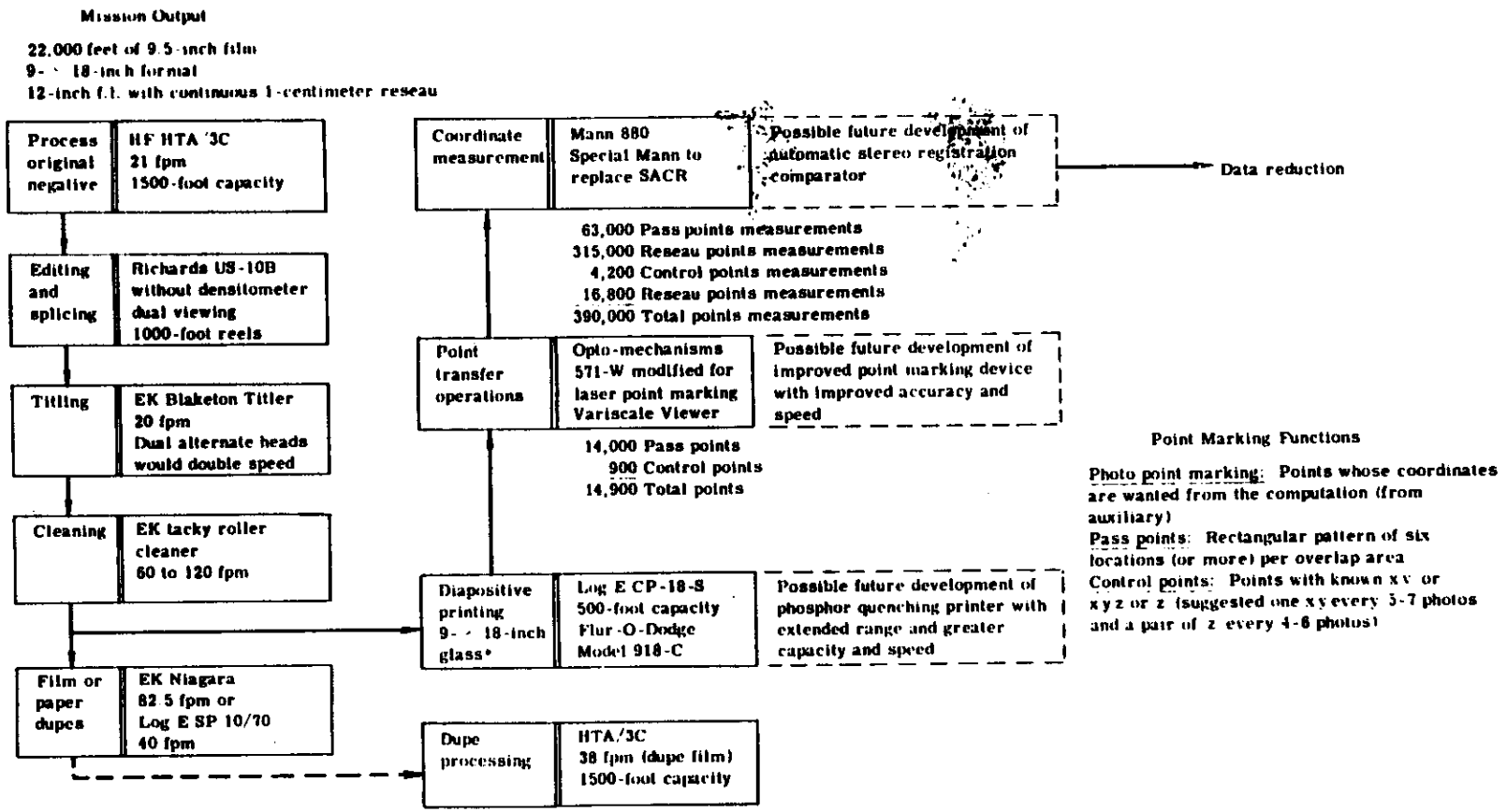

*Aerographic positive plates, 0.250-inch thickness, 0.0005 inch per linear inch flatness tolerance.

Fig. 3-7 — Ground handling of mission photography, block diagram

suitable precision through an explicit function. This would permit a significant conservation of storage and time in the final data reduction.

It appears from a survey of existing equipment that the Richards US-10B with dual viewing would be the most appropriate means of performing the editing task. Film titling and cleaning represent no significant problem since suitable efficient equipment is readily available from commercial sources.

The final essential product of the photographic laboratory is the production of glass diapositives from the original negatives, on which the photogrammetric measurement will be performed. At present, the Log E CP-18-S and Flur-O-Dodge Model 918-C appear to be the most appropriate equipment selections. However, it is envisioned that current proposals for the development of a phosphor quenching printer will lead to equipment that will greatly enhance this aspect of the photographic phase.

Planning and point selection for the photogrammetric measurements will necessitate paper prints of the terrain pictures from equipment such as the Eastman Kodak Niagara or Log E SP 10/70, which are also able to produce copy negatives. The resulting materials would be processed by the HTA/3C.

The preceding steps constitute the initial phase of the data handling. The significant bottleneck in this production is that of editing and inspecting the original negatives. It will therefore be necessary, from a production aspect, that a battery of editing personnel and equipment be available. Assuming that one person might edit 50 frames per day, it would require a minimum of 10 sets of equipment worked two shifts per day in order to accomplish this task in two weeks of elapsed time.

In view of the preceding comments, it would appear that the requirements of the photolaboratory would require approximately thirty people, and the following equipment.

Item	Quantity	Use
HTA/3C processor	1	Processing of original film, duplicating, printing
Richards US-10B dual viewing table	10	Editing and inspection
Blaketon Titler	1	Film titling
Eastman Kodak Tacky Roller	1	Film cleaning
Log E SP 10/70 or Eastman Kodak Niagara	1	Duplicating negatives; producing paper prints
Log CP-18-S or Flur-O-Dodge 918-C	1	Diapositive printing

This facility would prepare the photography from one mission for photogrammetric measurements in approximately three weeks elapsed time.

The photogrammetric activities conclude with the measurement of the required image coordinates. Prior to this, there is an enormous task in the selection and transfer of points, the identification of control, and the extraction of information from the data blocks.

The selection and transfer of pass points, as well as the identification of control, is initially performed on paper prints, as a matter of convenience. These points are then transferred to the diapositives and permanently marked. It would appear that since it might be necessary to mark and transfer a large number of points, this task would be most economically solved with the use of the 571-W comparison viewer produced by Opto-Mechanisms that has been modified for point marking. It must be mentioned, however, that the development of point marking devices with improved accuracies and speed are to be expected in the near future.

The implication associated with point marking devices is that the coordinates of the marked points will be measured with a monocomparator. This is not necessarily true, but, owing to the large format size and the scarcity of appropriate instruments, it appears that the monocomparator technique is the most feasible. Again, the future development of accurate automated stereo registration comparators would appear to be imminent, and could greatly enhance the mensuration time.

An alternative approach would be to use existing 9- × 9-inch mensuration equipment, if each of the 9- × 18-inch frames is used to produce two abutting 9- × 9-inch diapositives. There is no serious objection to the technique, since the two segments are integrally united through the reseau image. This does, however, increase the amount of time that will be necessary for diapositive printing, point marking and transfer, and the mensuration task. This task is somewhat facilitated by minimizing the number of reseau points to be measured, namely by measuring only those four points that enclose a point of interest, and performing a differential connection for film shrinkage.

So far these comments have been concerned with measuring the terrain photographs. In addition, the extraction of pertinent recorded data such as exposure time, altimeter data, etc., could be efficiently performed during the preliminary point selection on the paper prints. Information contained in the data blocks of the stellar photography could also be efficiently extracted at the time that the star identification phase is performed.

Although automation of much of the stellar reduction is possible, the combined reseau and image points to be measured for the terrestrial photography alone is in the order of 400,000, a formidable number of measurements that could be accomplished in two man years using present equipment and techniques. In addition to this, the transfer and marking of some 15,000 points will entail a minimum effort of 1/3 man year.

The semiautomatic stellar identification procedures will require a future one man year of effort, which is approximately the same as required for the selection and identification of terrain images. By these computations, a grand total in the order of five man years, implying a staff of 20, supported by equipment, could produce the desired measurements (per mission) in three months of elapsed time. Unfortunately, although certain tasks will be performed concurrently, measurements of the terrestrial photographs cannot be efficiently produced until all ground control and pass points have been finally selected on the paper prints. A more detailed study of these operational problems is desirable before a sound estimate of manpower requirements can be established, but it is provisionally estimated that a capable staff of 50, supported by efficient equipment, would suffice to perform this task (per mission) in a four-month period.